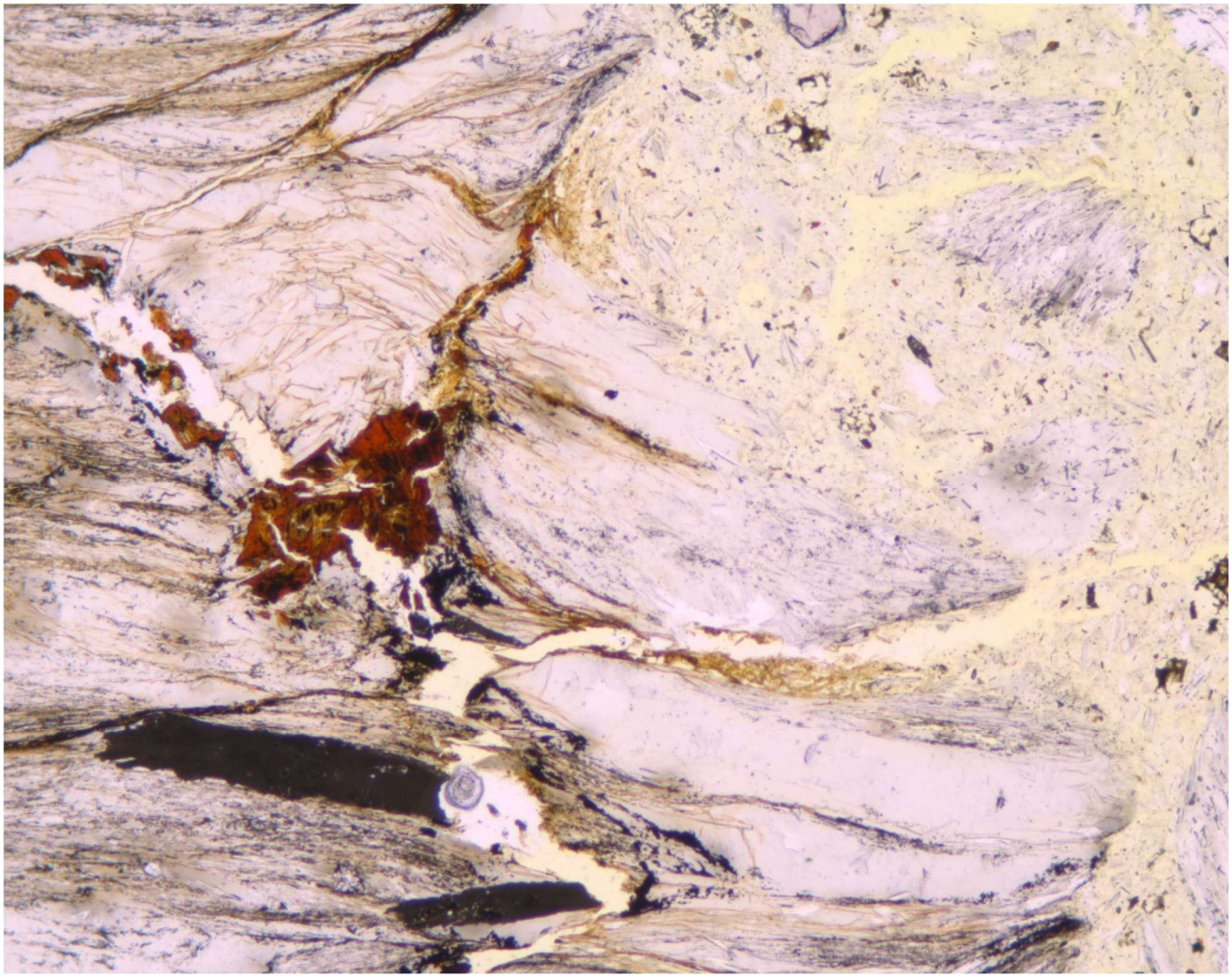

Sample 20511/B11 Polished thin section showing oxidisation of sulfides and evidence of expansion caused by internal sulfate attack.

Department of Housing, Local Government and Heritage, and Geological Survey Ireland

Pyrrhotite-bearing concrete investigation, Co. Donegal

Laboratory Analysis Services in support of Geological Survey Ireland's "Irish Construction Materials" Project: Concrete Products

Phase 1 Report

1283831-01 (02)

MARCH 2025

CONTENTS

RSK DOCUMENT CONTROL ..... **V**
EXECUTIVE SUMMARY ..... **VI**
GLOSSARY ..... **I**
1 INTRODUCTION **3**
1.1 Context 3
1.2 Instructions 4
1.3 Objective 4
2 SITE WORK **6**
2.1 Sampled properties 6
2.2 Sampling 6
3 SAMPLES – RSK **8**
4 METHODS **10**
4.1 Petrographic examination – ASTM C856-20 and I.S. 465 7.3, ... 10
4.2 SEM/EDX analysis 10
4.3 XRD analysis (semi-quantitative) 11
4.4 Compressive strength of core samples – BS EN 12504-1:2019 11
4.5 Compressive strength of masonry blocks – BS EN 772-1:2011+A1:2015 11
4.6 Density – BS EN 12390-7:2019+AC:2020 11
4.7 Density – BS EN 772-13:2000 12
4.8 Cement content – BS 1881-124:2015+A1:2021 12
4.9 Total sulfur – BS EN 1744-1: 2009+A1:2012 12
4.10 Acid soluble sulfate content – BS EN 1744-1:2009+A1:2012 12
4.11 Water soluble sulfate content – BS EN 1744-1:2009+A1:2012 13
4.12 Pyrite/Pyrrhotite content 13
4.13 Determination of sulfate – BS EN 196-2:2013 13
4.14 Determination of sulfide – BS EN 196-2:2013 14
4.15 RICS - The Mundic Problem, Stage 3 expansion testing 14
4.16 Accelerated Oxidisation testing of concrete blocks, adapted version of CSA A23,1:19/A23.2:19 Attachment P3 (informative) 14
5 LABORATORY PROGRAM **16**
6 SAMPLE PROCESSING **17**
6.1 Sub-sampling 17
7 RESULT SUMMARIES **18**
7.1 Optical microscopy (OM) 18
7.1.1 Constituent properties 18
7.1.2 Quantitative compositional mix proportions 18
7.1.3 Sulfides 21
7.1.4 Deposits observed 21
7.1.5 Photomicrographs 22
7.2 SEM/EDX 31
7.2.1 Phase maps 31
7.2.2 ‘Free’ muscovite mica analysis 31
7.2.3 Sulfides 33
7.2.4 Sulfide associated deterioration 34

7.3 XRD 36
7.4 Chemical and physical testing 37
7.4.1 Compressive strength 38
7.4.2 Density 38
7.4.3 Cement content 39
7.4.4 Total sulfur (TS) 40
7.4.5 Acid soluble sulfate (AS) 41
7.4.6 Water soluble sulfate content (WSS) 43
7.4.7 Pyrite and pyrrhotite content 43
7.4.8 Sulfide content 45
7.5 RICS - The Mundic Problem, Stage 3 expansion testing 45
7.6 Oxidisation testing of concrete block, adapted version of CSA A23,1:19 Attachment P3 (informative) 45
8 DISCUSSION 46
8.1 Sample integrity 46
8.2 Aggregates 46
8.2.1 Abundance and composition 46
8.2.2 Physical properties 47
8.2.3 Sulfides 47
8.2.4 Mica content 51
8.3 Cement matrix 53
8.3.1 Cement content 53
8.3.2 Internal sulfate attack (ISA) 54
8.3.3 Acid attack 56
8.4 Physical properties 56
8.5 Condition summary of test property structural elements 58
8.5.1 Outer leaf 58
8.5.2 Inner leaf 59
8.5.3 Rising wall 59
8.5.4 Foundation 60
8.6 Control property 61
8.7 Summary of main factors in the concrete deterioration 61
9 CONCLUSIONS 62
10 REMARKS 66

TABLES

Table 3-1 Samples received by RSK 9
Table 5-1 Laboratory program assignment 16
Table 7-1 Constituents and void contents 18
Table 7-2 OM sulfide abundance 21
Table 7-3 OM deposits observed 21
Table 7-4 Petrographic summary table 30
Table 7-5 Table of calculated ‘free’ muscovite mica content 32
Table 7-6 SEM/EDX observations 34
Table 7-7 XRD Semi-quantitative compositional data 36
Table 7-8 Chemical and physical data 37

FIGURES

Figure 2-1 Examples of sampling areas 7
Figure 3-1 Examples of as-received samples 8
Figure 7-1 Quantitative compositional mix proportions 18
Figure 7-2 Scanned images of polished slices – Inner leaf 19
Figure 7-3 Scanned images of polished slices – Outer leaf 19
Figure 7-4 Scanned images of polished slices – Rising wall 20
Figure 7-5 Scanned images of polished slices – Foundation 20
Figure 7-6 Photomicrographs – Outer Leaf – Test property 7MV 22
Figure 7-7 Photomicrographs – Outer Leaf – Test property 21GD 22
Figure 7-8 Photomicrographs – Outer Leaf – Test property 28AW 23
Figure 7-9 Photomicrographs – Outer Leaf – Control property C 23
Figure 7-10 Photomicrographs – Inner Leaf – Test property 7MV 24
Figure 7-11 Photomicrographs – Inner Leaf – Test property 21GD 24
Figure 7-12 Photomicrographs – Inner Leaf – Test property 28AW 25
Figure 7-13 Photomicrographs – Inner Leaf – Control property C 25
Figure 7-14 Photomicrographs – Rising Wall – Test property 7MV 26
Figure 7-15 Photomicrographs – Rising Wall – Test property 21GD 26
Figure 7-16 Photomicrographs – Rising Wall – Test property 28AW 27
Figure 7-17 Photomicrographs – Foundation – Test property 7MV 27
Figure 7-18 Photomicrographs – Foundation – Test property 21GD 28
Figure 7-19 Photomicrographs – Foundation – Test property 28AW 28
Figure 7-20 Photomicrographs – Foundation – Control property C 29
Figure 7-21 Photomicrographs – Microporosity 29
Figure 7-22 SEM/EDX phase maps 31
Figure 7-23 SE Images of ‘free’ muscovite mica 31
Figure 7-24 Mean ‘free’ muscovite mica proportion of binder 32
Figure 7-25 BSE images of sulfides present within samples 33
Figure 7-26 Foundation deterioration – Control property 34
Figure 7-27 BSE images showing evidence of concrete deterioration 35
Figure 7-28 Compressive strength data 38
Figure 7-29 Density data 39
Figure 7-30 Cement content data 39
Figure 7-31 Total sulfur data (aggregate equivalent) – Acid digestion 40
Figure 7-32 Total sulfur data (aggregate equivalent) – HTC 41
Figure 7-33 Acid soluble sulfate data – BS EN 1744-1 42
Figure 7-34 Acid soluble sulfate data – BS EN 196-2 42
Figure 7-35 Water soluble sulfate data 43
Figure 7-36 Calculated pyrite content data 44
Figure 7-37 Calculated pyrrhotite content data 44
Figure 7-38 Sulfide content data (whole sample) 45
Figure 8-1 Comparison of ‘free mica’ content to OM determined soundness 52
Figure 8-2 Cross section of element condition 60

APPENDICES

APPENDIX A - CHAIN OF CUSTODY
APPENDIX B - IGSL SAMPLING REPORT EXTRACT – SAMPLING LOCATIONS
APPENDIX C - CERTIFICATES OF TEST
APPENDIX D - AS-RECEIVED PHOTOGRAPHS

RSK DOCUMENT CONTROL

Report No.: 1283831-01 (02)

Title: Pyrrhotite-bearing concrete investigation, Co. Donegal - Laboratory Analysis Services in support of Geological Survey Ireland's "Irish Construction Materials" Project: Concrete Products Phase 1

Client: Department of Housing, Local Government and Heritage and Geological Survey Ireland

Date: 14 March 2025

RSK Office: 18 Frogmore Road, Hemel Hempstead, Hertfordshire, HP3 9RT

Status: Final

Author	Alex Smith Principal Geomaterials Scientist	**Technical reviewer**	Dr Ian Blanchard Associate Director
Signature		Signature	
Date:	14 March 2025	Date:	14 March 2025

EXECUTIVE SUMMARY

Damage to housing typically built between the late 1990s to early 2010s in NW Ireland has been previously attributed to excessive fine, disseminated 'free' muscovite mica and reactive sulfide-related deterioration. To investigate the topic The Irish Government funded a research framework in 2022, in which RSK was awarded funding. RSK was instructed to investigate the long-term performance of the affected concrete, pyrrhotite (a reactive sulfide) oxidisation and its effect on the physical properties of deteriorated concrete blocks. To fulfil these research aims, a set of concrete samples was taken and supplied to RSK in 2023. Samples comprised inner leaf, outer leaf, rising wall (if present) concrete masonry block and foundation mass concrete samples from three test properties, exhibiting pyrrhotite and deterioration, and samples from one control property exhibiting sulfides but no evident deterioration. This Phase 1 report presents the initial characterisation of the sample set, providing a baseline for further analysis in Phase 2 and 3 of the research programme. Testing included detailed petrographic and instrumental techniques supplemented by suites of chemical and physical testing. The aggregate (PHY) used within the test property concrete chiefly contained metamorphic phyllite and quartzite rocks and derived minerals. The phyllite contained sulfides including pyrrhotite, pyrite, chalcopyrite and rare pentlandite in addition to muscovite mica and other mica group minerals. The use of PHY resulted in abundant 'free' mica and common pyrrhotite both as discrete cement matrix-set and variably internally and marginally aggregate particle-set grains. Chemical analyses indicated sulfur contents within PHY that exceeded the specific restriction in European standards for sulfur content within pyrrhotite-bearing aggregates for use in concrete. However, total sulfur determined by acid digestion did not show the expected total sulfur levels consistent with the petrographically observed or as determined by sulfide determined by acid digestion or HTC total sulfur tests on PHY-bearing concretes. The EN 1744-1 total sulfur acid digestion methodology was thought to have returned underestimations due to the presence of complex geological materials involved and sulfides not being fully digested in the test method. The amount of pyrrhotite present within the PHY-bearing concrete exhibited significant but varied amounts of *in situ* oxidisation to iron oxides/hydroxides and other compounds, leading to some corresponding degree of highly localised internal sulfate attack (ISA) and weakening of the cement matrix within all PHY-bearing building elements. The above-ground oxidisation and ISA-related deterioration appear to be exacerbated by the presence of moisture ingress through the cracked external render into the outer leaf combined with an oxidising environment within the outer and inner leaves. However, the PHY concrete only exhibited relatively rare, localised abundances of ISA-related, expansive and strength-reducing sulfate deposits (ettringite, gypsum, thaumasite etc.) for the degree of *in situ* sulfide oxidisation. The deficiency in ISA-type sulfate deposits may be caused by the migration of dissolved sulfate into the adjacent cementitious sand-cement mortar or render, which showed thaumasite formation at the interface with the outer and inner leaf, in selected PHY-bearing concrete blocks. Additionally, the significant carbonation and associated pH reduction of the cement matrix above ground appears to have suppressed ISA. When compared to the control property, the type, abundance, and morphology of the pyrrhotite present in PHY concretes were found to be the most significant causal factors in the observed deterioration. Excessive 'free mica' within PHY concrete may have aided its susceptibility to but not be the primary cause of deterioration. The degree of deterioration through sulfide oxidisation and ISA, within PHY-bearing concrete elements was generally relatively ordered outer leaf>inner leaf>rising wall>foundation with the inverse order generally applicable to sample integrity. This investigation suggests that the presence of remnant unoxidised pyrrhotite, conditions for sulfide oxidisation and ISA in all PHY-bearing concrete indicates the potential for further deterioration. A degree of risk is advised for all elements due to the progression of these deterioration mechanisms albeit at different rates and along different reaction pathways. The PHY-bearing mass concrete foundations are generally the strongest building element investigated and in the best condition, however any low risk assigned to these foundations, given similar exposure conditions, may only be tentatively assigned in this report given the data available. More commentary will be provided on this assertion in the Phase 2 and 3 reports.

GLOSSARY

21GD – 21 Glendale Drive (test property)

28AW – 28 Abbotts Wood (test property)

7MV – 7 Mulroy View (test property)

AOI – Area of interest

ASS – Acid soluble sulfate

BSE – Backscatter electron

C – Carrowmore (control property)

CPL – Circular-polarised light

C-S-H – Calcium silica hydrates

DPM – Damp-proof membrane

EDX – Energy dispersive X-ray

F – Foundation

GSI – Geological Survey Ireland

HTC – High temperature combustion

IL – Inner leaf

In situ – Whilst present within concrete

ISA – Internal sulfate attack

ITZ – Interfacial transition zone, cement-aggregate interfacial zone within the cement matrix.

NSAI – National Standard Authority of Ireland

OL – Outer leaf

OM – Optical microscopy

OS – Oxidisable sulfates

PPL – Plane-polarised light

Pre-existing – Before use within concrete

RL – Reflected light

RW – Rising wall

SE – Secondary electron

SEM – Scanning electron microscope

TPS – Total potential sulfate

TS – Total sulfur

TSA – Thaumasite form of sulfate attack

WSS – Water soluble sulfate

XPL – Cross-polarised light

XRD – X-Ray Diffraction

1 INTRODUCTION

1.1 Context

Concrete blocks containing deleterious aggregates were found to have been used in the Northwest of Ireland's domestic construction, primarily in the late 1990s until the late 2000s. During a period of Irish economic growth referred to as the 'Celtic Tiger' and its associated building boom. Initially, the issue was thought to be chiefly related to either or both muscovite mica contents or reactive pyrite (with different causes in different areas) and thought possibly to affect approximately 5,000 homes.[1] The scale of the problem led to the establishment of a multi-billion euro fund to assist the affected homeowners, and the introduction of Irish standard I.S. 465 giving methods to investigate the affected concrete.[2] However, the recent experience of consultants and academic research have highlighted the presence and oxidisation reactions of pyrrhotite as the most common cause of deterioration in many of the affected properties, especially in the north-west of the country, through the mechanism of internal sulfate attack (ISA).[3,4]

Concrete blocks affected by ISA typically experience a primary deterioration mechanism triggered by the expansive oxidisation (rusting) of iron sulfides, resultant release of sulfuric acid and subsequent dissolution, alteration and weakening of the cement matrix eventually leading to conversion or failure of the concrete. These reactions are in part represented by the following equations well documented in the literature.[5,6,7]

$Fe_{(1-x)}S$ (pyrrhotite) + $(2-x/2)O_2$ + $xH_2O \rightarrow (1-x)Fe^{2+} + SO_4^{2-} + 2xH^+$

$Fe^{2+} + 1/4O_2 + 2H^+ \rightarrow Fe^{3+} + 1/2H_2O$

$Fe^{3+} + 3H^2O \rightarrow Fe(OH)_3$ (ferric oxyhydroxide, expansive) + $3H^+$

H_2SO_4(sulphuric acid) + $Ca(OH)_2$ (portlandite) $\rightarrow CaSO_4.2H_2O$ (gypsum)

$3(CaSO_4.2H_2O) + C_3A + 26H_2O \rightarrow C_3A \cdot 3CaSO_4 \cdot H_{32}$ (ettringite)·

[1] McCarthy, D. Kane, N. Lee, F. Blaney, D. Report of the Expert Panel on Concrete Blocks, 2017, https://www.gov.ie/en/publication/0218f-report-of-the-expert-panel-on-concrete-blocks/.

[2] I.S. 465:2018+A1:2020, Assessment, Testing and Categorisation of Damaged Buildings Incorporating Concrete Blocks Containing Certain Deleterious Materials and Amendment 1, National Standards Authority of Ireland, 2020

[3] A. Leemann, B. Lothenbach, B. Münch, T. Campbell, P. Dunlop, The "mica crisis" in Donegal, Ireland – a case of internal sulfate attack? Cem. Concr. Res. 168 (2023).

[4] C. Brough, B. Staniforth , C. Garner , R. Garside , R. Colville , J. Strongman , J. Fletcher, High risk concrete blocks from County Donegal: The geology of defective aggregate and the wider implications, Construction and Building Materials 408 (2023) 133404

[5] A. Rodrigues, J. Duchesne, B. Fournier, B. Durand, P. Rivard, M. Shehata, Mineralogical and chemical assessment of concrete damaged by the oxidation of sulfide-bearing aggregates: Importance of thaumasite formation on reaction mechanisms, Cement and Concrete Research, Volume 42, Issue 10, 2012, Pages 1336-1347, ISSN 0008-8846,

[6] R. Zhong, K. Wille, Deterioration of residential concrete foundations: the role of pyrrhotite-bearing aggregate, Cem. Concr. Compos. 94 (2018) Pages 53–61.

[7] Jana, D, Concrete Deterioration from the Oxidation of Pyrrhotite: A State-of-the-Art Review, Chapter 5, Maher, M.L.J, Pyrite and Pyrrhotite, 2023, Pages 139-221, ISBN 979-8-88697-329-7, Nova Science Publishers, Inc.

1.2 Instructions

To address the deterioration of thousands of homes affected by concrete block deterioration, the Irish Government Department of Housing, Local Government and Heritage in conjunction with the Geological Survey of Ireland (GSI) and National Standards Authority of Ireland (NSAI) established a research framework titled 'Laboratory Analysis Services in support of Geological Survey Ireland's "Irish Construction Materials" Project: Concrete Products'. Under this framework, GSI provided RSK and other research partners with a set of research topics to assess. These topics are summarised as follows:

- Long-term performance of the concrete blocks under Irish environmental conditions, e.g. accelerated ageing testing.
- Whether and under what circumstances the pyrrhotite within concrete blocks could oxidise.
- Risk of oxidation occurring within the range of environmental conditions found in Ireland.
- If oxidation occurs, what effect that process has on the integrity, dimensional properties, and compressive strength of the blocks relative to their state when received for testing.
- Risk of retention of pyrrhotite-bearing blockwork in affected dwelling.

It should be noted that RSK's submission was primarily limited to the underlined research topics.

The framework further expanded on the 4th research topic.

- If pyrrhotite alteration occurs in the concrete blocks assessed, does it:
  1. result in the expansion of the samples?
  2. affect the compressive strength of the samples?
  3. significantly impact the integrity of the samples?

To investigate the provided research topics GSI provided RSK with a sample set of pyrrhotite-bearing concrete blocks including some with adhered render and mortar, and mass concrete, from buildings that have previously been evaluated in accordance with I.S. 465.[8] The sample set included a mixture of blocks and cores taken from the inner leaves, outer leaves, rising walls (excluding the control property) and foundations of four buildings, three test properties and one control property. The sample set was designed to be representative of blocks *in situ* (in use) to understand the risk posed by pyrrhotite and reflect the aggregate constituents of damaged and undamaged properties selected.

1.3 Objective

To investigate the instructed research topics (underlined in **1.2**) RSK developed a three-phase investigation as follows.

- Phase 1 – Initial characterisation of the received samples

[8] I.S. 465:2018+A1:2020, See [2]

- Phase 2 – Accelerated ageing and oxidisation (expansion) testing
- Phase 3 – Post-expansion testing, characterisation and comparison

This report is exclusively limited to the analysis conducted on samples supplied to RSK. It forms the Phase 1 initial characterisation of the samples to establish the as-received (*in situ*) condition of the supplied samples. The characterisation will concentrate on the following:

- As-received condition
- Sulfide and sulfate contents
- Mica content
- Physical properties
- Composition of the samples
- Evidence of deterioration mechanisms
- Factors influencing the observed deterioration mechanisms

The results and conclusions presented herein will form the baseline for the Phase 2 long-term performance of concrete blocks under accelerated ageing conditions.

Purposely, only the preparation for Phase 2 is partially covered herein as this was part of the initial sub-sampling of the samples. Phase 2 and Phase 3 are to be covered in subsequent RSK reports, 1283831-03 and 1283831-04.

2 SITE WORK

IGSL provided RSK with the sampling locations and details in a report entitled 'Donegal Concrete Blocks GSI Research Programme, Sampling Operations Record, April 2023', of which an extract is attached in **Appendix B** of this report.[9]

2.1 Sampled properties

The properties were selected by Donegal County Council and advised to have been taken from four vacated houses in Co. Donegal. Three of the houses were considered test properties, these were 15-25 years old and were known to have experienced structural damage/defects typical of the area identified in accordance with I.S. 465.[10,11] The other 'control' property was known to have been constructed in the 1980's and be in good condition. The properties are listed below.

Test Properties

- 7 Mulroy View, Co. Donegal, (7MV)
- 21 Glendale Drive, Co. Donegal, (21GD)
- 28 Abbotts Wood, Co. Donegal, (28AW)

Control Property

- Carrowmore, Co. Donegal, (C)

The properties are constructed of poured mass concrete strip foundations with rising walls made of flat-laid precast concrete blocks (aggregate cement masonry units) built up from the foundations to a dampproof membrane (DPM). Above the DPM, there is a cavity wall made up of two leaves of concrete blocks cemented by a sand cement mortar (see **Figure 2-1**). The wall cavities at all properties, were filled with apparent polystyrene-type insulation of various appearances. The outer leaf is often coated with a painted external render, whilst the inner leaf is coated by an internal plaster. The control property is notable for not being constructed with a DPM or a rising wall. Instead, both leaves extend to the foundations below ground.

2.2 Sampling

The sampling was advised to have been conducted on behalf of Donegal County Council by Crana Cranes Ltd (advised to be a Donegal County Council approved sub-contractor for I.S. 465[12] sampling) under the supervision of IGSL (at the request of GSI). The sampling took place between 9th-12th January 2023, in conditions which appeared to be wet or overcast with saturated groundwater conditions based on supplied photographic evidence (**Figure 2-1**). The IGSL engineering geologist was advised to be Sean

[9] Quigley. P, (2023) 'Donegal Concrete Blocks GSI Research Programme, Sampling Operations Record', IGSL.

[10] Quigley. P, (2023) Donegal Concrete Blocks, IGSL. See [9]

[11] I.S. 465:2018+A1:2020, See [2]

[12] I.S. 465:2018+A1:2020, See [2]

Cunningham who oversaw the works and photographed and recorded sample locations (see **Appendix B**).

Figure 2-1 Examples of sampling areas

1st Row Left – 7MV inner leaf sampling location. 1st Row Right – 21GD rising wall and foundation sampling location. 2nd Row Left – 28AW An outer leaf sampling location. 2nd Row Left – C outer leaf sampling location. Photos taken from IGSL Sampling Reports. Source IGSL.

A selection of blocks and cores were extracted from the inner leaf, outer leaf, rising wall (where possible) and strip foundation building elements. Core samples were taken by coring rigs using approximately 100 mm inner diameter barrels. Trial pits were excavated with a digger to expose the foundations and rising walls (see **Figure 2-1**). More details of the sampling can be found in the sampling report and **Appendix B**.[13]

[13] Quigley. P, (2023) Donegal Concrete Blocks, IGSL. See [9]

3 SAMPLES – RSK

The samples received by RSK were advised to have first been transported from the sampled properties to IGSL's laboratory in Naas, Co. Kildare. There, samples were assigned to RSK and other research partners.

RSK received the assigned 46 sample batch comprised of concrete blocks and concrete cores from the four properties on 28th March 2023. After a request for a further six samples from 28AW in February 2024, in total, RSK received 52 samples for analysis (see **Appendix A**).

Samples were photographed (see **Figure 3-1**, **Appendix D**) logged into RSK's laboratory sample management system and given unique sample references (see **Table 3-1**).

Figure 3-1 Examples of as-received samples

Photos of a variety of as-received sample types and conditions from across all four properties. 1st Row Left, 7MV IL intact. 1st Row Right, 21GD RW intact. 2nd Row Left, 28AW OL disintegrated. 2nd Row Right, C F fragmented. For references see Table 3-1.

Table 3-1 Samples received by RSK

Location	RSK Ref	Client Sample Ref	Sample type	Element	Client Area Location	Date Sampled	As-received condition
7MV	20511/B1	1A	Block	Inner Leaf	I, GE	10/01/2023	F/C
	20511/B2	1B	Block	Inner Leaf	I, GE	10/01/2023	In
	20511/B3	1G	Block	Inner Leaf	I, GE	10/01/2023	SC
	20511/C1	1L	Core	Inner Leaf	I, GE	10/01/2023	In
	20511/B4	2A	Block	Outer Leaf	E, FF, W	10/01/2023	In
	20511/B5	2D	Block	Outer Leaf	E, FF, W	10/01/2023	In
	20511/C2	2I	Core	Outer Leaf	E, FF, W	10/01/2023	In
	20511/C3	2M	Core	Outer Leaf	E, FF, W	10/01/2023	In
	20511/C4	3B	Core	Rising Wall	E, FF, W	10/01/2023	In
	20511/C5	3F	Core	Rising Wall	E, FF, W	10/01/2023	In
	20511/C6	3I	Core	Rising Wall	E, FF, W	10/01/2023	F
	20511/C7	4B	Core	Foundation	E, FF, W	10/01/2023	F/C
	20511/C8	4E	Core	Foundation	E, FF, W	10/01/2023	In
	20511/C9	4G	Core	Foundation	E, FF, W	10/01/2023	In
21GD	20511/B13	1A	Block	Inner Leaf	I, GE	09/01/2023	SD
	20511/B14	1D	Block	Inner Leaf	I, GE	09/01/2023	In
	20511/C22	1G	Core	Inner Leaf	I, GE	09/01/2023	In
	20511/B15	2B	Block	Inner Leaf	I, GE	09/01/2023	In
	20511/C23	2E	Core	Inner Leaf	I, GE	09/01/2023	SD
	20511/B18	3A	Block	Outer Leaf	E, GE	09/01/2023	In
	20511/B16	3D	Block	Outer Leaf	E, GE	09/01/2023	In
	20511/B17	3F	Block	Outer Leaf	E, GE	09/01/2023	In
	20511/C24	3J	Core	Outer Leaf	E, GE	09/01/2023	In
	20511/C25	4D	Core	Rising Wall	E, GE	09/01/2023	In
	20511/C26	4H	Core	Rising Wall	E, GE	09/01/2023	In
	20511/C27	5B	Core	Foundation	E, GE	09/01/2023	In
	20511/C28	5E	Core	Foundation	E, GE	09/01/2023	In
28AW	20511/B8	1A	Block	Inner Leaf	I, GE	11/01/2023	In
	20511/B9	1E	Block	Inner Leaf	I, GE	11/01/2023	SD
	20511/B10	1I	Block	Inner Leaf	I, FF	11/01/2023	In
	20511/B11	2A	Block	Outer Leaf	E, GE	11/01/2023	C
	20511/B12	2F	Block	Outer Leaf	E, GE	11/01/2023	F/C
	20511/C16	2I	Core	Outer Leaf	E, GE	11/01/2023	Di
	20511/C17	2M	Core	Outer Leaf	E, GE	11/01/2023	Di
	20511/C18	3B	Core	Rising Wall	E, GE	11/01/2023	In
	20511/C19	3F	Core	Rising Wall	E, GE	11/01/2023	In
	20511/C20	4A	Core	Foundation	E, GE	11/01/2023	In
	20511/C21	4D	Core	Foundation	E, GE	11/01/2023	In
	20954/B1	2H	Block	Outer leaf	E, GE	11/01/2023	F/C
	20954/C1	2K	Core	Outer leaf	As E, GE	11/01/2023	In
	20954/C2	2L	Core	Outer leaf	As E, GE	11/01/2023	In
	20954/C3	3H	Core	Rising wall	E, GE	11/01/2023	In
	20954/C4	3I	Core	Rising wall	E, GE	11/01/2023	In
	20954/C5	4C	Core	Foundation	E, GE	11/01/2023	In
C	20511/B6	1A	Block	Inner Leaf	I	12/01/2023	In
	20511/C10	1E	Core	Inner Leaf	I	12/01/2023	F
	20511/C11	1F	Core	Inner Leaf	I	12/01/2023	In
	20511/B7	2B	Block	Outer Leaf	E, FF	12/01/2023	In
	20511/C12	2F	Core	Outer Leaf	E, FF	12/01/2023	In
	20511/C13	3A	Core	Below GL	E, GE	12/01/2023	In
	20511/C14	4A	Core	Foundation	E, GE	12/01/2023	In
	20511/C15	4C	Core	Foundation	E, GE	12/01/2023	F

I-Interior, E-Exterior, GE-Gable end, FF-Front Facing, W-West, As-Assumed, F-Fragmented, C-Crumbly, In-Intact, SC-Slightly Crumbly, SD-Slight deterioration, Di-Disintegration

4 METHODS

A programme of analysis was selected (**see Section 5**) for received concrete samples to characterise the material, investigate the cause of any observed deterioration and determine whether any further residual expansion was possible within the different elements of the properties investigated. The test methods specified include a suite of physical, petrographic and chemical testing to quantify and qualitatively evaluate and compare the relevant concrete components, particularly sulfide minerals, sulfur content, sulfates, 'free mica', sulfide oxidisation and ISA.

Further details of the methodologies used can be found in the test certificates presented in **Appendix C**.

4.1 Petrographic examination – ASTM C856-20[14] and I.S. 465 Clause 7.3[15]

For investigated samples, one polished and one coverslipped thin section and a polished slice (approximately up to 100×100×20 mm sized) were produced using either the minimum of water required or alternative grinding media. Examination of the concrete was conducted using a polarising Zeiss Axioscope A1 petrographic microscope, utilising reflected, transmitted and reflected UV, light sources.

4.2 SEM/EDX analysis

SEM/EDX analysis was conducted at an RSK-approved sub-contractor with on-instrument consultation given as needed by RSK personnel. Various sizes of concrete samples ranging from 25×25×25mm to 50×30×25 mm were vacuum impregnated with epoxy resin, polished to a 3-micron finish, and carbon-coated on a single face for analysis.

A JEOL 6480 LV SEM equipped with an Oxford Instruments X-MAX80 SD X-ray detector and INCA X-ray analysis system was used to image the samples and perform the EDX analysis. EDX analyses the characteristic X-rays produced by the interaction between the primary electron beam and the sample. The technique identifies all elements present with atomic numbers of 5 (boron) and greater with a detection limit of approximately 0.1 weight % with all measurements semi-quantitative. The SEM was chiefly operated at an accelerating voltage of 15 kV.

The percentage content for each of the samples investigated was determined through the analysis of three areas of interest (AOI). The AOIs were selected away from coarse aggregate particles, focusing on the binder, to characterise <63 µm sized 'free' muscovite mica and discrete sulfide content present. To achieve this EDX phase maps were produced at appropriate magnifications utilising Oxford Instruments Aztec Software.

[14] ASTM C856-20, Standard practice for petrographic examination of hardened concrete, ASTM, 2020

[15] I.S. 465:2018+A1:2020, See [2]

The AOI phase maps were post-processed and had area proportions calculated to obtain average mineral proportions, binder content and derived calculations using ImageJ 1.53k1.[16]

4.3 XRD analysis (semi-quantitative)

XRD analysis was conducted at an RSK-approved sub-contract using a fully automated Bruker D8 powder diffractometer employing copper kα radiation (λ=0.15406nm) and an energy dispersive Si detector. The samples were continuously spun during data collection and were scanned using a step size of 0.02° 2θ between the range of 5°-80° 2θ. Phase identification using XRD is achieved by comparing the diffraction pattern obtained from the unknown, to a standard database that is compiled by the International Centre for Diffraction Data (ICDD).

4.4 Compressive strength of core samples – BS EN 12504-1:2019

A set of 1:1 length-to-diameter ratio concrete core samples were sub-sampled, prepared (ground) and tested in accordance with BS EN 12504-1.[17] Compressive strengths were compared to cube strength specifications. Deviating sample 20511/C5 was not a full cylinder as it had a small slice missing from the side with a length of approximately 38 mm at the top of the core and 17 mm at the bottom.

4.5 Compressive strength of masonry blocks – BS EN 772-1:2011+A1:2015

Six portions of masonry units were sawn to smaller sizes in the cross-sectional proportion and tested in an as-laid orientation following conditioning to the air-dry condition in BS EN 772-1 Clause 7.3.2a.[18] The samples were prepared by grinding. The normalised compressive strength is the compressive strength corrected for the conditioning method and shape factor in accordance with BS EN 772-1 Annex A.[19]

4.6 Density – BS EN 12390-7:2019+AC:2020

As-received dry densities were measured in accordance with BS EN 12390-7[20] on 1:1 cored concrete samples to provide a check on sample compaction.

[16] Image J 1.53k, Wayne Rasband and contributors, National Institutes of Health, USA, http://imagej.nih.gov/ij

[17] BS EN 12504-1:2019. Testing concrete in structures. Part 1 – Cored specimens. Taking, examining and testing in compression. BSI, London, 2019.

[18] BS EN 772-1:2011+A1:2015Methods of test for masonry units Determination of compressive strength, BSI, London, 2015

[19] BS EN 772-1 See[18]

[20] BS EN 12390-7:2019+AC:2020, Testing hardened concrete - Density of hardened concrete, BSI, London, 2020

4.7 Density – BS EN 772-13:2000

Gross received dry densities were calculated in accordance with BS EN 772-13[21] on sawn geometrically shaped sub-samples taken from concrete block samples to provide a check on sample compaction. Please note that concrete block density results are not available in **Appendix C**.

4.8 Cement content – BS 1881-124:2015+A1:2021

Analysis was performed on 1 kg of material either previously tested for compressive strength or the remnants of the sample after sub-sampling. The analyses for insoluble residue, soluble silica and calcium oxide were carried out in accordance with BS 1881-124:2015+A1:2021, Clause 6.[22] Note, that the cement content calculated as kg/m^3 used the determined densities for some samples, whereas other samples used the determined densities from the same or near similar element (See **Appendix C**).

4.9 Total sulfur – BS EN 1744-1: 2009+A1:2012

The total sulfur content was determined in accordance with BS EN 1744-1, Clause 11.1 acid digestion method.[23] The extraction was conducted using hydrogen peroxide and dilute hydrochloric acid, and the sulfur was precipitated as barium sulfate. The result is reported to the nearest 0.1% by mass of dry aggregate (sample). Note, that the test method describes testing aggregate samples. In this case, the concrete samples were initially prepared to pass a 2 mm sieve before the specified preparation procedure (as per aggregate samples) was conducted. Concerns have been raised about the reliability of the results obtained by this technique, which appears to significantly under-estimate the total sulfur of samples where petrographic examination confirms the presence of sulfide minerals.

Subsequently, additional testing was undertaken wherein powdered samples were directly tested for total sulfur content utilising high-temperature combustion and infra-red analysis (LECO). This method is provided as an option in BS EN 1744-1 Clause 11.2,[24] although the acid digestion method is the reference method. A similar HTC method is described in the Canadian standard CS-A23.1 as the preferred method for determining total sulfur in aggregate. Note Sample 20511/B17 was prepared to pass a 125 µm sieve before the specified preparation was conducted.

4.10 Acid soluble sulfate content – BS EN 1744-1:2009+A1:2012

The acid soluble sulfate content was determined in accordance with BS EN 1744-1, Clause 12.[25] The extraction was conducted using dilute hydrochloric acid and the sulfate was precipitated as barium sulfate. The sulfate content is reported to the nearest 0.1%

[21] BS EN 772-13:2000, Methods of test for masonry units - Determination of net and gross dry density of masonry units (except for natural stone), BSI, London

[22] BS 1881-124:2015+A1:2021, Testing Concrete - Methods for analysis of hardened concrete, BSI, London

[23] BS EN 1744-1:2009+A1:2012, Tests for chemical properties of aggregates - Chemical analysis, BSI, London

[24] BS EN 1744-1, See [23]

[25] BS EN 1744-1, See [23]

by mass of dry aggregate (sample). Note, that the test method describes testing aggregate samples. In this case, the concrete samples were additionally prepared to pass a 2 mm sieve before the specified preparation procedure (as per aggregate samples) was conducted. The test method may cause some dissolution of acid soluble pyrrhotite[26] and therefore the results obtained may represent more sulfur than consistent with the total sulfate content of the sample.

4.11 Water soluble sulfate content – BS EN 1744-1:2009+A1:2012

The water-soluble sulfate content was determined in accordance with BS EN 1744-1, Clause 10.[27] The 2:1 water extract was treated with an excess of barium chloride to precipitate the sulfate as barium sulfate, which was determined gravimetrically. The result was expressed as SO_3 to the nearest 0.01% by mass of dry aggregate (sample). Note the test method describes testing aggregate samples. In this case, the concrete samples were additionally prepared to pass a 2 mm sieve before the specified preparation procedure (as per aggregate samples) was conducted. The resulting material was tested to determine the water-soluble sulfate content in accordance with BS EN 1744-1 for fine aggregate.[28]

4.12 Pyrite/Pyrrhotite content

The tests for acid soluble sulfate and total sulfur (HTC) were carried out in accordance with BS EN 1744-1:2009 + A1:2012.[29] The oxidisable sulfides were calculated from the determined acid soluble sulfate content and total sulfur content according to the formula provided in TRL 447 Table 8.1 and simple conversion of oxidisable sulfates into a pyrite or pyrrhotite content.[30] It should be noted that the calculated values are the maximum potential values for these mineral contents and should be treated with caution.

4.13 Determination of sulfate – BS EN 196-2:2013

The sulfate content was determined in accordance with BS EN 196-2:2013.[31] The acid extract was treated with an excess of barium chloride to precipitate the sulfate as barium sulfate, which was determined gravimetrically. The result is expressed as sulfur trioxide, SO_3 by weight of sample and of cement and converted to SO_4. Note that the method is for testing cement while the samples are concrete blockwork and mass concrete. The standard details the calculation for reporting the sulfate content by mass of sample. A further calculation was performed to report the sulfate by mass of cement. This was performed following BS 1881-124:2015+A1:2021 and using the determined cement content.[32] This calculation is not included in BS EN 196-2:2013.[33]

[26] Deer, W A, Howie, R A, and Zussman, J. An introduction to the rock-forming minerals. The Mineralogical Society, 2013.

[27] BS EN 1744-1, See [23]

[28] BS EN 1744-1, See [23]

[29] BS EN 1744-1, See [23]

[30] Reid J M, Czerewko M A and Cripps J C. Sulfate specification for structural backfills. TRL Report TRL447. Crowthorne, Transport Research Laboratory, 2005, 2nd edn

[31] BS EN 196-2:2013 Method of testing cement - Chemical analysis of cement, BSI, London

[32] BS 1881-124, See [22]

[33] BS EN 196-2, See [31]

4.14 Determination of sulfide – BS EN 196-2:2013

The sulfide content of the sample was determined in accordance with BS EN 196-2:2013, clause 4.4.5.[34] Note that the method is for testing cement while the samples tested comprised concrete blocks and mass concrete. A conversion factor based on sample density (measured) and calculated aggregate content (1700 kg/m^3 from point count) was applied to the values to calculate the sulfide content of aggregates.

4.15 RICS - The Mundic Problem, Stage 3 expansion testing

Expansion testing was conducted in accordance with RICS guidance note 'The mundic problem, 3rd edition'.[35] The Stage 3 test is primarily applicable to concrete blocks from a specific area of the Southwest region of the UK where spoil from metalliferous mining activities have been used locally as aggregate. Therefore, any criteria should not be thought to apply outside of that regional use. The method involves measuring the unconstrained linear expansion of concrete cores that have been exposed to a water-saturated atmosphere at a constant temperature of 38°C for at least 250 days. The testing period can be expanded to at least 350 days if the expansion shown is progressing at a slow rate when 250 days of exposure is reached. The majority of samples were kept in exposure conditions for 350 days, to provide further time for any reactions to occur.

4.16 Accelerated Oxidisation testing of concrete blocks, adapted version of CSA A23,1:19/A23.2:19 Attachment P3 (informative)

To determine residual oxidisation potential and the possibility of thaumasite formation an adaption of the test method developed by Andrea Rodrigues at Université Laval and published in CSA A23, 1:19/CSA A23, 2:19, P3.[36] The methodology describes a procedure for determining the potential deleterious character of sulfide-bearing aggregates through a two-phase accelerated mortar bar test. In this study, the methodology was adapted to test the concrete core samples with similar sample sizes and stud arrangements specified within RICS guidance note The mundic problem, 3rd edition.[37]

To prepare the sub-samples three pairs of bespoke titanium DEMEC Gauge studs spaced at 50 mm separation were fixed at equal intervals (120°) around the circumference of a set of up to four 75 mm diameter cores taken from the investigated elements (dependent on sample availability).

Cores undergo immersion in 6% sodium hypochlorite for 3hrs±15min and are then removed, weighed and measured as a zero reading then left to dry for 3hrs±15min. After

[34] BS EN 196-2, See [31]

[35] RICS Guidance Note. (2015). The Mundic Problem, RICS Professional Guidance Note, UK. 3rd edition. London: Royal Institution of Chartered Surveyors (RICS). ISBN 978 1 78321 094 7

[36] CSA A23.1:19/CSA A23.2:19 Concrete materials and methods of concrete construction/Test methods and standard practices for concrete, P3, Pages 370-381, CSA, Canada, ISBN 978-1-4883-0744-7

[37] RICS, The Mundic Problem, See [35]

drying samples are stored above a saturated sodium chloride solution (75 %RH) at 80 °C.

Every week, the cores undergo two immersion periods in the 6% sodium hypochlorite (as specified above) and once a week, after an immersion period, the length, mass and condition of each core are taken and recorded.

After 13 weeks of storage at 80 °C and 75 %RH (P3 Phase 1) between immersions, samples transition to storage above water at 4 °C (P3 Phase 2) and continue the twice-weekly immersions in sodium hypochlorite and once-a-week measurements.

Samples were taken off test if they had disintegrated, lost structural integrity or had lost measuring studs repeatedly in P3 Phase 1. In P3 Phase 2 the same sample deterioration required measurements were stopped but disintegrated samples continued to go through the cycling but in a perforated holding container to permit the possibility of thaumasite formation to occur and allow an equal comparison (where possible).

5 LABORATORY PROGRAM

Table 5-1 Laboratory program assignment

Location	RSK Sample Ref	Petrographic thin section/polished block examination	SEM/EDX	XRD	Compressive strength	Density	Cement content	Total sulfur (Acid digestion)	Total sulfur (HTC)	Acid soluble sulfate content	Water soluble sulfate content	Pyrite/pyrrhotite content	Determination of sulfate	Determination of sulfide	CSA A23.1 P3 Oxidisation	RICS - The Mundic Problem Stage 3 Expansion Testing
7MV	20511/B2	X	X	X	X	X	X	X	X	X	X	X	X	X		XXXX
	20511/B3			X											XXX	
	20511/B4	X	X	X	X	X	X	X	X	X	X	X	X	X		XXXX
	20511/B5			X											XXX	
	20511/C4	X	X	X												XX
	20511/C5			X	X		X	X	X	X	X	X	X		XX	
	20511/C6			X											X	X
	20511/C7	X	X	X	X	X	X	X	X	X	X	X	X	X		XX
	20511/C8														X	X
	20511/C9														XX	XX
21GD	20511/B13	X	X	X	X		X	X	X	X	X	X	X	X		
	20511/B14															XXXX
	20511/B15			X											XXX	
	20511/B16															XXXX
	20511/B17			X	X		X	X	X	X	X	X	X	X	XXX	
	20511/C24	X	X	X												
	20511/C25	X	X	X												XX
	20511/C26			X	X		X	X	X	X	X	X	X	X	XX	
	20511/C27	X	X	X												X
	20511/C28			X	X		X	X	X	X	X	X	X	X	X	
28AW	20511/B8															XXXX
	20511/B9	X	X	X	X		X	X	X	X	X	X	X	X		
	20511/B10			X											XXX	
	20511/B11	X	X	X					X							XXXX
	20511/B12			X	X										XXX	
	20511/C16						X	X		X	X	X	X			
	20511/C18	X	X	X												XX
	20511/C19			X	X		X	X	X	X	X	X	X	X	X	
	20511/C20	X	X													X
	20511/C21			X	X		X	X	X	X	X	X	X	X	X	
	20954/B1														XX	XX
	20954/C3														XXX	
	20954/C4															XX
	20954/C5														X	X
C	20511/B6	X	X	X			X	X	X	X	X	X	X	X	XXX	XXX
	20511/C11				X											
	20511/B7	X	X	X			X	X	X	X	X	X	X	X	XXX	XXX
	20511/C12				X											
	20511/C13								X							
	20511/C14	X	X	X			X	X		X	X	X	X	X		
	20511/C15						X	X		X	X	X	X	X		

X represents tests assigned; multiple X's represent the number of sub-samples assigned.

6 SAMPLE PROCESSING

6.1 Sub-sampling

Sub-sampling was conducted on the samples once they had equilibrated to laboratory conditions whilst protecting the samples from excessive carbonation and drying out.

Blocks were sub-sampled for RICS Stage 3 testing[38] and the residual oxidisation potential CSA test[39] using dry coring techniques. This was conducted to minimise the flow of water through the samples, which could result in additional oxidisation or unrecorded alteration of the as-sampled state. If, however, dry coring failed to retrieve samples due to the extra stress caused by dry coring and poor sample condition a minimal amount of water was employed to facilitate sample retrieval. It was noted that many of the test property blocks were not in a suitable condition for any intact sub-sampling to be conducted. Other sub-sampling was conducted through diamond sawing using the minimum amounts of water or without the use of water.

[38] RICS, The Mundic Problem, See [35]

[39] CSA A23.1/CSA A23.2, Concrete test methods, P3, See [36]

7 RESULT SUMMARIES

To better illustrate the results, condensed summaries are produced in the following section. Full details of the results can be found in **Appendix C**.

7.1 Optical microscopy (OM)

The following section consists of summaries of the petrographic data collected by OM.

7.1.1 Constituent properties

Table 7-1 Constituents and void contents

Property	7MV				21GD				28AW				C (Control)		
Element	IL	OL	RW	F	IL	OL	RW	F	IL	OL	RW	F	IL	OL	F
Aggregate Type (REF)	All-in Phyllite (PHY)				All-in Phyllite (PHY)				All-in Phyllite (PHY)				All-in Sandstone (SST)		
Cement type	Portland-type cement														
Void content % (estimated)	15-20	10-20	10-15	0.5	20-25	10-20	10-15	1.5	15-20	20-25	10-15	2-3	15-25	15-20	5-8
Void content % (measured)	18.9	11.7	14.4	1.5	22.7	15.7	13.5	0.9	19.9	21.2	12.6	2.4	20.8	19.4	10.4

7.1.2 Quantitative compositional mix proportions

Figure 7-1 Quantitative compositional mix proportions

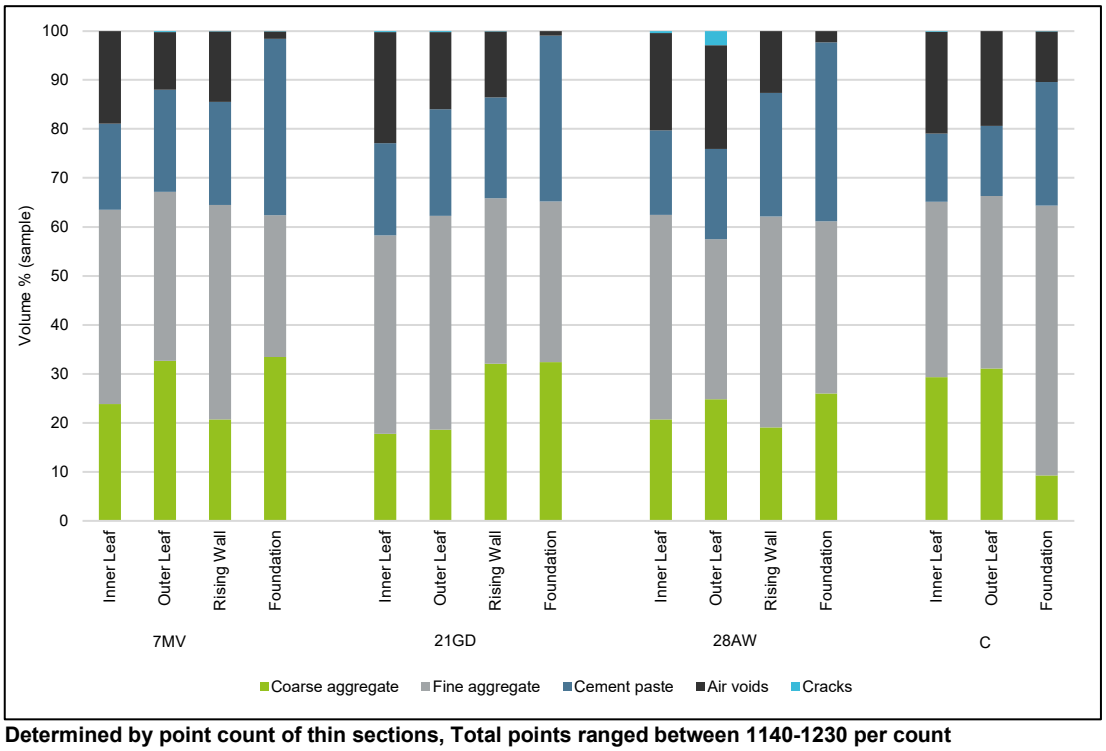

Determined by point count of thin sections, Total points ranged between 1140-1230 per count

Figure 7-2 Scanned images of polished slices – Inner leaf

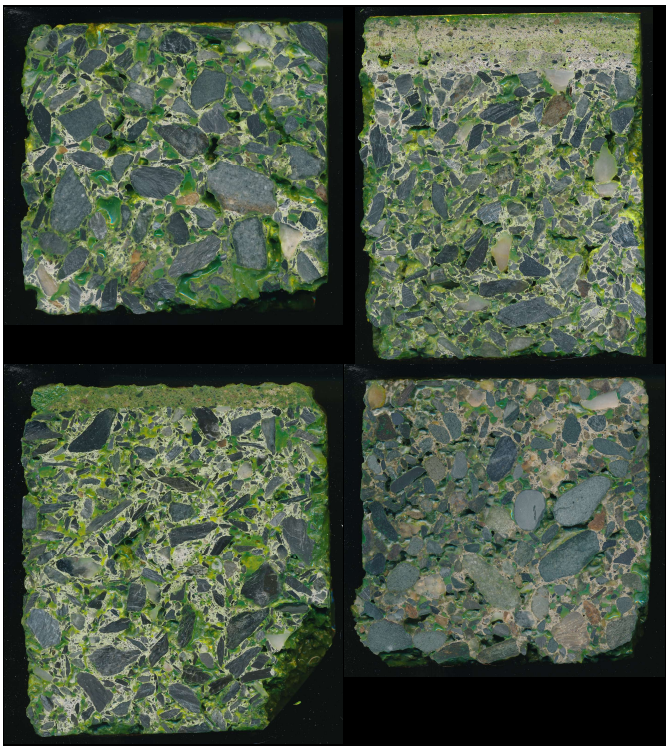

Upper left to bottom right – 7 MV, 21 GD, 28 AW, C, Traces of mortar can be seen on 21GD and 28AW samples.

Figure 7-3 Scanned images of polished slices – Outer leaf

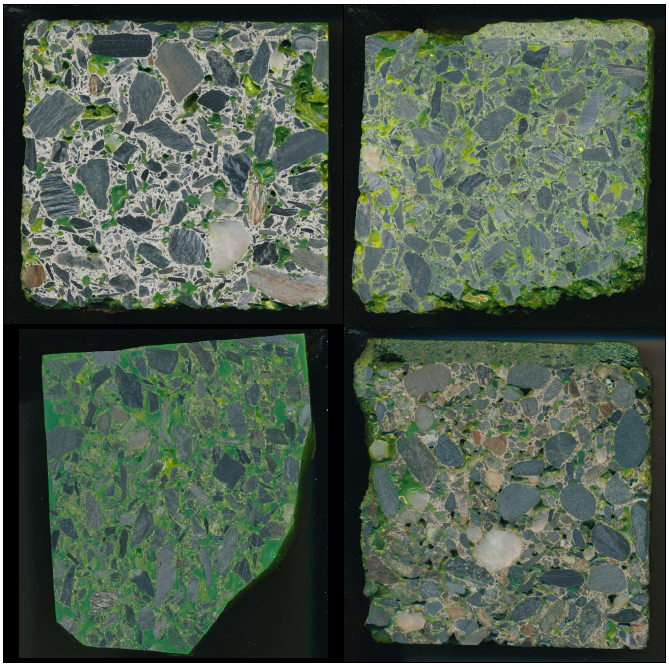

Upper left to bottom right – 7MV, 21GD, 28AW, C. Traces of mortar can be seen on 21GD and C samples.

Figure 7-4 Scanned images of polished slices – Rising wall

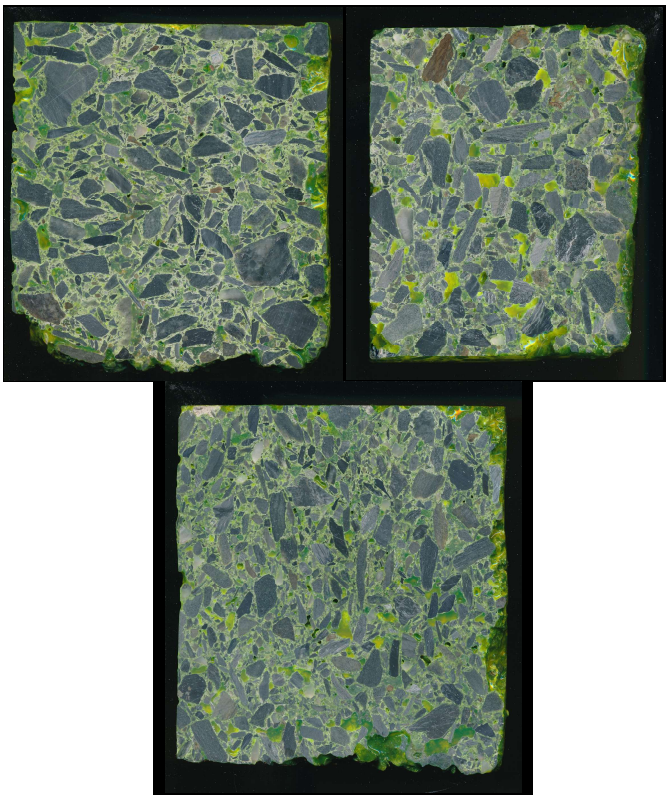

Upper left to bottom right – 7MV, 21GD, 28AW

Figure 7-5 Scanned images of polished slices – Foundation

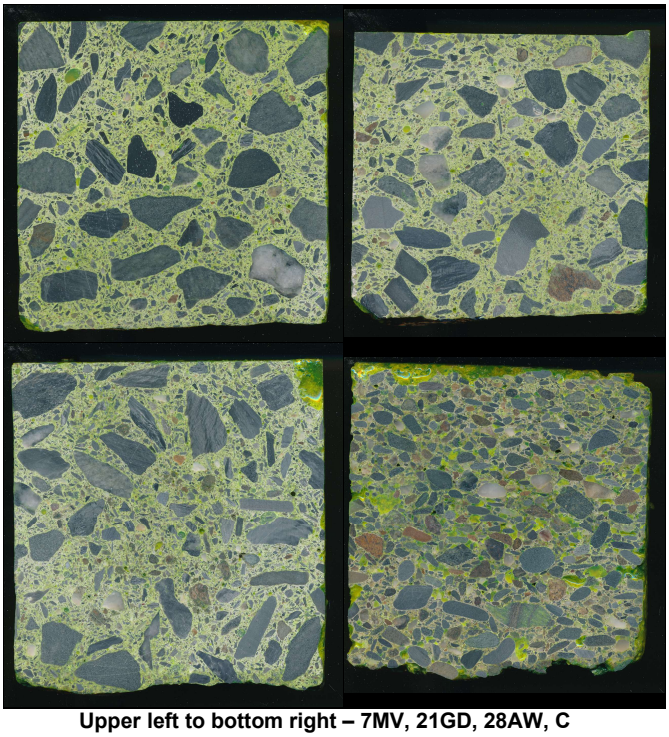

Upper left to bottom right – 7MV, 21GD, 28AW, C

7.1.3 Sulfides

Table 7-2 OM sulfide abundance

Property		7MV	21GD	28AW	C (Control)
Aggregate		PHY			SST
Pyrrhotite	Aggregate	XXX			X
	Matrix	XXX			X
Pyrite	Aggregate	XX			XX
	Matrix	XX			X
Chalcopyrite	Aggregate	X			-
	Matrix	X			-

X denotes relative abundances – XXX high abundance, XX moderate abundance, X lower abundance, - absent. Most common sulfides included only, excluded pentlandite and other rare trace minerals.

7.1.4 Deposits observed

Table 7-3 OM deposits observed

Property	7MV				21GD				28AW				C (Control)		
Element	I	O	R	F	I	O	R	F	I	O	R	F	I	O	F
Iron oxide/hydroxide	xx	xx	xx	xx	xxx	xx	xx	x	xx	xxx	xx	x	xx	xx	xx
Secondary Ettringite	x	x	x	-	xx	x	x	x	x	xx	xx	-	-	-	xx
Secondary Calcite	-	x	-	-	x	-	xx	x	-	-	-	-	-	-	-
Secondary Gypsum	-	-	x	-	-	-	x	x	-	-	x	xx	-	-	-
Thaumasite	-	-	x	-	xx	xx	-	-	-	-	-	-	-	-	-
Silicate Gel (remnant paste)	-	-	-	-	-	-	-	x	-	-	-	-	-	-	-
Other	-	-	-	-	-	xx	x	-	-	-	-	-	-	-	-

x denotes relative abundances – xxx high abundance, xx moderate abundance, x lower abundance, - absent. Other deposits included secondary portlandite and other deposits

7.1.5 Photomicrographs

Figure 7-6 Photomicrographs – Outer Leaf – Test property 7MV

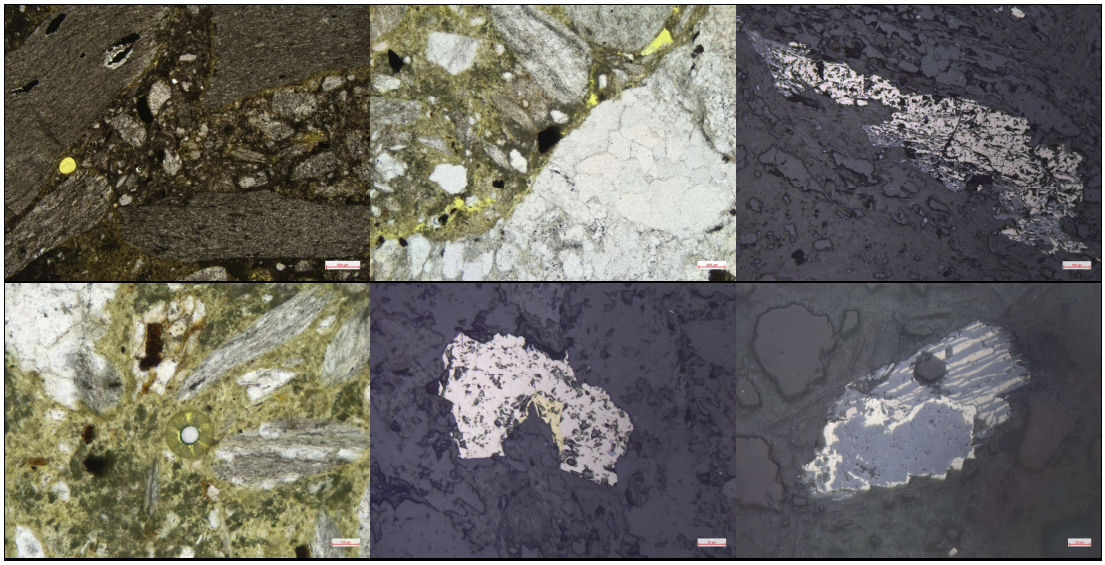

Outer leaf 7MV, 20511 B4 – 1st Row Left (CPL) – Showing phyllite aggregate containing pyrite and pyrrhotite. 1st Row Centre (PPL) – Showing Quartzite and phyllite aggregate particles with discrete pyrrhotite and pyrite fine aggregate particles set within the patchy high microporosity cement matrix. 1st Row Right (RL) – Striped oxidisation of pyrrhotite within an aggregate particle. 2nd Row Left, (PPL) – Secondary ettringite deposits within an air void (centre) set in an area of weak cement matrix. Note the traces of oxidisation of pyrrhotite (black/brown). 2nd Row Centre (RL) – Aggregate-set fresh pyrrhotite, chalcopyrite and pyrite. 2nd Row Right (RL) – Striped pyrrhotite oxidisation and pyrite rim within the same matrix-set fine aggregate particle.

Figure 7-7 Photomicrographs – Outer Leaf – Test property 21GD

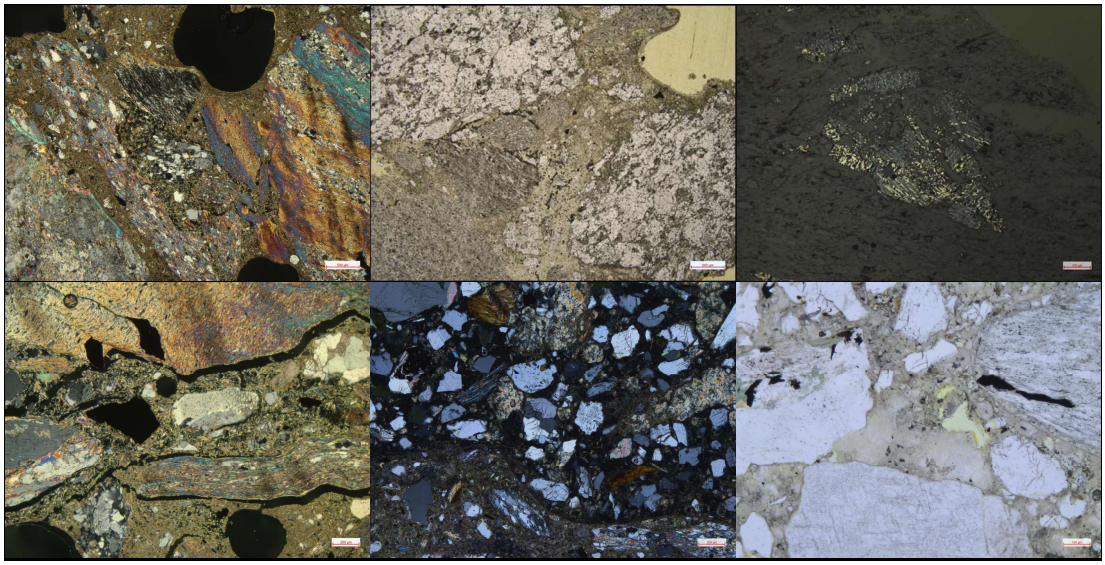

Outer Leaf 21GD, 20511/C24 – 1st Row Left (CPL) – Phyllite aggregate within the cement matrix with relatively high pyrrhotite content. 1st Row Centre (PPL) – Phyllite and quartzite aggregate particles with partially depleted cement matrix. 1st Row Right (RL) – Nearly completely oxidised fragmented pyrrhotite aggregate particles set within fractured cement matrix. 2nd Row Left (CPL) – Highly fractured concrete block and weak cement matrix, with oxidisation of aggregate set pyrrhotite. 2nd Row Centre (CPL) and Right (PPL) – Views of mortar directly adjacent to the concrete block showing extensive thaumasite formation.

Figure 7-8 Photomicrographs – Outer Leaf – Test property 28AW

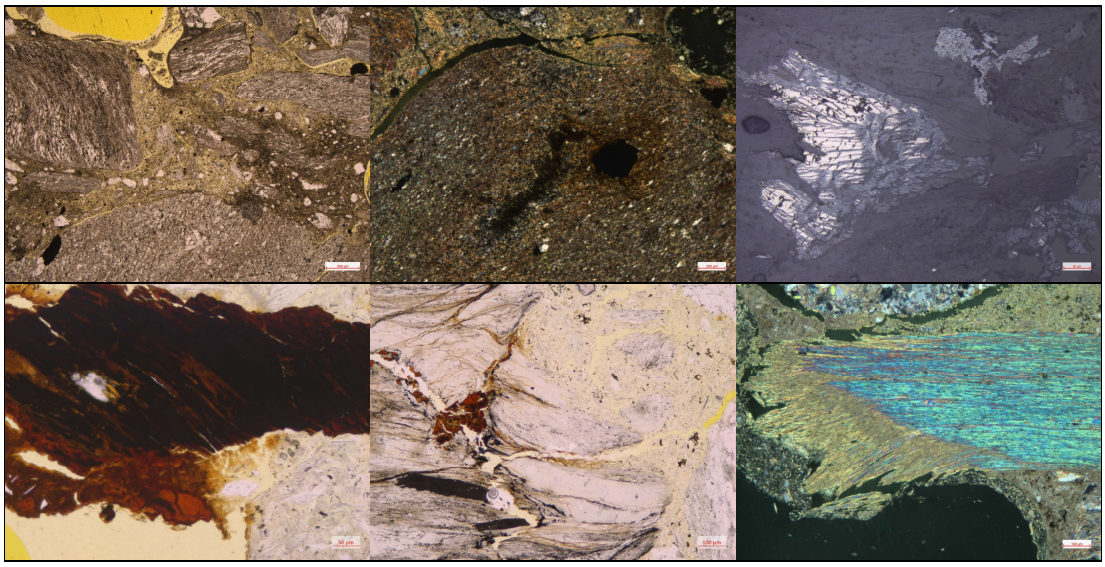

Outer Leaf 28AW, 20511/B11 – 1st Row Left (PPL) – Phyllite aggregate within the pale yellowish-grey weak, cracked cement matrix. 1st Row Centre (CPL) – Phyllite aggregate particle with oxidised pyrrhotite with associated staining (of aggregate) and associated cracking of the surrounding cement matrix. 1st Row Right (RL) – Significantly oxidised fragmented pyrrhotite within a fractured phyllite aggregate particle. 2nd Row Left (PPL) – Striped oxidised pyrrhotite particle with pale brown matrix beneath converted by *in situ* internal sulfate attack. 2nd Row Centre (PPL) – Fractured phyllite particle caused by oxidisation of pyrrhotite (brown). 2nd Row Right (CPL) – Phyllite aggregate particle showing splitting along cleavage planes, resulting in a poor bond with the surrounding cement matrix.

Figure 7-9 Photomicrographs – Outer Leaf – Control property C

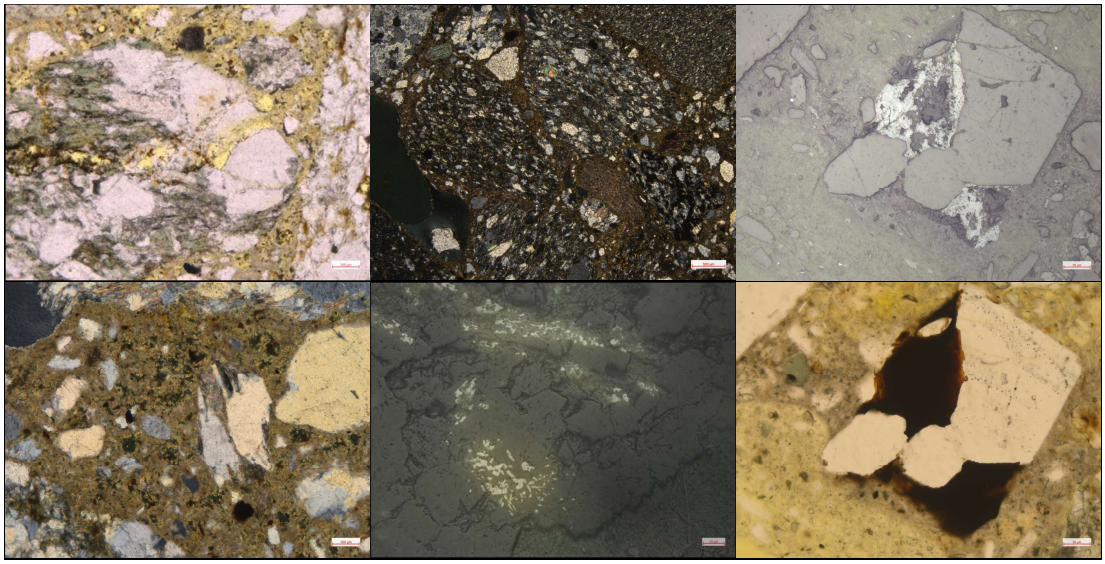

Outer Leaf C, 20511/B7 – 1st Row Left (PPL) – Internally cracked sandstone particle, note the cracking does not run into the nearly complete carbonated cement matrix. 1st Row Centre (CPL) – Sandstone and Siltstone aggregate and rare phyllite aggregate particles set within cement matrix. 1st Row Right (RL) – Partially *in situ* oxidised pyrite showing slight staining (darkening) of the surrounding cement matrix. 2nd Row Left (CPL) – Highly carbonated cement matrix with quartz fine aggregate particles. 2nd Row Centre (RL) – Sulfide minerals oxidised before use in concrete with no associated deposits or deterioration. 2nd Row Right (PPL) – View of the image directly above.

Figure 7-10 Photomicrographs – Inner Leaf – Test property 7MV

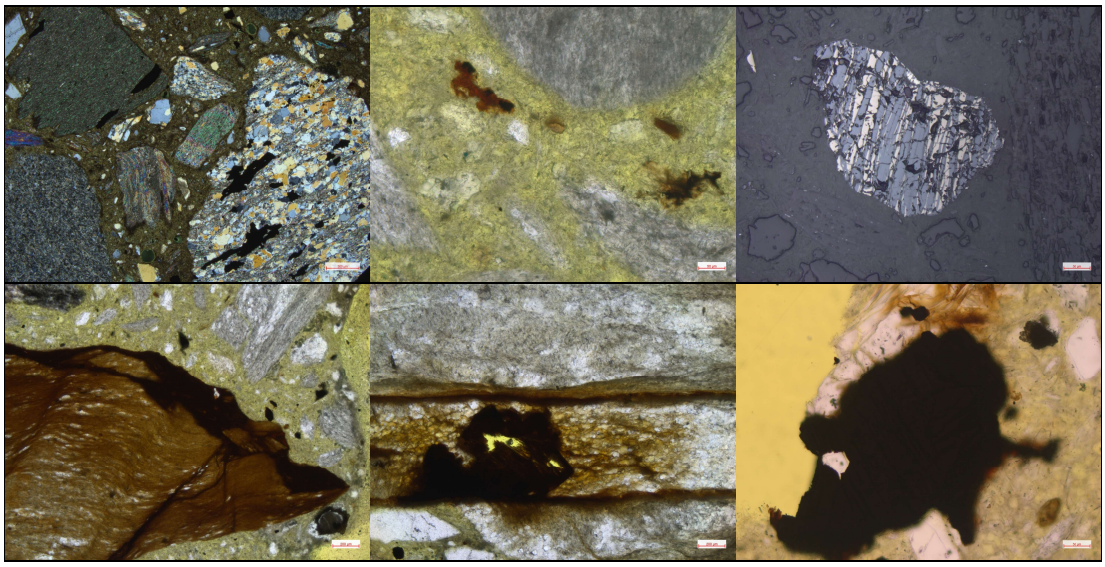

Inner Leaf 7MV, 20511/B2 – 1st Row Left (CPL) – Showing phyllite and quartzite aggregate containing pyrite and pyrrhotite. 1st Row Centre (PPL) – oxidisation of pyrrhotite set within the highly microporous cement matrix. 1st Row Right (RL) – Striped oxidisation of pyrrhotite set within the matrix. 2nd Row Left, (PPL) – Pre-existing oxidisation of iron sulfides within phyllite aggregate particle. 2nd Row Centre (PPL) – oxidisation of iron sulfides within phyllite aggregate particles exploiting veining/cleavage. 2nd Row Right (PPL) – evidence of limited *in situ* oxidisation of pyrrhotite within the cement matrix.

Figure 7-11 Photomicrographs – Inner Leaf – Test property 21GD

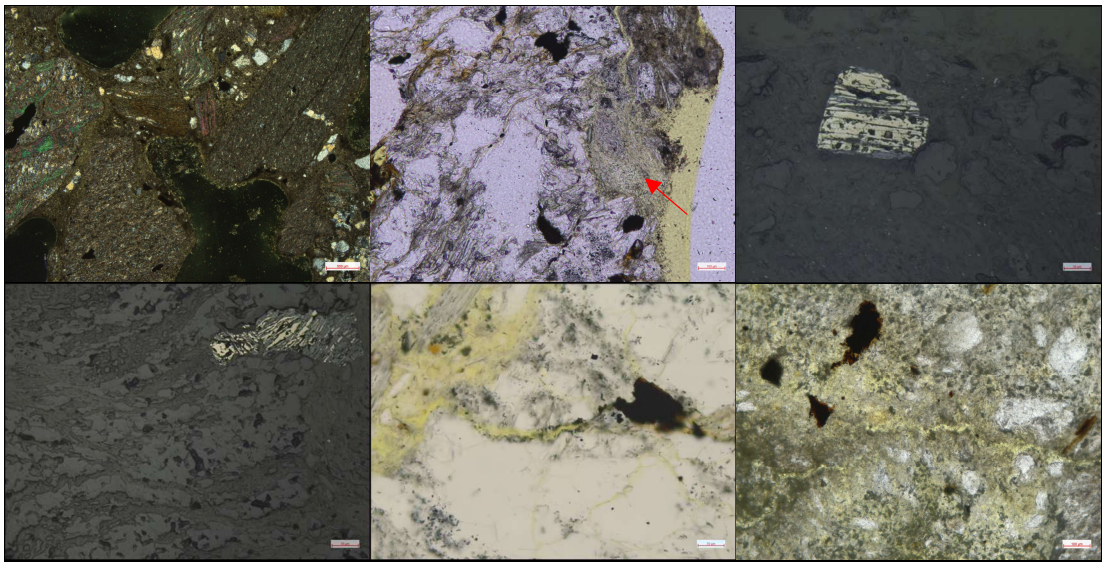

Inner leaf 21GD, 20511/B13 – 1st Row Left (CPL) – Phyllite aggregate with relatively high pyrrhotite content. 1st Row Centre (PPL) –Quartzite aggregate particle with adjacent possible thaumasite replacing cement matrix (red arrow). 1st Row Right (RL) – Striped *in situ* pyrrhotite oxidisation of matrix set aggregate particle. 2nd Row Left (RL) – Striped *in situ* pyrrhotite oxidisation of aggregate set pyrrhotite. Note that where the pyrrhotite is exposed to the cement matrix (far right) the degree of oxidisation is higher. 2nd Row Centre (CPL) – Crack running from oxidised pyrrhotite within phyllite through aggregate into the cement matrix. 2nd Row Right (PPL Hybrid) – *In situ* oxidisation of sulfides within the cracked cement matrix, which appeared to show very fine secondary sulfate formation.

Figure 7-12 Photomicrographs – Inner Leaf – Test property 28AW

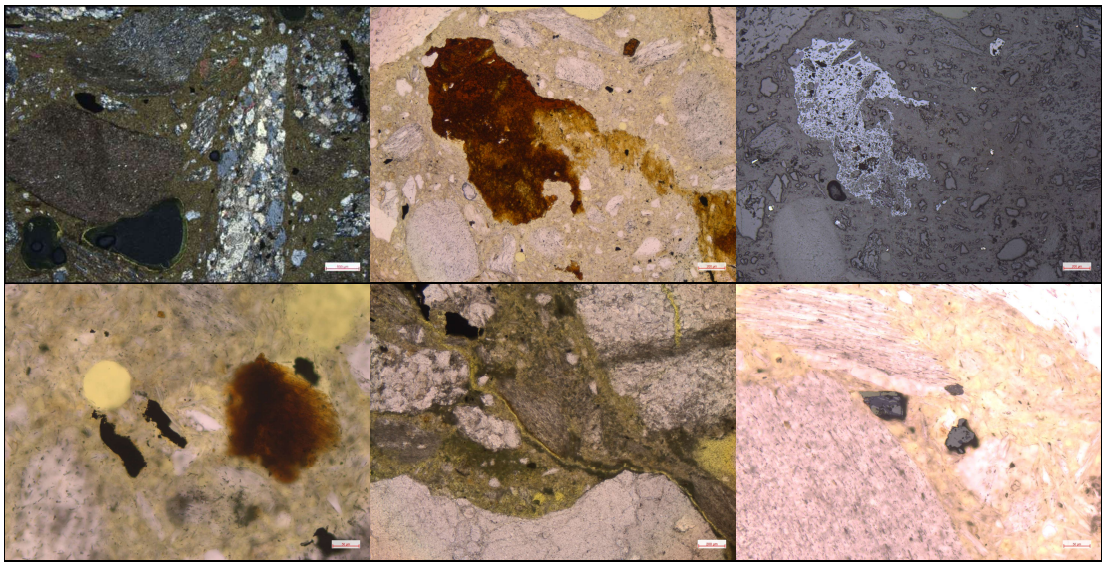

Inner leaf 28AW, 20511/B9 – 1st Row Left (CPL) – Phyllite and quartzite aggregate set within a weak cement matrix. 1st Row Centre (PPL) – Significant oxidisation of a matrix-set pyrrhotite aggregate particle and associated staining/conversion of the surrounding cement matrix. 1st Row Right (RL) – Same view as 1st row centre, significantly oxidised fragmented pyrrhotite aggregate particle. 2nd Row Left (PPL) – Contrast in oxidisation of pyrite-coated grains (black, two, centre left), Pyrrhotite (brown stain) and chalcopyrite (black, above pyrrhotite). 2nd Row Centre (PPL) –Weak, cracked cement matrix. 2nd Row Right (RL/PPL Hybrid) – *In situ* oxidisation of discrete pyrrhotite particles within the matrix. Black rim (oxides within the matrix).

Figure 7-13 Photomicrographs – Inner Leaf – Control property C

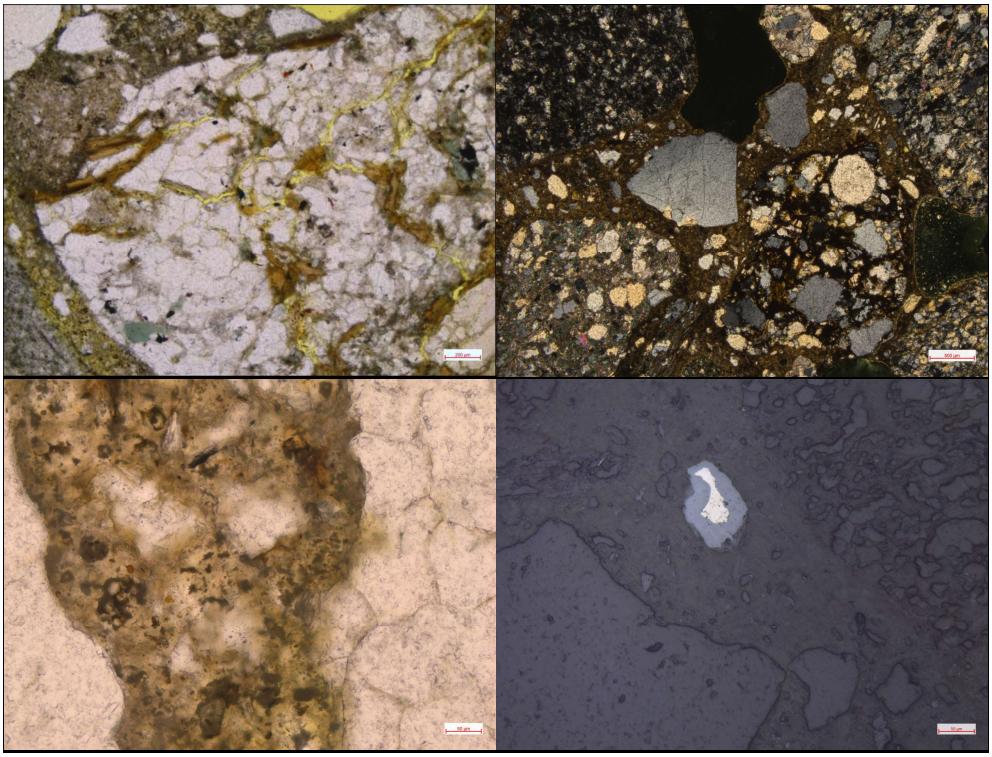

Inner Leaf – C, 20511/B6 – 1st Row Left (PPL) – Showing sandstone/quartzite aggregate containing internal fracturing and iron sulfides, 1st Row Right (CPL) – Sandstone/quartzite aggregate set in cement matrix with large voids. 2nd Row Left (PPL) and 2nd Row Right (RL) – evidence of limited oxidisation of pyrite within the cement matrix.

Figure 7-14 Photomicrographs – Rising Wall – Test property 7MV

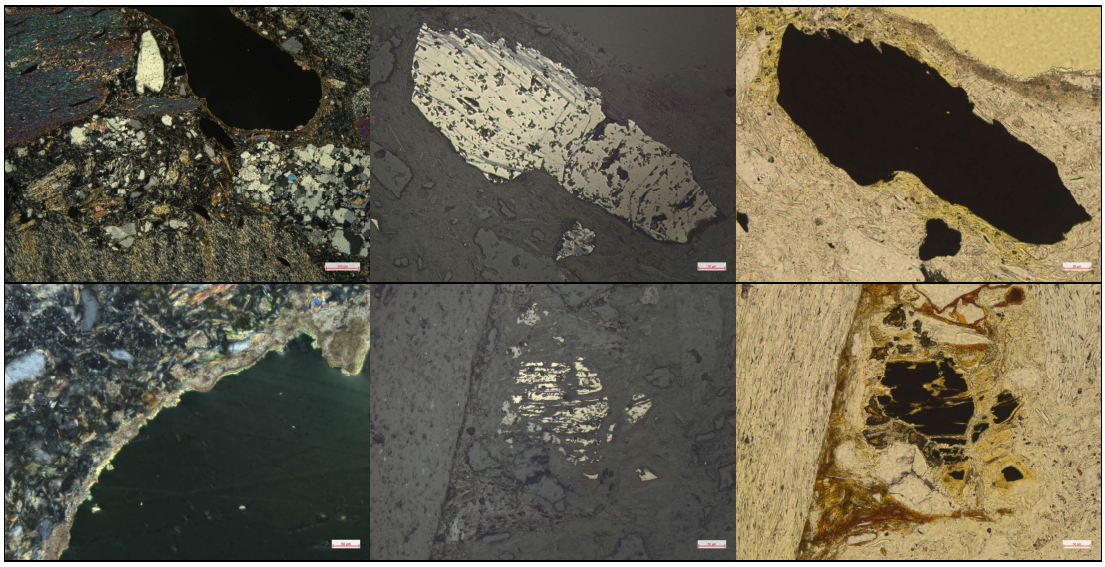

Rising Wall 7MV, 20511/C4 – 1st Row Left (CPL) – Phyllite and quartzite aggregate set within a cement matrix. 1st Row Centre (RL) –Limited striped oxidisation of a matrix-set pyrrhotite aggregate particle. 1st Row Right (PPL) – Same view as 1st row centre, showing weak cement matrix around sulfide particle. 2nd Row Left (CPL) – Secondary calcite lining an air void. 2nd Row Centre (RL) – *In situ* partially striped oxidised and cracked matrix-set pyrrhotite grain surrounded by converted/stained cement matrix. 2nd Row Right (PPL) – Same view as 2nd Row Centre, staining and matrix conversion are more apparent.

Figure 7-15 Photomicrographs – Rising Wall – Test property 21GD

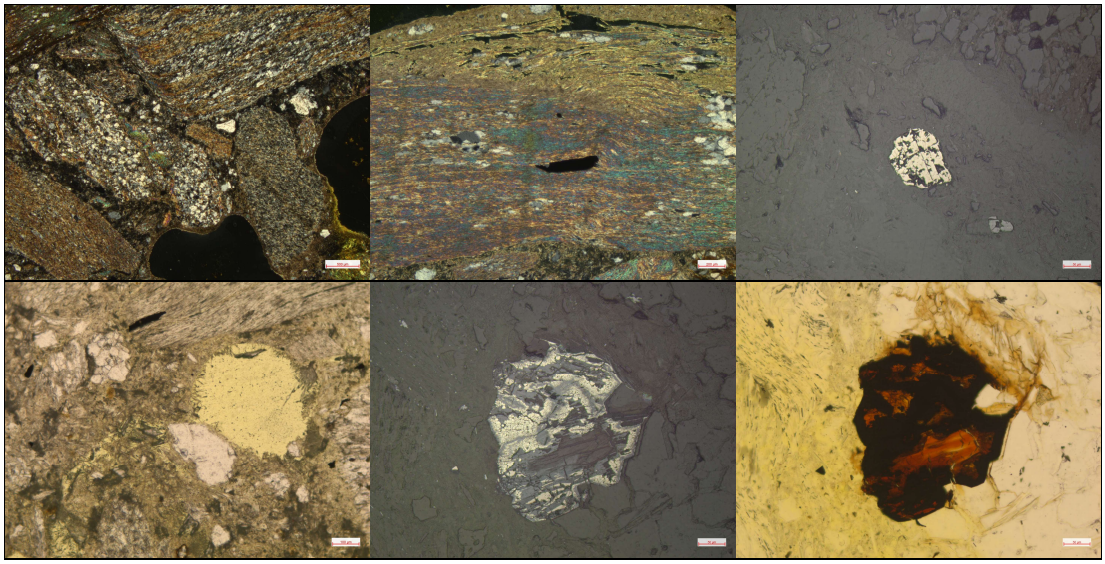

Rising Wall 21GD, 20511/C25 – 1st Row Left (CPL) – Phyllite and quartzite aggregate set within cement matrix. 1st Row Centre (CPL) – Flaking phyllite aggregate particle showing poor bond to the cement matrix. 1st Row Right (RL) – Unoxidised (fresh) matrix-set pyrrhotite aggregate particle. 2nd Row Left (PPL) – Cracking in the cement matrix and associated secondary ettringite deposits (fibrous). 2nd Row Centre (RL) – Partially oxidised aggregate-set (but on outer rim) pyrrhotite grain showing an odd pattern of oxidisation. 2nd Row Right (PPL) – Same view as 2nd Row Centre showing only limited iron staining of the cement matrix and more extensive iron oxide/hydroxide staining of the aggregate particle.

Figure 7-16 Photomicrographs – Rising Wall – Test property 28AW

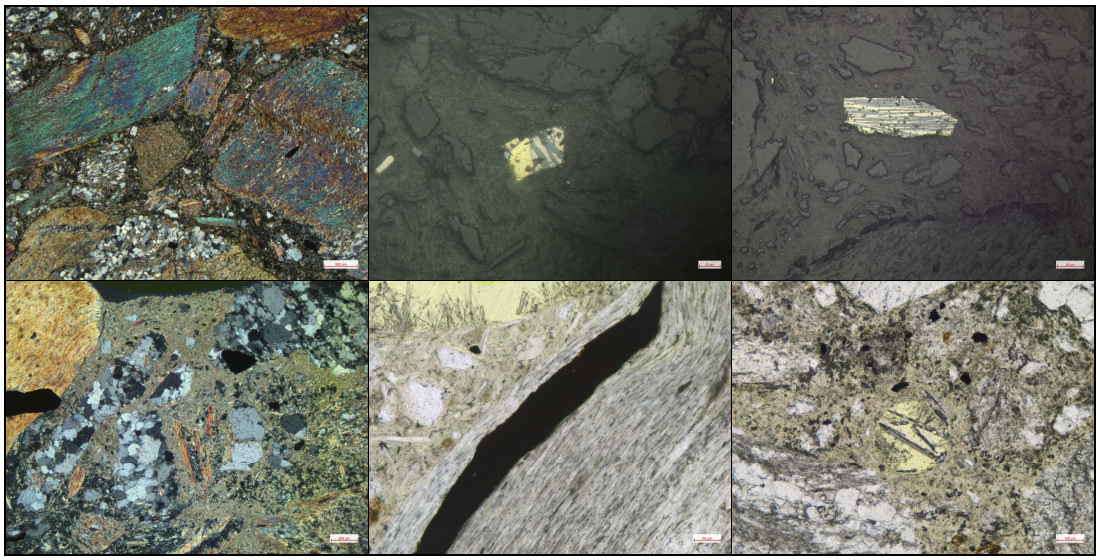

Rising Wall 28AW, 20511/C18 – 1st Row Left (CPL) – Phyllite and quartzite aggregate set in cement matrix. 1st Row Centre (RL) – Chalcopyrite and striped oxidised pyrrhotite matrix-set grain. 1st Row Right (RL) – Striped oxidisation of aggregate-set pyrrhotite grain. 2nd Row Left (CPL) – Carbonated cement matrix at the outer surface. 2nd Row Centre (PPL) – elongate pyrrhotite and chalcopyrite grain set within a phyllite particle. 2nd Row Right (PPL) – Air void exhibiting secondary gypsum, set within a mica-rich cement matrix.

Figure 7-17 Photomicrographs – Foundation – Test property 7MV

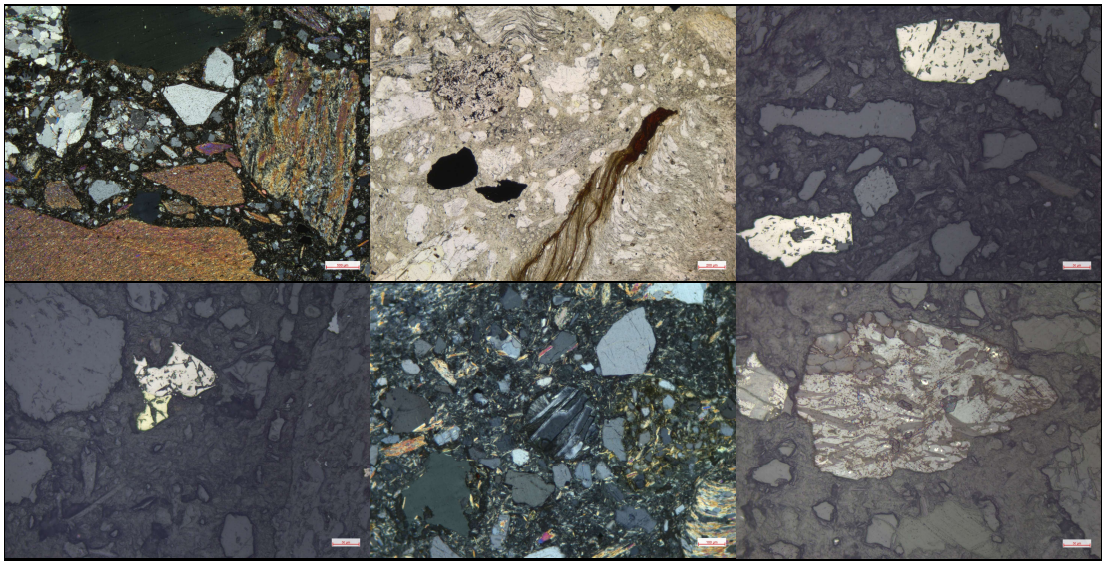

Foundation 7MV, 20511/C7 – 1st Row Left (CPL) – Phyllite and quartzite aggregate set within a cement matrix. 1st Row Centre (RL) – Oxidisation of a matrix-set pyrrhotite particle with iron-rich staining along cleavage planes of the phyllite but not running into the cement matrix (pre-existing). 1st Row Right (RL) –Fresh non-oxidised pyrrhotite (white/very pale brown) matrix-set aggregate particles. 2nd Row Left (RL) – Chiefly fresh chalcopyrite and pyrrhotite matrix-set aggregate grain. 2nd Row Centre (CPL) – An air void infilled with secondary gypsum (centre). 2nd Row Right (RL) – Partially oxidised sulfide grain primarily composed of pyrrhotite and iron oxide/hydroxides.

Figure 7-18 Photomicrographs – Foundation – Test property 21GD

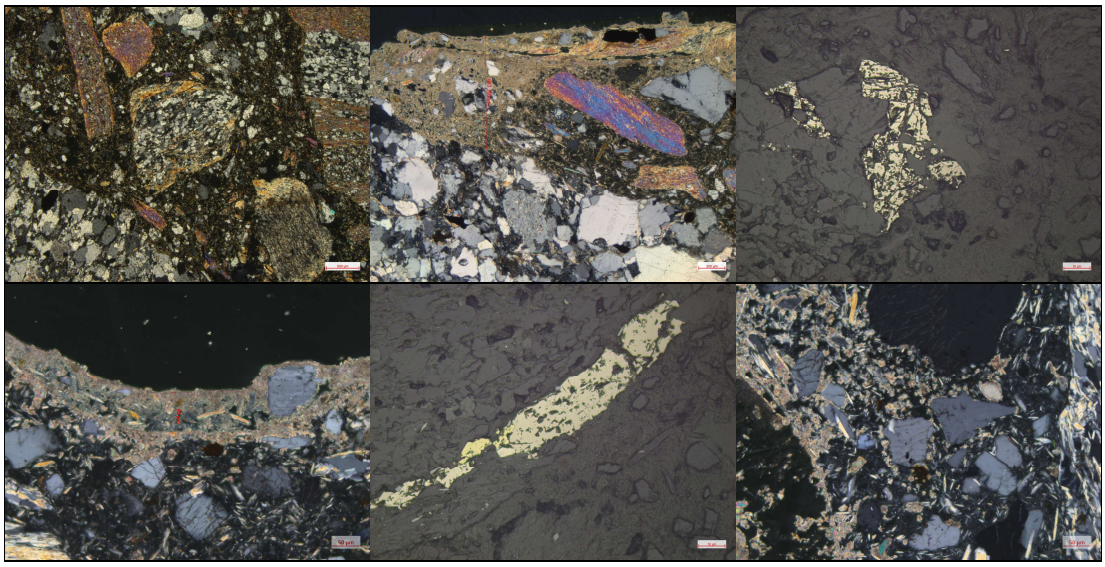

Foundation 21GD, 20511/C27 – 1st Row Left (CPL) – Phyllite and quartzite aggregate set within cement matrix. 1st Row Centre (CPL) – Flaking phyllite aggregate particle showing internal cracking/delamination void running out into the cement matrix and to the outer surface (top). 1st Row Right (RL) – Traces of striped pyrrhotite oxidisation in aggregate-set pyrrhotite aggregate particle. 2nd Row Left (PPL) – Rare traces of secondary calcite, ettringite and gypsum within a crust at the edge of an air void associated with minor depletion of the adjacent cement matrix. 2nd Row Centre (RL) – Chiefly fresh pyrrhotite and chalcopyrite aggregate-set grain with only traces of surface oxidisation. 2nd Row Right (PPL) – Isolated trace of secondary carbonation (pale pink rosettes) of the cement matrix associated with acidic solution interaction with the cement matrix.

Figure 7-19 Photomicrographs – Foundation – Test property 28AW

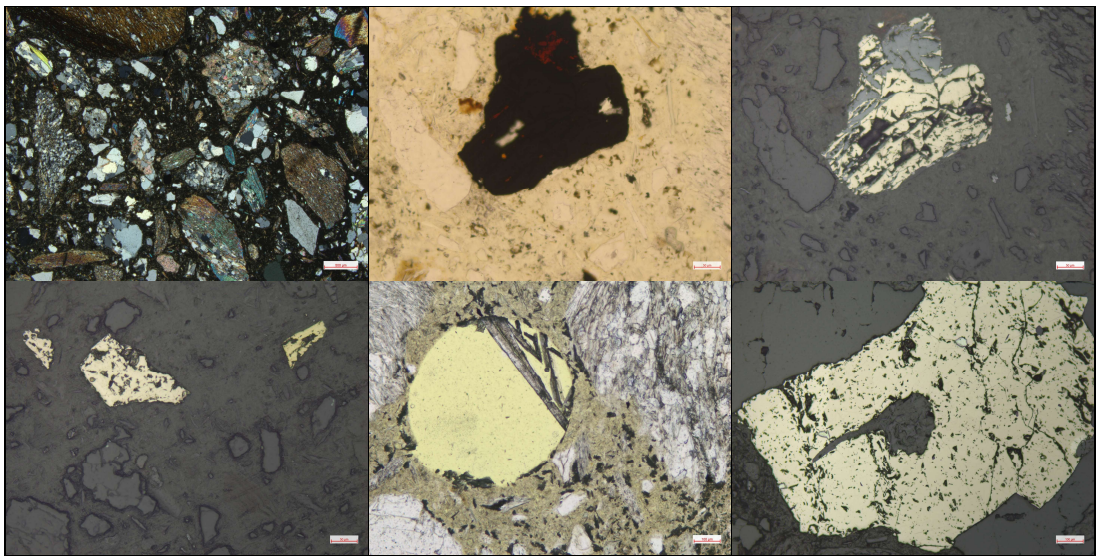

Foundation 28AW, 20511/C20 – 1st Row Left (CPL) – Phyllite, quartzite and meta-sandstone aggregate set in the cement matrix. 1st Row Centre (PPL) – Striped oxidised pyrrhotite matrix-set grain with evidence of some *in situ* oxidisation. 1st Row Right (RL) – Same image as 1st Row Centre, striped oxidisation of aggregate-set pyrrhotite grain exhibiting some inclusions. 2nd Row Left (RL) – Chiefly fresh pyrrhotite and chalcopyrite (right) matrix-set grains. 2nd Row Centre (PPL) – Secondary gypsum (white) bridging air void (yellow). 2nd Row Right (PPL) – Coarse, aggregate-set, fresh pyrrhotite grain with minor inclusions of pyrite and other minerals.

Figure 7-20 Photomicrographs – Foundation – Control property C

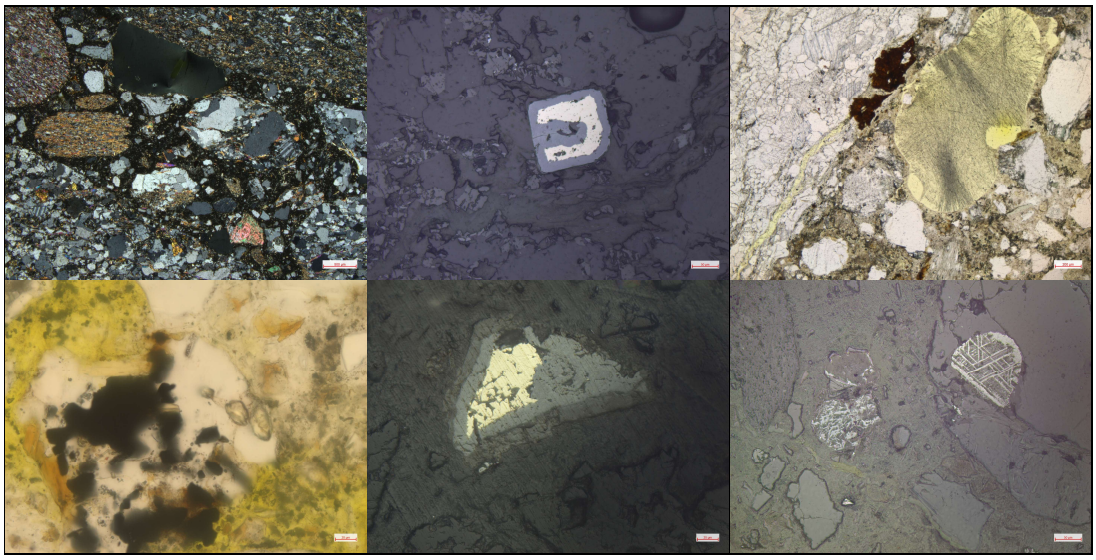

Foundation – C, 20511/C14 – 1st Row Left (CPL) – Sandstone/quartzite and rare phyllite aggregate particles set within the cement matrix. 1st Row Centre (RL) surface oxidised pyrite (no evidence of *in situ* oxidisation). 1st Row Right (PPL) – Sandstone/quartzite aggregate particle with oxidised pyrrhotite and associated cracking. The air void (yellow) is infilled with secondary ettringite. 2nd Row Left (PPL) – Highly magnified view of the weak, low cement, high microporosity cement matrix (yellow) and aggregate particle showing trace *in situ* oxidisation of pyrite. 2nd Row Centre (RL) – Matrix-set pyrite grain that exhibits surface oxidisation but that was not associated with staining or cracking of the cement matrix. 2nd Row Right (RL) – Pre-existing partial oxidisation of pyrrhotite (left) and other metallic minerals with complex intergrowths, set within an aggregate particle (right).

Figure 7-21 Photomicrographs – Microporosity

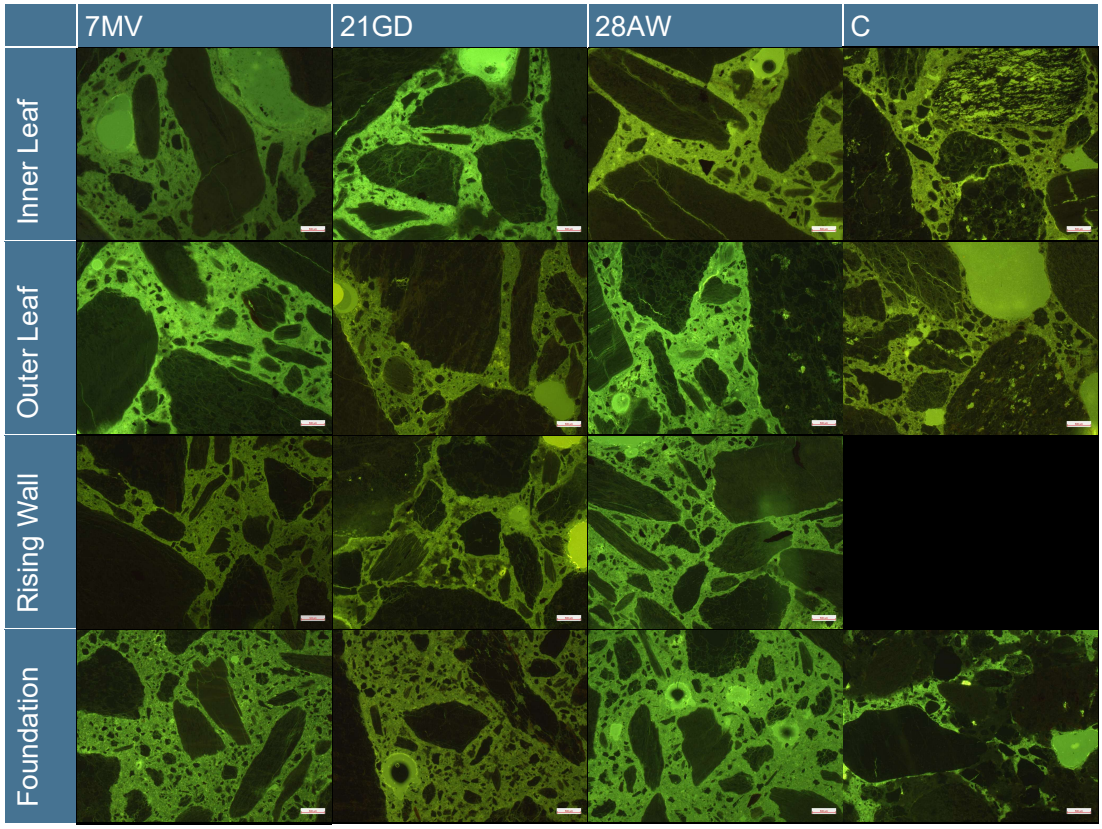

Relative microporosity photomicrographs, 2.5x objective, 250 ms exposure, reflected UV light, fluorescent resin.

Table 7-4 Petrographic summary table

Location	7MV				21GD				28AW				C		
RSK Sample ref.	20511/B2	20511/B4	20511/C4	20511/C7	20511/B13	20511/C24	20511/C25	20511/C27	20511/B9	20511/B11	20511/C18	20511/C20	20511/B6	20511/B7	20511/C14
Client sample ref.	1B	2A	3B	4B	1A	3J	4D	5B	1E	2A	3B	4A	1A	2B	4A
Sample type	Block	Block	Core	Core	Block	Core	Core	Core	Block	Block	Core	Core	Block	Block	Core
Element	Inner Leaf	Outer Leaf	Rising Wall	Foundation	Inner Leaf	Outer Leaf	Rising Wall	Foundation	Inner Leaf	Outer Leaf	Rising Wall	Foundation	Inner Leaf	Outer Leaf	Foundation
Client area location	Interior, Gable End	Exterior, Front Facing, West	Exterior, Front Facing, West	Exterior, Front Facing, West	Interior, Gable End	Exterior, Gable End	Exterior, Gable End	Exterior, Gable End	Interior, Gable End	Exterior, Gable End	Exterior, Gable End	Exterior, Gable End	Interior	Exterior, Front Facing	Exterior, Gable End
Mica															
Visible evidence of deterioration of the concrete blocks	Sound but potentially susceptible	Sound but potentially susceptible	Sound but potentially susceptible	Sound	Sound but potentially susceptible	Unsound	Sound but potentially susceptible	Sound but potentially susceptible	Sound but potentially susceptible or unsound	Unsound	Sound but potentially susceptible	Sound but potentially susceptible	Sound	Sound	Sound
Presence of "free muscovite mica"	Common	Numerous	Numerous	Numerous	Common	Numerous	Numerous	Numerous	Numerous	Numerous	Numerous	Numerous	Rare	Common	Rare
Evidence of moisture ingress	Common	Common	Numerous	Numerous	Common	Common	Abundant	Abundant	Numerous	Abundant	Abundant	Abundant	Rare	Common	Abundant
Microcracking	Rare	Rare	Few	Rare	Few	Common	Rare	Rare	Rare	Numerous	Rare	Rare	Rare	Rare	Rare
Degradation/Weakening of cement matrix (evidence of leaching of cement hydrates)	Common	Common	Rare	Rare	Common	Common	Common	Common	Very Common	Common	Rare	Rare	Rare	Rare	Rare
Relative microporosity	High	Excessive	High	High	High	High	High	High	Excessive	Excessive	High	High	High	High	Moderate
Sulfides															
Visible evidence of deterioration or degradation of the concrete blocks/aggregate	Sound but potentially susceptible	Sound but potentially susceptible	Sound but potentially susceptible	Sound but potentially susceptible	Sound but potentially susceptible	Unsound	Sound but potentially susceptible	Sound but potentially susceptible	Sound but potentially susceptible or unsound	Unsound	Sound but potentially susceptible	Sound but potentially susceptible	Sound	Sound	Sound
Presence of problematic lithologies*	Major	Major	Major	Major	Major	Major	Major	Major	Major	Major	Major	Major	Trace/minor	Trace/Minor	Trace/Minor
Presence of gypsum or secondary sulfates	Few	Few	Rare	Few	Rare	Numerous	Few	Few	Rare	Few	Few	Few	Absent	Absent	Few
Presence of reactive forms of sulfide (chiefly pyrrhotite)	Numerous	Numerous	Numerous	Numerous	Numerous	Numerous	Numerous	Numerous	Numerous	Numerous	Numerous	Numerous	Rare	Few	Few
Cracking/ microcracking	Few	Few	Few	Rare	Few	Numerous	Rare	Rare	Numerous	Numerous	Few	Few	Rare	Rare	Rare
Degradation/Weakening of cement matrix (evidence of leaching of cement hydrates)	Common	Common	Rare	Rare	Common	Common	Common	Common	Very common	Common	Rare	Rare	Rare	Rare	Very Rare
MICA - Overall	**High**	**Critical**	**High**	**High**	**High**	**Critical**	**High**	**High**	**Critical**	**Critical**	**High**	**High**	**High**	**High**	**High**
SULFIDES - Overall	**Critical**	**Critical**	**Critical**	**Critical**	**Critical**	**Critical**	**Critical**	**Critical**	**Critical**	**Critical**	**Critical**	**Critical**	**Low/medium**	**Low/medium**	**Low/medium**
SULFIDES – Excluding common Risk factors (*)	**High**	**High**	**Low/medium**	**Low/medium**	**High**	**Critical**	**High**	**High**	**Critical**	**Critical**	**Low/medium**	**Low/medium**	**Low/medium**	**Low/medium**	**Low/medium**
Key	Negligible	Low/Medium	High	Critical	**Petrographically assessed against criteria from I.S. 465:2018+A1:2020 Table 3 (mica) and Table 5 (pyrite or other sulfides).[40] *Related to common geological factors**										

[40] I.S. 465:2018+A1:2020, See [2]

7.2 SEM/EDX

7.2.1 Phase maps

For detailed methodology please see **4.2**.

Figure 7-22 SEM/EDX phase maps

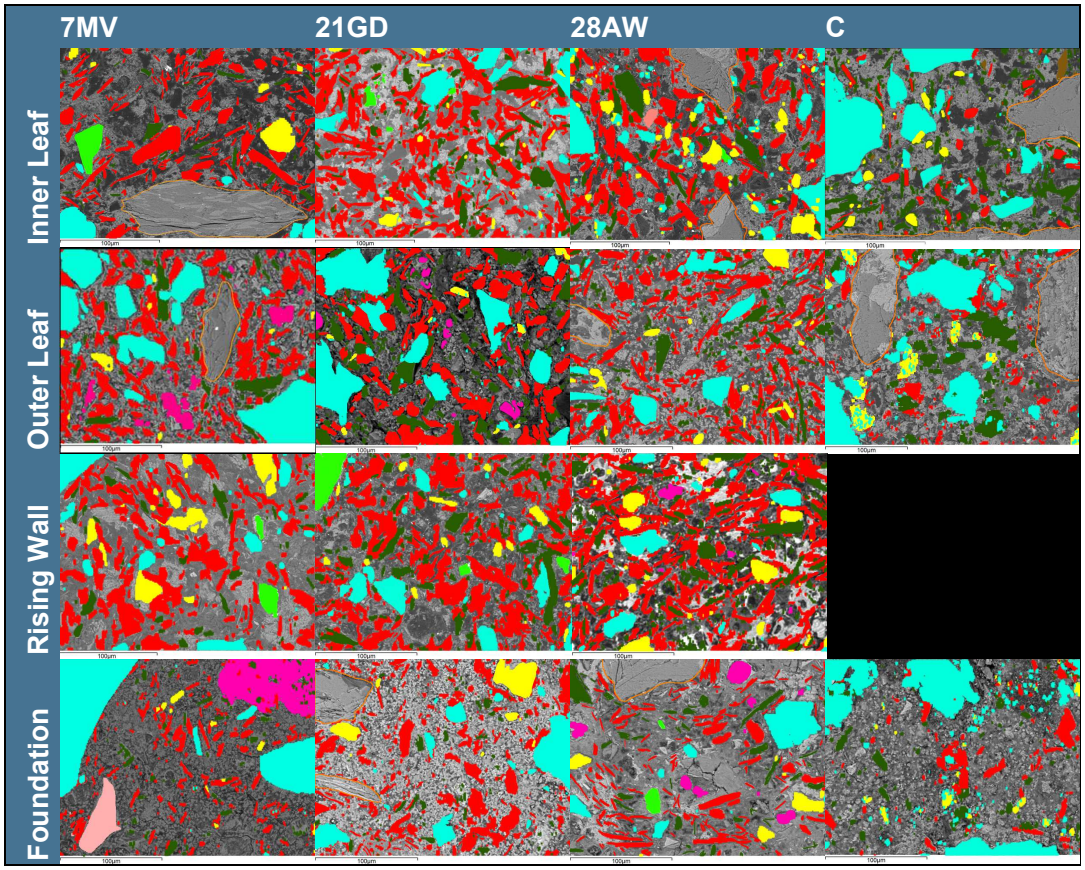

Muscovite mica (red), chlorite (dark green), quartz (light blue), feldspar (yellow), calcite (pale pink), sulfate (magenta), iron oxide (brown) and sulfide (bright green). The orange outline indicates micaceous aggregate particles eliminated from the calculation. Phase maps are set on BSE Images. Only one of three AOIs is presented here for each element.

7.2.2 'Free' muscovite mica analysis

'Free' muscovite mica content was calculated in accordance with I.S. 465:2018+A1:2020 Annex C Clause C.2 and is presented in **Table 7-5** and **Figure 7-24**.[41]

Figure 7-23 SE Images of 'free' muscovite mica

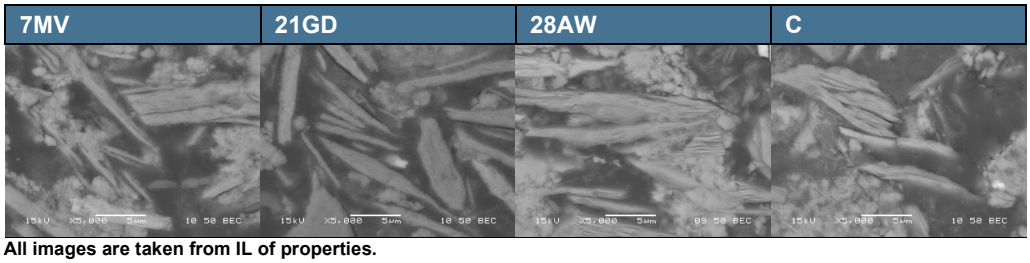

All images are taken from IL of properties.

[41] I.S. 465:2018+A1:2020, See [2]

The relative appearances of muscovite mica across the properties can be seen in more detail in **Figure 7-23**.

Table 7-5 Table of calculated 'free' muscovite mica content

Location		Volume %			
Property	Element	Fine aggregate excluding muscovite mica	Free muscovite mica	Binder	Free muscovite mica proportion of binder (mean)
7MV	Inner leaf	18	19	59	**24**
	Outer leaf	18	26	50	**34**
	Rising wall	12	25	57	**30**
	Foundation	12	11	73	**13**
21GD	Inner leaf	18	28	48	**36**
	Outer leaf	22	22	53	**30**
	Rising wall	20	23	53	**31**
	Foundation	11	16	72	**18**
28AW	Inner leaf	24	28	45	**39**
	Outer leaf	19	22	56	**28**
	Rising wall	18	31	47	**40**
	Foundation	11	16	70	**18**
C	Inner leaf	27	5	64	**8**
	Outer leaf	33	7	59	**10**
	Foundation	18	5	76	**6**

The methodology of 'free' mica determination can be found in 4.2

Figure 7-24 Mean 'free' muscovite mica proportion of binder

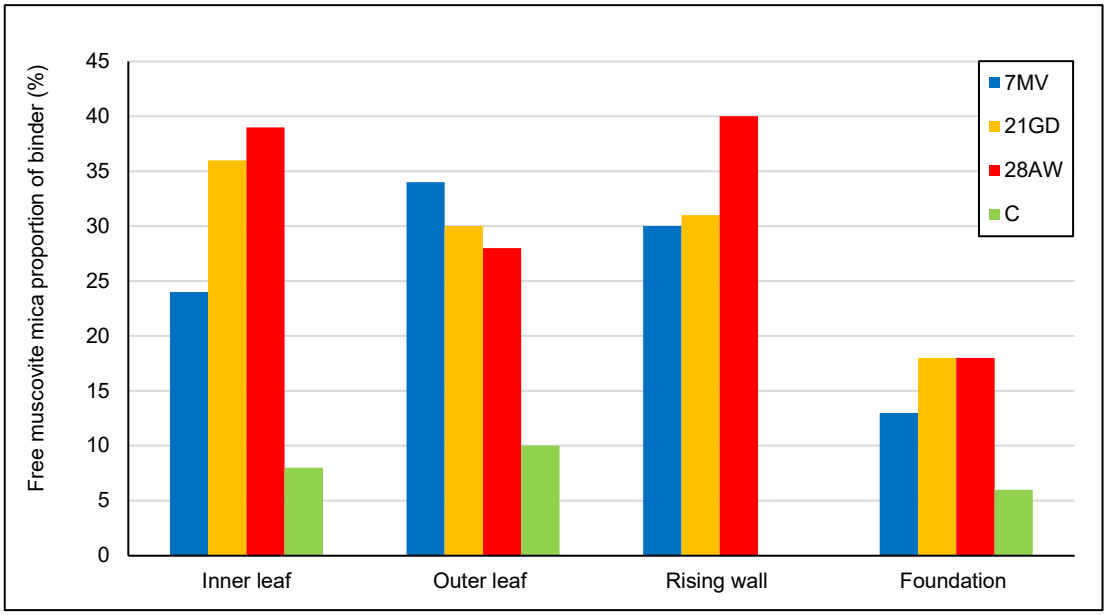

7.2.3 Sulfides

The abundance and types of sulfides were determined by the aggregate type present (test properties – PHY, reference property – SST) as presented in **Figure 7-25**. Concretes that contained PHY exhibited common pyrrhotite, pyrite and rare chalcopyrite. By comparison concretes containing SST contained sporadic pyrite, including potentially reactive framboidal pyrite, and pyrrhotite. Irrespective of composition, all samples exhibited both aggregate-set and matrix-set sulfides (**Figure 7-25**). Therefore, the primary variable in the SEM/EDX investigation of sulfides was their composition, degree of oxidisation, and associated deterioration (**Table 7-6**).[42]

Figure 7-25 BSE images of sulfides present within samples

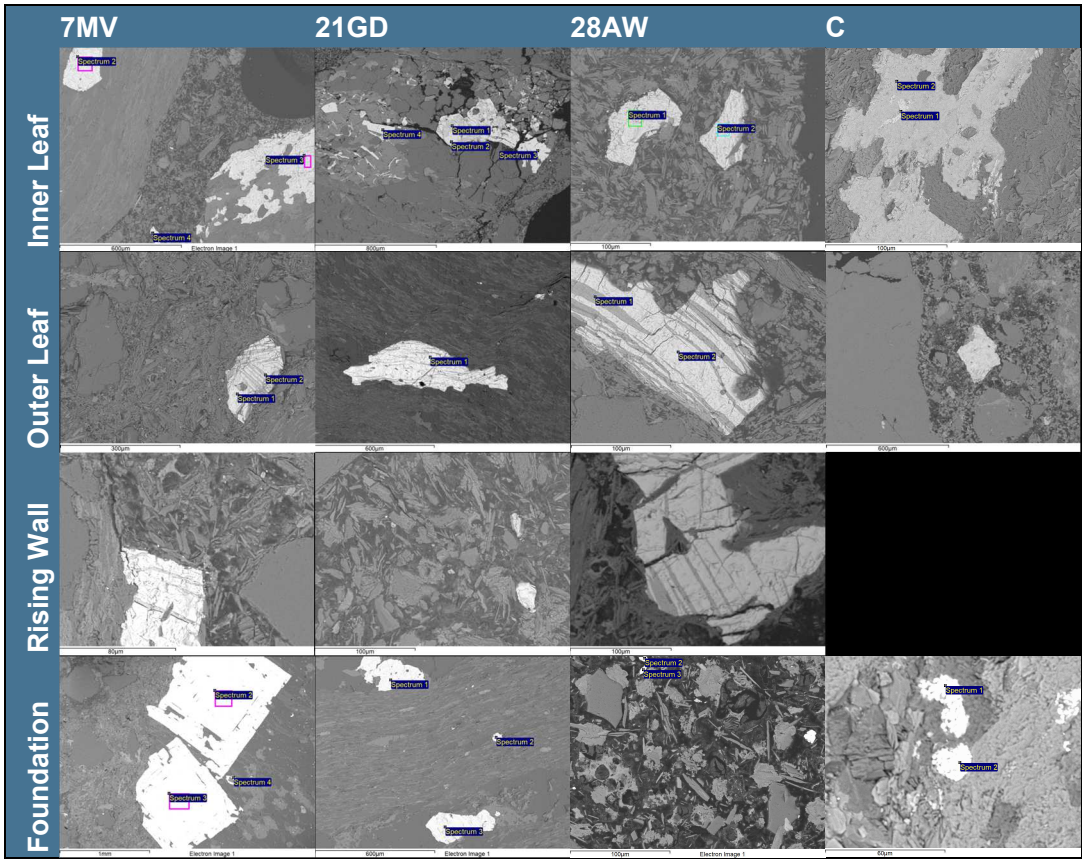

BSE Images, representative of sulfide mineralogy in the concrete samples. Blue boxes represent spectra locations. For further details see Appendix C. Dark grey striping represents striped oxidisation of pyrrhotite (e.g. 2nd Row Centre Right). Views show both aggregate-set sulfides (e.g. 1st Row Far Left, 1st Row Far Right, 3rd Row Far Left, 3rd Row Centre Right) and matrix-set sulfides (e.g. 2nd Row Far Left and 4th Row Centre Right). 4th Row Far Right shows aggregate-set framboidal pyrite

Typically observed oxidisation patterns included striped pyrrhotite oxidisation and surface pyrite oxidisation (**Figure 7-25**). Only limited amounts of framboidal pyrite were observed within C (**Figure 7-25**), which were not observed to be oxidised.

[42] I.S. 465:2018+A1:2020, Annex C C.3 See [2]

7.2.4 Sulfide associated deterioration

The observed secondary deposits and matrix replacements are described in **Table 7-6**. The presence of thaumasite was chiefly located within the adjacent render base coat or mortar, left attached to the concrete blocks within the inner and outer leaves of 21GD (**Figure 7-26**). The thaumasite within the mortar/render either directly replaces the cement matrix or infills voids.

Table 7-6 SEM/EDX observations

Property	Test Properties (7MV, 21GD, 28AW, location if specific)				Control Property (C)		
Element	IL	OL	RW	F	IL	OL	F
Degree/frequency of *In situ* oxidisation	XX	XXX	X	X	-	-	-
Pre-existing oxidisation	X	X	X	X	X	X	X
Striped Oxidisation of Pyrrhotite	XX	XXX	X	X	-	-	X
Cracking associated with oxidised sulfides	XX	XXX	X	-	-	-	-
Thaumasite (location)	X (Mortar 21GD)	X (Mortar 21GD)	X (21GD)	X (7MV)	-	-	-
Secondary Ettringite	X	XX	X (7MV, 28 AW)	X (7MV, 28AW)	-	-	-
Secondary gypsum	X (21GD)	-	XX (28AW)	X (28AW)	-	-	-
Secondary Calcite	X (21GD)	XX	X (7MV)	X (21GD)	-	-	X
Leaching	X	XX	X	X	-	-	X

x denotes relative abundances/degree – xxx high, xx moderate, x lower, - absent

Other locations where thaumasite was observed included voids within the foundation of 28AW and traces possibly replacing the cement matrix of the rising wall of 21GD (**Figure 7-27**). Other secondary deposits, including sulfates like ettringite and gypsum, were predominantly found below the DPM in the rising walls and the foundation of the test properties. In contrast, the control property only showed small amounts of secondary calcite within the foundation (**Figure 7-26**).

Figure 7-26 Foundation deterioration – Control property

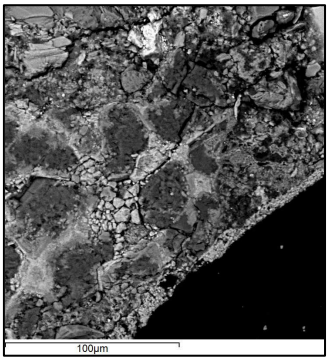

BSE Image of C F (20511/C14) Limited secondary calcite lining an air void (black)

Figure 7-27 BSE images showing evidence of concrete deterioration

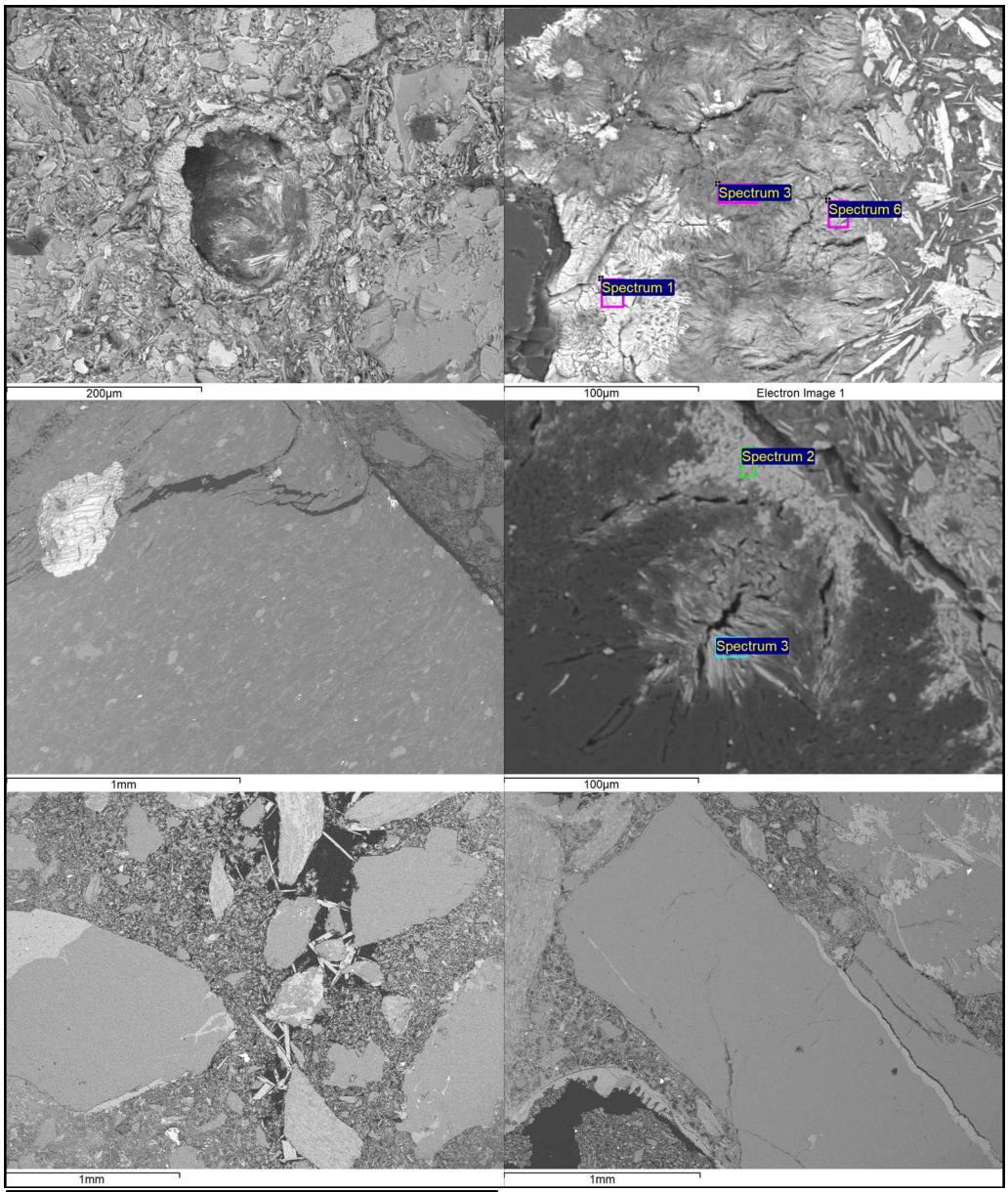

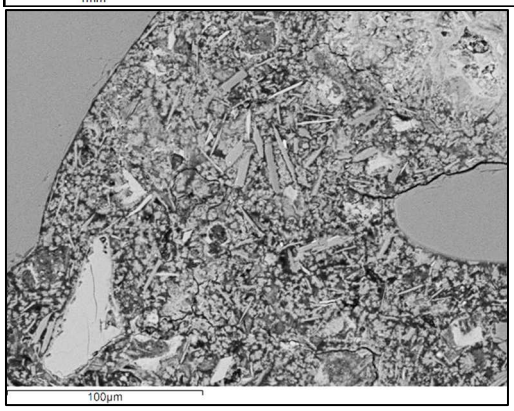

BSE SEM Images. 1st Row Left – 21GD IL (20511/B13) Secondary calcite and secondary calcium sulfate (gypsum) lining an air void. 1st Row Right – 21GD IL (20511/B13) Thaumasite, other calcium sulfates and calcium silica sulfates within adjacent to the attached mortar. 2nd Row Left – 28AW OL (20511/B11) Cracked phyllite particle with the crack emanating from a partially *in situ* oxidised pyrrhotite particle. 2nd Row Right – 7MV RW (20511/C4) Secondary ettringite (Spectrum 3) and secondary calcite (Spectrum 2) within an air void. 3rd Row Left – 28AW F (20511/C20) Secondary elongate gypsum mineralisation within cracks. 3rd Row Left – 7MV RW (20511/C4) Secondary calcite (lower left) lining the edges of an air void and cracking through a quartz aggregate particle. 4th Row – 7MV F (20511/C7) An area of converted cement matrix in the top right corner comprised a mass of thaumasite and ettringite with associated cracking

7.3 XRD

The semi-quantitative XRD data is summarised and presented within **Table 7-7**. Other components not necessarily important to this investigation have been amalgamated. These other components primarily include quartz, calcite and quartz. Further details can be found in **Appendix C** and **4.3**.

Table 7-7 XRD Semi-quantitative compositional data

Location		Composition, approx. %							
		Mica Group Minerals			Sulfides		Sulfates		
Property	Element	Chlorite	Muscovite (mica)	Paragonite	Pyrite	Pyrrhotite	Ettringite	Gypsum	Other Components
7MV	Inner leaf	32.9	41.1	0.8	0.1	0.2	0.4	0.4	24.1
	Inner leaf	49.4	37.3	1.0	0.1	0.1	-	0.1	12.0
	Outer leaf	42.7	40.5	0.6	0.1	0.1	0.3	0.2	15.5
	Outer leaf	38.2	33.9	1.0	-	0.2	0.4	-	26.5
	Rising wall	50.4	31.1	0.6	0.1	0.1	0.2	0.1	14.5
	Rising wall	40.8	29.0	0.5	0.1	0.1	0.3	0.2	29.1
	Foundation	36.8	42.0	0.7	0.1	0.1	0.5	0.3	19.5
21GD	Inner leaf	47.0	33.8	0.6	-	0.1	0.2	0.1	18.2
	Inner leaf	43.2	40.3	0.5	-	0.1	0.2	0.1	15.7
	Outer leaf	49.9	38.0	0.5	0.1	0.1	0.2	-	11.3
	Outer leaf	38.5	46.4	0.5	0.1	0.1	0.2	0.2	14.0
	Rising wall	40.6	44.6	0.6	0.1	0.1	0.3	0.1	13.7
	Rising wall	42.0	43.8	0.4	-	0.1	0.2	0.1	13.5
	Foundation	45.5	37.4	0.6	0.1	0.1	0.3	0.1	16.0
	Foundation	42.0	37.5	0.7	-	0.1	0.4	0.1	19.1
28AW	Inner leaf	20.4	41.7	1.0	-	0.1	-	0.1	36.6
	Inner leaf	41.0	48.2	0.7	0.1	0.1	-	0.1	9.8
	Outer leaf	46.5	43.1	0.6	-	0.1	-	-	9.8
	Outer leaf	49.9	24.6	0.7	-	0.1	0.3	0.1	24.4
	Rising wall	47.0	37.1	0.8	-	0.1	0.3	0.2	14.5
	Foundation	41.6	44.1	0.7	-	0.1	0.2	0.1	13.1
C	Inner leaf	43.1	23.2	0.9	-	0.1	0.4	0.1	32.0
	Outer leaf	48.4	21.5	0.9	0.1	0.1	0.4	0.1	28.5
	Foundation	38.6	22.3	1.1	-	0.1	0.3	0.3	37.5

7.4 Chemical and physical testing

A summary of chemistry and physical testing is presented in **Table 7-8** and followed by graphical representations of each test and any relevant information as required. Note that in all graphical representations, there was no rising wall in C, rather than a zero result.

Table 7-8 Chemical and physical data

Standard	Test	Property / Element	7MV IL	7MV OL	7MV RW	7MV F	21GD IL	21GD OL	21GD RW	21GD F	28AW IL	28AW OL	28AW RW	28AW F	C IL	C OL	C Low OL	C F
EN 1744-1	Total sulfur – Acid digestion (TS)	*S % mass (sample)*	0.3	0.3	0.1	0.2	0.4	0.4	0.1	0.2	0.3	0.2	0.2	0.2	0.1	0.1	-	0.1
	Total sulfur – Acid digestion (TS)	*S % mass (aggregate)*	0.2	0.2	0.0	0.0	0.3	0.3	0.0	0.0	0.2	0.1	0.1	0.0	0.0	0.0	-	0.0
	Total sulfur – HTC (TS)	*S % mass (sample)*	0.75	0.84	1.01	0.72	0.71	1.01	0.63	0.70	1.00	0.90	0.72	0.87	0.19	0.27	0.32	-
	Total sulfur – HTC (TS)	*S % mass (aggregate)*	0.65	0.74	0.91	0.52	0.61	0.91	0.53	0.50	0.90	0.80	0.62	0.67	0.09	0.17	0.22	-
	Acid soluble sulfate (AS)	*SO_4 % mass*	0.3	0.3	0.3	0.5	0.6	0.5	0.3	0.4	0.3	0.2	0.4	0.4	0.2	0.3	-	0.2
	Water soluble sulfate (WSS)	*SO_3 % mass*	0.06	0.01	0.01	0.01	0.20	0.23	0.17	0.01	0.10	0.04	0.02	0.01	0.13	0.13	-	0.01
TRL447, table 8.1. (HTC)	Total potential sulfate (TPS)	*SO_4 % mass*	1.95	2.22	2.73	1.56	1.83	2.73	1.59	1.50	2.70	2.40	1.86	2.01	0.27	0.51	0.66	-
	Oxidisable sulfides (OS)	*SO_4 % mass*	1.65	1.92	2.43	1.06	1.23	2.23	1.29	1.10	2.40	2.20	1.46	1.61	0.07	0.21	-	-
	Equivalent pyrite content	*FeS_2 % mass*	1.03	1.20	1.52	0.66	0.77	1.39	0.81	0.69	1.50	1.38	0.91	1.01	0.04	0.13	-	-
	Equivalent pyrrhotite content	*FeS % mass*	1.51	1.76	2.23	0.97	1.13	2.04	1.18	1.01	2.20	2.02	1.34	1.48	0.06	0.19	-	-
	Aggregate content modifier	-	1.29	1.28	1.29	1.32	1.31	1.20	1.23	1.33	1.29	1.21	1.21	1.33	1.24	1.34	-	1.32
EN 196-2	Sulfide content	*S^{2-} % mass (sample)*	0.25	0.53	0.50	0.32	0.37	0.35	0.44	0.43	0.46	0.31	0.37	0.25	0.03	0.41	-	0.08
		S^{2-} % mass (aggregate)	0.32	0.68	0.64	0.42	0.48	0.42	0.54	0.57	0.59	0.38	0.45	0.33	0.04	0.55	-	0.11
	Acid soluble sulfate content	*SO_4 % mass*	0.22	0.29	0.25	0.28	0.49	0.59	0.23	0.26	0.30	0.19	0.22	0.43	0.23	0.30	-	0.12
BS 1881-124	Cement content	*kg/m³*	110	130	180	310	110	180	150	270	100	80	140	250	80	110	-	160
EN 12390-7	As-received density	*kg/m³*	-	-	2190	2240	-	-	2090	2260	-	-	2050	2260	2240	2270	-	2130
EN 772-13	Gross dry density of masonry unit	*kg/m³*	2170	2150	-	-	2170	1990	-	-	2370	2010	-	-	2060	-	-	-
EN 12504-1	Compressive strength	*N/mm²*	-	-	12.8	29.9	-	-	5.9	14.2	-	-	5.9	22.2	14.1	12.8	-	-
EN 772-1	Normalised Compressive Strength	*N/mm²*	7.9	8.6	-	-	9.1	10.1	-	-	8.6	7.2	-	-	-	-	-	-

28AW IL taken from as received mass and dimensions and C F Density taken from petrographic calculations and as received masses only

7.4.1 Compressive strength

The limited suite of compressive strength results is presented in **Figure 7-28**. For more details on methodology and measurements see **4.4**, **4.5**, and **Appendix C**. Where block sub-samples were tested, compressive strength results were normalised for shape factors to allow comparison with other masonry units. Where core sub-samples were tested, compressive strength results are presented as core compressive strengths.

Figure 7-28 Compressive strength data

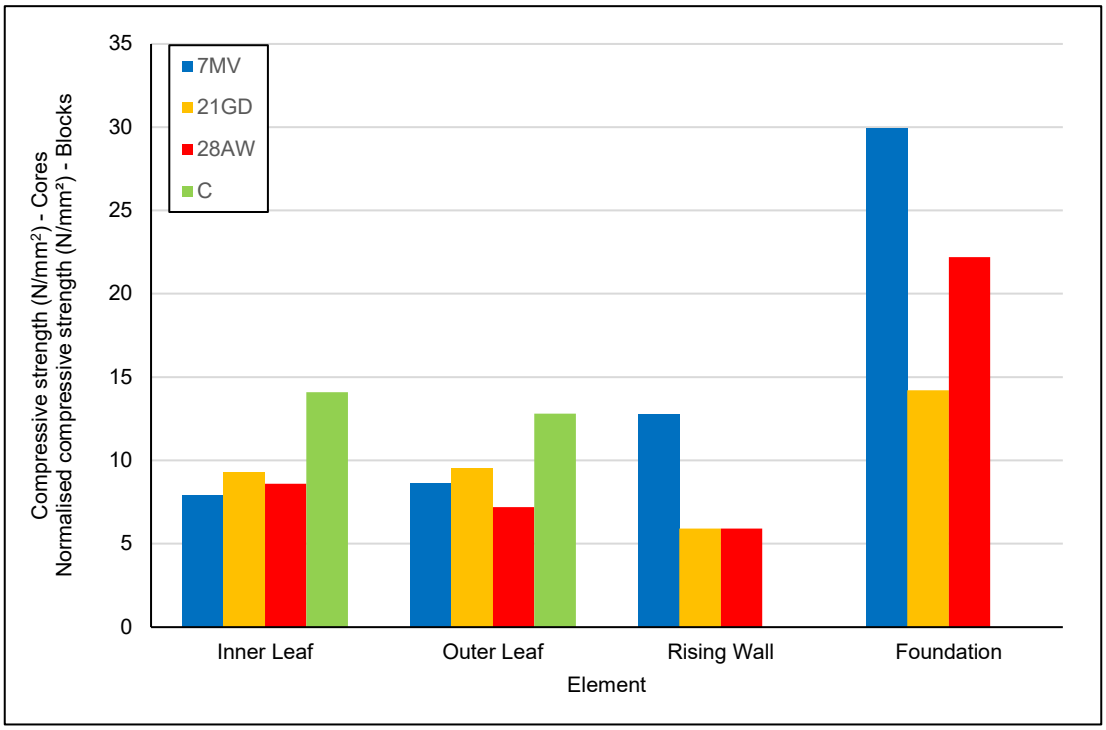

Block sub-samples BS EN 772-1:2011+A1:2015[43] – Inner Leaf and Outer Leaf 7MV, 21GD, 28AW only. All other sub-samples were cores either sub-sampled from core or block samples and tested in accordance with BS EN 12504-1:2019[44]. N=1. Where no test was conducted this was due to limited sample availability and the prioritisation of other testing.

7.4.2 Density

Results of density testing on block and core sub-samples are presented in **Figure 7-29**. For more details on methodology and measurements see **4.6**, **4.7**. and **Appendix C** (core densities only). Block density data was derived from internal unpublished calculations and are not necessarily taken from the same block sub-sample as the compressive strength sub-sample.

[43] BS EN 772-1 See [18]

[44] BS EN 12504-1:2019. See [17]

Figure 7-29 Density data

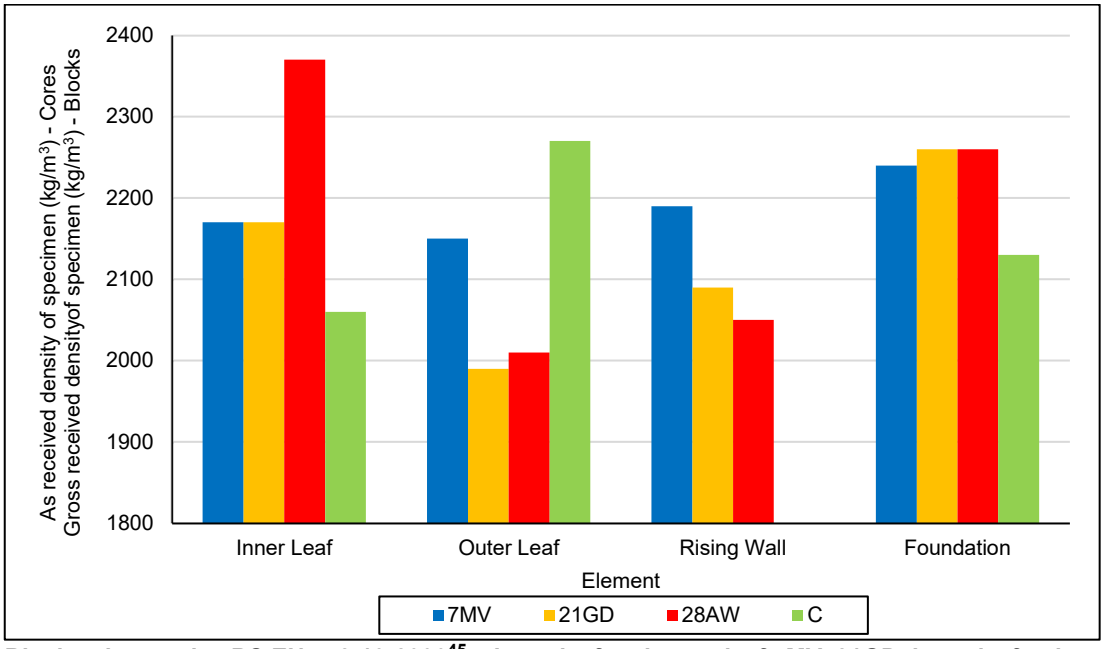

Block sub-samples BS EN 772-13:2000[45] – Inner leaf and outer leaf 7MV, 21GD, inner leaf only – C, outer leaf only – 28AW. All other sub-samples were cores either sub-sampled from core or block samples and tested in accordance with BS EN 12390-7:2019+AC:2020.[46] N=1.

7.4.3 Cement content

The results of cement content testing are presented in **Figure 7-30**. For more details on methodology and measurements please see **4.8** and **Appendix C**.

Figure 7-30 Cement content data

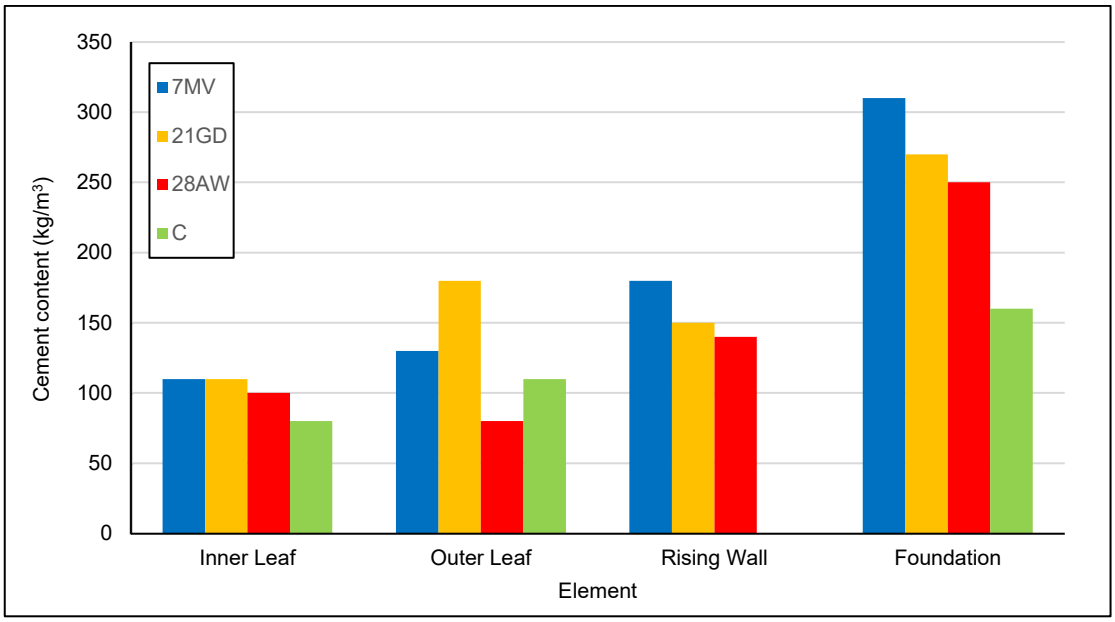

Samples tested in accordance with BS 1881-124:2015+A1:2021.[47] N=1. Note no rising wall within Property C.

[45] BS EN 772-13, See [21]

[46] BS EN 12390-7, See [20]

[47] BS 1881-124, See [22]

7.4.4 Total sulfur (TS)

Results of total sulfur content testing are presented in **Figure 7-31** for acid digestion and **Figure 7-32** for HTC. For more details on methodology and measurements please see **4.9** and **Appendix C**. Results presented in **Figure 7-31**, **Figure 7-32** and **Table 7-8** have a 0.1 % mass S reduction applied to the data to account for the contribution of sulfur from the cement present within a typical standard Irish concrete block as noted within I.S.465:2018+A1:2020, E3.[48] A reduction for the mass concrete total sulfur values of 0.2 % mass S was similarly applied, calculated using a typical cement content of 14 % for general strip foundations.[49]

Figure 7-31 Total sulfur data (aggregate equivalent) – Acid digestion

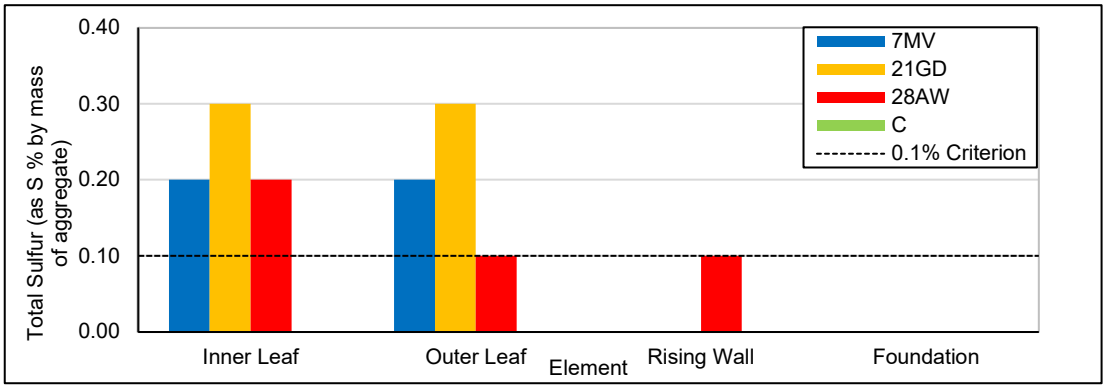

Samples tested in accordance with EN 1744-1:2009+A1:2012 Clause 11.1.[50] N=1. Note a 0.1 % S reduction has been applied to determined results to account for the sulfur contributed by cement in a typical standard Irish concrete block as per I.S.465:2018+A1:2020.[51] A 0.2 % S reduction has been applied in a similar method but for typical mass concrete foundations. The applied reduction has resulted in some 0.00 S % mass results, this does not indicate a lack of results apart from C Rising wall (non-existent). The 0.1 % by dry mass of aggregate criterion for aggregates containing pyrrhotite is taken from EN 12620:2002+A1:2008[52].

[48] I.S. 465:2018+A1:2020, See [2]

[49] NHBC Standards 2024, Site mixed concrete grade ST3

[50] BS EN 1744-1, See [23]

[51] I.S. 465:2018+A1:2020, See [2]

[52] EN 12620:2002+A1:2008 Aggregates for concrete. CEN, Brussels

Figure 7-32 Total sulfur data (aggregate equivalent) – HTC

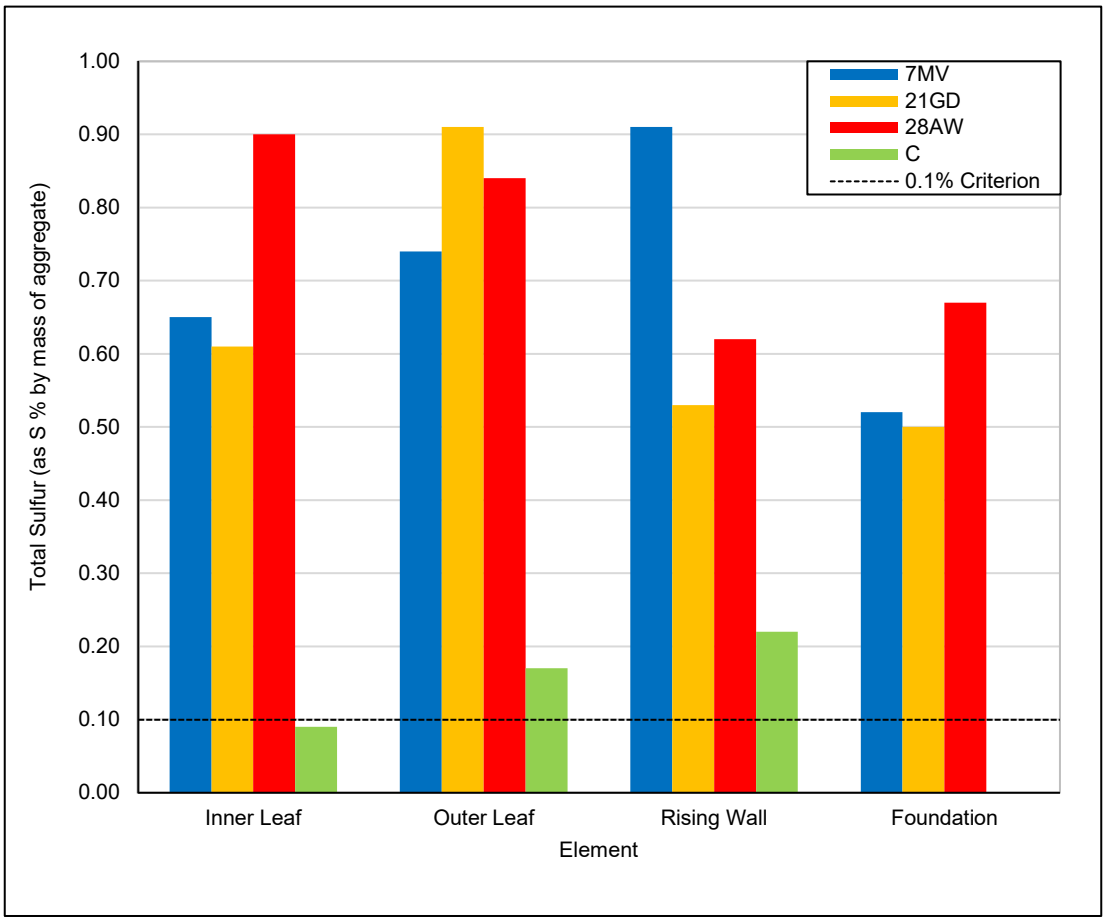

Samples tested in accordance with EN 1744-1:2009+A1:2012 Clause 11.2.[53] N=1. Note a 0.1 % S reduction has been applied to determined results to account for the sulfur contributed by cement in a typical standard Irish concrete block as per I.S.465:2018+A1:2020[54]. A 0.2 % S reduction has been applied in a similar method but for typical mass concrete foundations. Note that the Carrowmore rising wall sample represented here is actually the lower outer leaf sample but represents the same position that the rising wall would occupy in the structure. Also, note that no foundation sample was tested for Carrowmore. The 0.1 % by dry mass of aggregate criterion for aggregates containing pyrrhotite is taken from EN 12620:2002+A1:2008[55], 6.3.2.

7.4.5 Acid soluble sulfate (AS)

Results of the employed methods of acid soluble sulfate content testing are presented in **Figure 7-33** and **Figure 7-34**. For more details on methodology and measurements please see **4.10, 4.13** and **Appendix C**. Note that EN 1744-1 and EN 196-2 data have been converted from SO_3 to SO_4 (by multiplication by a factor of 1.2) to allow comparison to criteria given in the aggregate standards.

[53] BS EN 1744-1, See [23]

[54] I.S. 465:2018+A1:2020, See [2]

[55] EN 12620:2002+A1:2008 Aggregates for concrete. CEN, Brussels

Figure 7-33 Acid soluble sulfate data – BS EN 1744-1

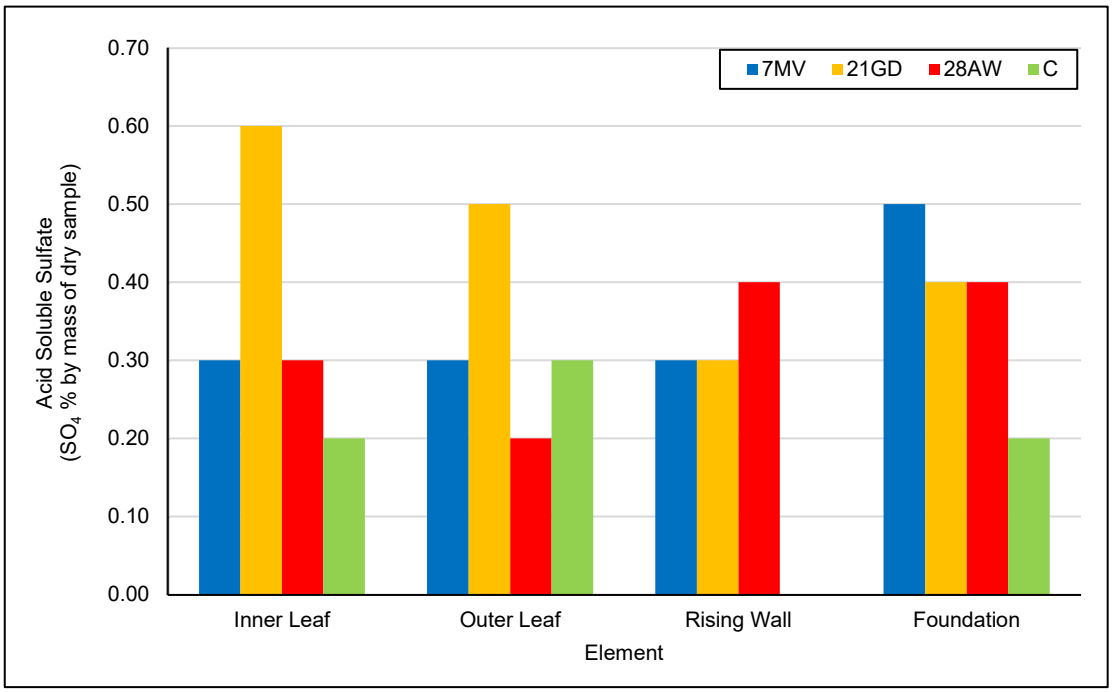

Samples tested in accordance with BS EN 1744-1:2009+A1:2012.[56] N=1.

Figure 7-34 Acid soluble sulfate data – BS EN 196-2

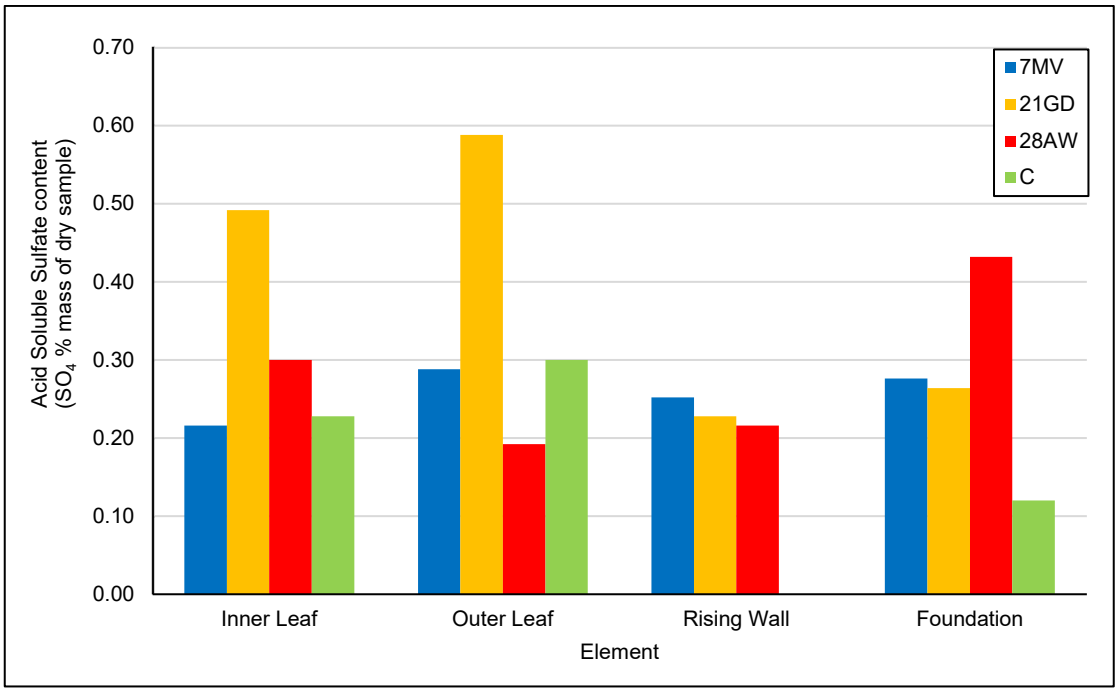

Samples tested in accordance with BS EN 196-2:2013.[57] N=1.

[56] BS EN 1744-1, See [23]

[57] BS EN 196-2, See [31]

7.4.6 Water soluble sulfate content (WSS)

Results of water-soluble sulfate content testing are presented in **Figure 7-35**. For more details on methodology and measurements please see **4.11** and **Appendix C**.

Figure 7-35 Water soluble sulfate data

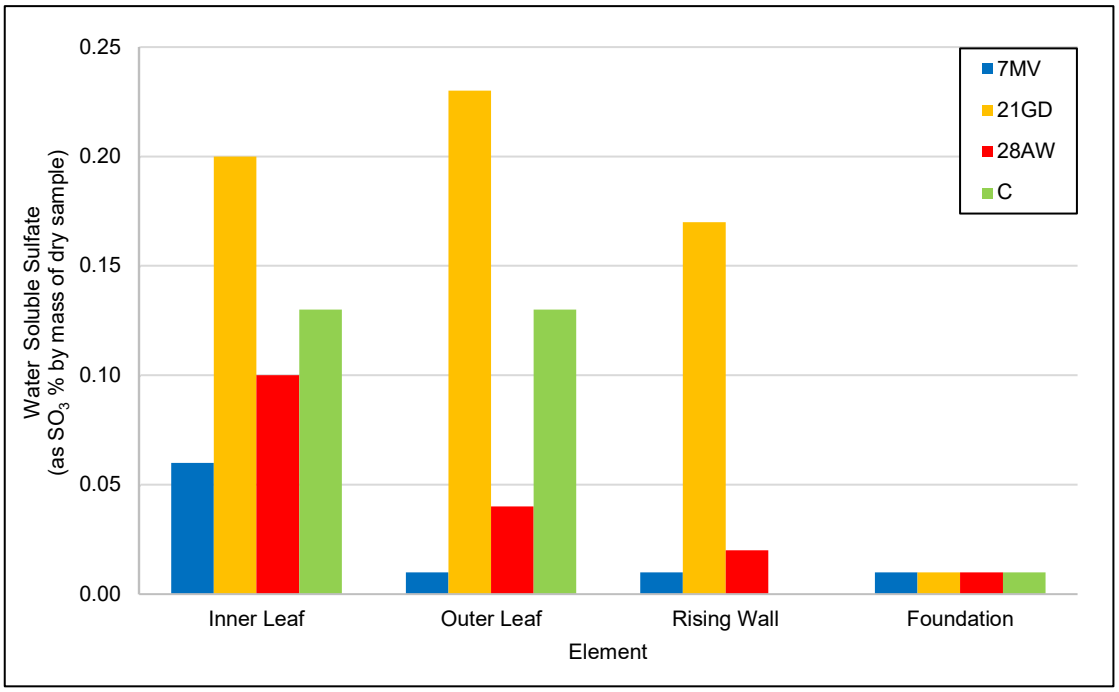

Samples tested in accordance with BS EN 1744-1:2009+A1:2012.[58] N=1. Results <0.01 represented as 0.01

7.4.7 Pyrite and pyrrhotite content

Results of pyrite and pyrrhotite content testing are presented in **Figure 7-36** and **Figure 7-37** respectively. The calculated maximum possible pyrite and pyrrhotite content represent values if all the oxidisable sulfides present were purely one mineral species. In this case, we know this not to be the case, but values are provided here for relative comparison. The values presented are calculated using TS (HTC) and ASS determined values (Table **7-8**, **7.4.4** and **7.4.5**). By calculating total potential sulfate (3 × TS) and subtracting AS, oxidisable sulfides (OS) as SO_4 is derived. OS can then be converted into the sulfide mineral species by simple conversion of molecular masses. The values presented (**Figure 7-36** and **Figure 7-37**) have been calculated using the total sulfur values that account for the contribution of sulfur from the cement, as opposed to the calculated values presented within **Appendix C**. For more details on methodology and measurements please see **4.12.**

[58] BS EN 1744-1, See [23]

Figure 7-36 Calculated pyrite content data

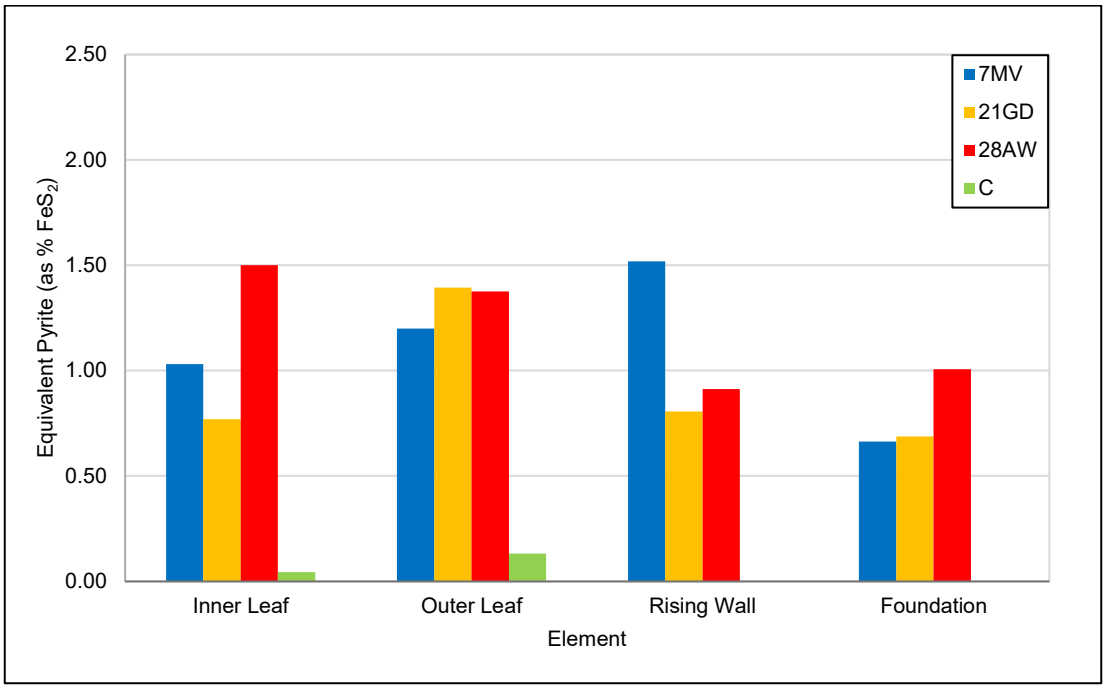

Based on calculations as described in TRL 447.[59] N=1. The results represent the maximum possible pyrite content based on TS (HTC) and ASS results assuming all sulfides are pyrite. Note no rising wall was present at C and no result for no calculation for C F.

Figure 7-37 Calculated pyrrhotite content data

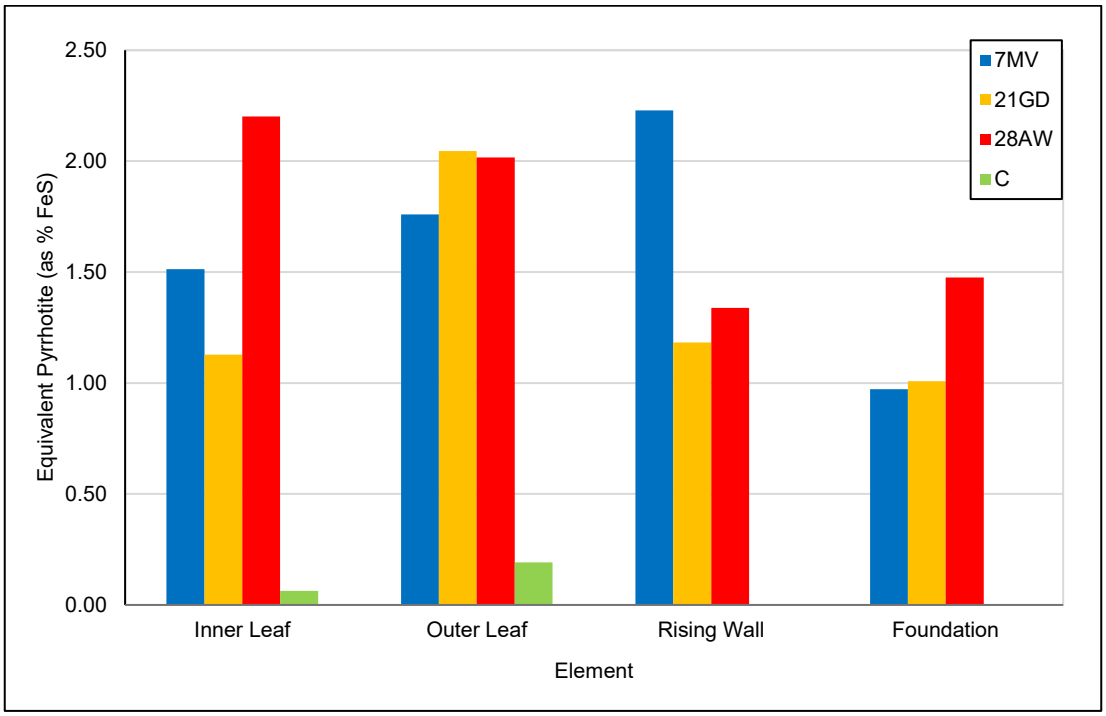

Based on calculations as described in TRL 447.[60] N=1. The results represent the maximum possible mineral content based on TS (HTC) and ASS results assuming all sulfides are pyrrhotite of FeS composition. Note no rising wall was present at C and no calculation for C F.

[59] TRL Report TRL447. See [30]

[60] TRL Report TRL447. See [30]

7.4.8 Sulfide content

The results of sulfide content testing are presented in **Figure 7-38**. For more details on methodology and measurements please see **4.14** and **Appendix C**.

Figure 7-38 Sulfide content data (whole sample)

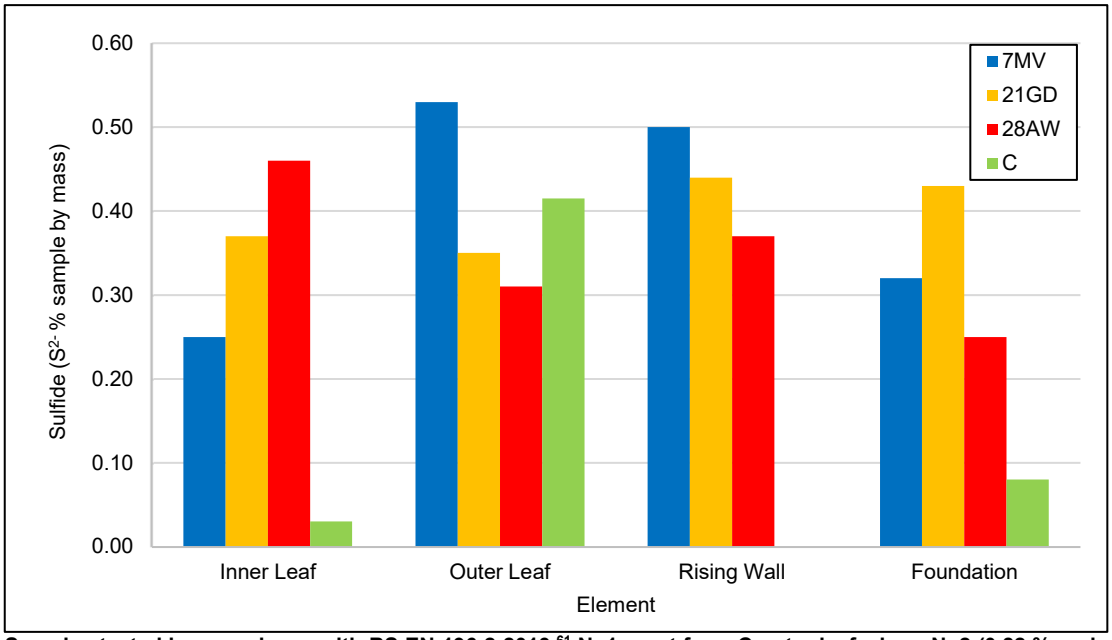

Samples tested in accordance with BS EN 196-2:2013.[61] N=1 apart from C outer leaf where N=2 (0.82 % and 0.01 %).

7.5 RICS - The Mundic Problem, Stage 3 expansion testing

Results are provided in 1283831-04 Phase 2 & 3 report.

7.6 Oxidisation testing of concrete block, adapted version of CSA A23,1:19 Attachment P3 (informative)

Results are provided in 1283831-04 Phase 2 & 3 report.

[61] BS EN 196-2, See [31]

8 DISCUSSION

8.1 Sample integrity

The condition in which the samples were received reflects their physical state and their ability to withstand the sampling technique used for extraction. Taking into account the consistency of the environmental conditions and the sub-contractor during the sampling from the properties, we can conclude that the concrete cores and blocks were extracted in a consistent manner using the same techniques for samples of the same physical type. Therefore, the conditions in which the samples were received should be comparable.

The as-received condition of the samples (see **Table 3-1**), when considered by percentage samples deteriorated, exhibited a consistent relative ranking of deterioration by element IL≈OL>F>RW, and by properties 28AW>C>7MV>21GD. It is noteworthy that the degree of deterioration varied significantly, ranging from disintegrated gravel in a bag to minor deterioration such as a small piece missing or broken off. The most severe physical deterioration was observed in 28AW OL samples, where disintegration was often complete. Conversely, 21GD samples predominantly exhibited intact or slightly deteriorated conditions. Notably, environmental conditions were also a factor in the as-received condition, with the below-ground level concrete samples found to be in the best condition, suggesting a lower degree of deterioration had occurred below-ground level. Additionally, the variation in condition within the same element was notable, suggesting localised deterioration as the result of local microenvironmental changes and variation in concrete quality or composition. Control samples were in a relatively misleading as-received condition in terms of relative property ranking as they were biased by a couple of minor sample failures and a lower number of samples. However, the general order of as-received condition based on qualitive comparison was F>RW>IL>OL.

8.2 Aggregates

8.2.1 Abundance and composition

Aggregate comprised approximately 60 % sample volume in all elements (**Figure 7-1**), allowing a relatively consistent comparison between the effects of the lithologies present. The most readily apparent contrast between the aggregates within the study was the clear compositional division evident between the PHY aggregate (phyllite and quartzite) utilised throughout the test property concretes and the SST aggregate (sandstone and siltstone) utilised in the control property concrete. Optical microscopy (**7.1**), SEM (**7.2**) and XRD (**Table 7-7**) results show that within PHY, phyllite was chiefly composed of muscovite mica, chlorite and paragonite mica group minerals with minor to trace iron sulfides. The quartzite component of the PHY chiefly comprised quartz with minor amounts of muscovite mica, feldspar and minor iron sulfides. When compared to the quartz and feldspar-rich sandstones and siltstones of the SST aggregate, PHY was significantly more micaceous and deficient in quartz whilst containing a higher abundance of iron sulfides.

Assuming a water:cement ratio of 0.65 the aggregate:cement ratios for the test property concrete blocks ranged between 6.5 to 10, in contrast to the control property concrete blocks, which ranged between 11 to 12 (**Appendix C**). Similarly, the mass concrete of the foundations returned lower aggregate:cement ratios (3.5 to 5.1) for the test properties and higher aggregate:cement ratios (4.9 to 6.2) for the control property. Given the consistent volume proportions for the aggregates, it seems likely that this is more reflective of the cement contents rather than variation within the aggregate content of the concretes.

8.2.2 Physical properties

Within PHY, chiefly only the phyllite was prone to flakiness and splitting with evidence of this both pre-existing (**Figure 7-15**) at some point during extraction, processing or within a stockpile, and as a reaction to *in situ* deterioration (**Figure 7-8**). Within concrete block samples, poor physical condition of the phyllite sporadically resulted in a poor cement-aggregate bond, irrespective of whether pre-existing or developed *in situ* deterioration (**Figure 7-8**). In contrast, whilst the SST aggregate within the control property exhibited some pre-existing fracturing, a good cement-aggregate bond was still observed (**Figure 7-9**). It can be suggested that the phyllite aggregate may not have been suitable for use within concrete due to its physical properties alone, including flakiness, fissile nature and tendency to easily split along cleavage planes generating fines. However, without appropriate physical test data for a similar, fresh PHY sample, little confidence can be given to any comparison with EN 12620[62] and S.R. 16[63] physical aggregate property requirements. More confidence can be placed in the conclusion that the poor physical properties of the PHY aggregate, as discussed above, have led to test property concrete blocks being relatively susceptible to deterioration compared to the SST-bearing concrete blocks of the control property. The increased cement content of the test property mass concrete foundations seems to restrict the apparent physical deficiencies of the PHY aggregate as no pre-existing cement: aggregate related weaknesses were readily observed.

8.2.3 Sulfides

The quantification of iron sulfide content was investigated by OM, SEM, EDX, XRD, and wet chemistry and HTC techniques. Qualitative OM estimates of aggregate content PHY-bearing elements consistently indicated iron sulfide content, primarily pyrrhotite with moderate amounts of pyrite and traces of chalcopyrite (see **Table 7-2**). The sulfides occurred as discrete matrix-set, typically fine grains, and as variously sized aggregate-set minerals, chiefly within phyllite and less abundantly within quartzite and schist aggregate particles. The SST aggregate also contained both discrete matrix-set and aggregate-set iron sulfides with a lower prevalence of discrete matrix-set grains. Relative to the PHY aggregates, the SST aggregates only included relatively moderate amounts of pyrite and traces of pyrrhotite and other metallic minerals (see **Table 7-2** and **Table 7-4**), primarily located within sandstone and siltstone particles; it was noted however that while the pyrite in the PHY aggregate is relatively coarse crystalline (therefore consistent with low reactivity forms), the SST aggregate additionally contains some traces of the

[62] EN 12620, See [52]

[63] S.R. 16:2016, Guidance on the use of I.S. EN 12620:2002+A1:2008 - Aggregates for concrete, 2016, NSAI, Dublin, Ireland

more reactive framboidal forms of pyrite. Only qualitative OM numeric estimates were determined for the discrete matrix-set iron sulfides, these all fell into trace (<2 % volume of aggregate) categories for the mineral occurrences described above in both test and control properties. OM and SEM/EDX analyses showed composition, abundance and morphology of the sulfides present within the samples were directly related to the aggregate type utilised.

As only semi-quantitative XRD analysis was conducted, the presence and quantity of XRD-detected sulfides were only judged sufficient to determine the possible presence of pyrite and pyrrhotite (see **Table 7-7**). Whereas pyrrhotite was indicated within all samples tested, pyrite was more sporadically detected, either indicating a lower relative abundance beyond that of detection or its absence. Whilst phase maps were produced using SEM/EDX analysis, these were principally limited to areas of high cement matrix abundance, to determine free mica content. Any semi-quantitative or quantitative determination of sulfide content using these phase maps was typically skewed towards discrete matrix-set sulfides and therefore was not reported.

The sulfide content of the concretes was analysed by multiple wet chemistry measurements including TS, ASS and sulfide content determinations and the calculation of sulfides as separate pyrite and as pyrrhotite. The use of multiple tests allows comparison of the results and highlights correlations and inconsistencies within the data. TS contents of the concrete can be thought of as the sum of the sulfur present as sulfate, both in the cement and aggregate, sulfide (primarily in the aggregate) and organic matter. Given the aggregate tested in this study, here TS can be thought to represent secondary sulfate, sulfide contents from the aggregate and a primary sulfate contribution from the cement, taken, likely slightly generously to be 0.1 % S (by mass of sample) for standard concrete blocks (I.S. 465:2018+A1:2020 E.3)[64] and calculated as 0.2 % S (by mass of sample) for mass concrete.

With the cement contribution deducted, the test property's total sulfur determined by the BS EN 1744-1 reference method (acid digestion) gave consistent results of 0.1 to 0.3 % S (by mass) for the inner and outer leaves, 0.0 to 0.1 % S (by mass) for the rising walls and 0.0 % S (by mass) for the foundations each sample analysed. The control property also indicated 0 % S by mass of aggregate for all elements. As previously noted, these are unrealistically low values, as there should always be around 0.1-0.2% total sulfur (by mass) just derived from the cement, and the petrography and SEM/EDX identified both sulfide and sulfate minerals present in the hardened concrete, sulfide principally in the aggregate, at levels apparently greater than these determined values. By comparison, the total sulfur of aggregate determined by EN 1744-1 high-temperature combustion method (LECO) returned total sulfur in the range of 0.6 to 1.0 % S (by mass) for the test properties' bulk concrete, which with the cement contribution deducted, indicated that the total sulfur of the PHY aggregate was likely to be in the approximate range of 0.5 to 0.9 % S (by mass). These results are more consistent with the visual evidence from petrography and other analyses. The control property returned total sulfur determined by high-temperature combustion (LECO) of 0.2-0.3 % S (by mass) for the bulk concrete and 0.1-0.2 % S (by mass) for the SST aggregate. Again, these results support the petrographic and SEM/EDX observations, in this case, the lower sulfide content within the SST aggregate used within the control property.

[64] I.S. 465:2018+A1:2020, See [2]

The determined values chiefly only represent single-point data and as such should be treated with caution, however, where further tests were performed using the same method (acid digestion only) on the same samples, results were consistent. The pyrrhotite-bearing PHY, present within the test properties, returned TS determined by HTC exceeding the maximum permitted TS of 0.1 % S (by mass) content given in EN 12620[65] for pyrrhotite-bearing aggregates.

The EN 1744-1[66] TS determinations by HTC combined with petrographic evidence indicate that for the combination of materials analysed, the issue lies with the EN 1744-1[67] TS by acid digestion test methodology. It was not clear whether the acid digestion methodology does not adequately digest the sulfur in the presence of cement and significant mica content was not immediately clear. However, the potential for TS determination by EN 1744-1 acid digestion[68] to underestimate total sulfur by 23-85% has been found to be caused by the presence of complex mineral species including feldspars and clay minerals. As such, the acid-digestion methodology is known to not be the favoured method of analysis.[69,70] It may be the case, in this instance, that the high mica group mineral content present within the samples has caused an underestimation of total sulfur. It should be noted that the test method used for the determination of total sulfur, from BS EN 1744-1[71] is the European harmonised standard for the assessment of sulfur in aggregate rather than in concrete, and it is possible therefore that the extraction method is insufficiently aggressive or that the released sulfur species tend to adsorb to other materials present in the standard, and are not wholly precipitated with barium chloride.

The sulfide as sulfur determinations in accordance with EN 196-2[72] can be converted to values for sulfur % mass for the aggregate if it is assumed that all the sulfide is present within the aggregate (as determined by optical microscopy and SEM analysis). The conversion factor is determined using the as-received densities of concrete (**Figure 7-29**) and the determined aggregate content (1700 kg/m^3) by point count (**7.1** and **Appendix C**). Using these values a multiplication factor of ~1.24-1.35 for concrete blocks and ~1.32 for the mass concrete foundations was calculated to deduce S^{2-} content within the aggregate (i.e. by removal in the calculation of the volume of cement and voids). This results in values of 0.32-0.68 S^{2-} % mass of dry aggregate for the test properties and between 0.04-0.54 S^{2-} % mass of dry aggregate for the control property. The outer leaf value for the control property is taken to be an unexplained outlier and was not able to be completely discounted. If the outlier is discounted a clear contrast between the 0.32-0.68 S^{2-} % (by mass) PHY aggregate and the <0.1 % S^{2-} (by mass) SST aggregate. Again, as seen in HTC TS determinations, PHY aggregates significantly exceed the 0.1 % S by mass limit for pyrrhotite bearing concrete aggregates specified in EN 12620.[73]

[65] EN 12620, See [52]

[66] BS EN 1744-1, See [23]

[67] BS EN 1744-1, See [23]

[68] BS EN 1744-1, See [23]

[69] TRL Report TRL447. See [30]

[70] Czerewko M A, Longworth I, Reid J M and Cripps J C (2016). Standardised terminology and test methods for sulfur mineral phases for the assessment of construction materials and aggressive ground. Quarterly Journal of Engineering Geology and Hydrogeology, 49: 245-265.

[71] BS EN 1744-1, See [23]

[72] BS EN 196-2, See [31]

[73] BS EN 196-2, See [31]

When considering observed OM and SEM/EDX evidence, in this circumstance, the EN 1744-1 acid digestion methodology[74] is deemed less representative of or consistent with, and possibly misleading with regards to, the observed presence of sulfides and sulfates within the samples than the EN 1744-1 TS HTC methodology % S or the EN 196-2 % S^{2-} values.

8.2.3.1 Sulfide oxidisation

Sulfide oxidisation is known to be related to the molar oxygen concentration (oxygen availability), pH, sulfide surface availability, reactivity of the sulfide mineral species and moisture condition.[75,76] With regards to different sulfide species present, pyrrhotite is known to be significantly more rapidly oxidised than pyrite, with pyrite reaction rates strongly controlled by mineral form.[77] Therefore, the pyrrhotite-rich PHY was expected to have a higher oxidisation potential and be of more concern, than the chiefly pyrite-dominated sulfides of the SST aggregate. Indeed, the sulfide type directly correlates to the two most common types (patterns) of oxidisation and their severity observed within the samples. Striped (or banded) oxidisation along crystallographic axes typically occurs within pyrrhotite (e.g. **Figure 7-16** and **Figure 7-25**), whilst surface oxidisation typically occurs along sulfide grain margins within pyrite but was also observed within pyrrhotite and chalcopyrite (see **Figure 7-9**, **Figure 7-13** and **Figure 7-20**). The striped pyrrhotite oxidisation was composed of bands of unreacted remnant pyrrhotite and iron oxide/hydroxide bands where oxidation had taken place. The striped oxidisation of the pyrrhotite was frequently associated with *in situ* oxidisation whereas surface oxidisation was more characteristic of pyrite and apparently pre-existing oxidisation of sulfides. The SST exhibited rare framboidal pyrite, in isolated clusters exhibiting limited oxidisation within the foundation of the test property.

In much the same way as the micaceous phyllite in PHY exhibited pre-existing physical deterioration from before use within the concrete, the degree of pre-existing oxidisation of sulfides within the rock formation, during processing or within the stockpile must also be considered. Fortunately, when evaluating *in situ* oxidisation of the iron sulfides, it was relatively straightforward to observe *in situ* iron-oxide/hydroxide staining of the cement matrix surrounding the iron sulfides and associated cracking running from reaction sites into the cement matrix, both of which indicated oxidisation had either initiated or continued when *in situ* within the concrete to date.

Concerning *in situ* surface-type oxidisation, three main trends are evident. Firstly, at most only traces of iron oxides and hydroxides diffused into the cement matrix, and the lack of related significant cracking was observed around sulfide grains exhibiting surface oxidisation. The lack of cement matrix interaction strongly suggested that the majority of this form of oxidisation pre-existed the aggregates' incorporation into the examined concrete (further discussed within **8.3.2**). Secondly, *in situ* surface oxidisation was the predominant type of oxidisation observed within the mass concrete foundations for all sulfide species. This variation in oxidisation type and related severity suggested that the

[74] BS EN 1744-1, See [23]

[75] Casanova, I. Agulló, L. Aguado, A. Aggregate expansivity due to sulfide oxidation — I. Reaction system and rate model, Cement and Concrete Research, Volume 26, Issue 7, 1996, Pages 993-998, ISSN 0008-8846,

[76] Jana, D, Concrete Deterioration from the Oxidation of Pyrrhotite, Chapter 5, See [7]

[77] Chopard, A, Benzaazoua, M, Plante, B, Bouzahzah, H and Marion, P.. (2015). Kinetic Tests to Evaluate the Relative Oxidation Rates of Various Sulfides and Sulfosalts. Proceedings of 10th International Conference on Acid Rock Drainage, Santiago, Chile.

moisture-saturated, likely gaseous oxygen-poor, environment of the mass concrete foundations negatively influences the type and degree of sulfide oxidisation.[78] Lastly, the striped oxidisation pattern was chiefly associated with *in situ* oxidisation of the pyrrhotite.

The degree of oxidation and associated minor expansion[79] within the striped pyrrhotite can be thought of as a proportional ratio of oxidised bands to remnant pyrrhotite within single pyrrhotite grains/crystals. OM and SEM/EDX analyses of the striped pyrrhotite and matrix interaction (see **7.1** and **7.2**) indicated that the highest degree of oxidisation occurred within the outer leaf of the test properties, particularly 28AW and 21GD where near complete pyrrhotite oxidisation was commonly observed. After the outer leaves the degree of oxidisation of pyrrhotite relatively decreased from the inner leaves followed by the rising wall and then lowest within the mass concrete of the foundations (as discussed above). The availability of oxygen correlated to the oxidisation progression of striped pyrrhotite between different building elements, similar to surface-type oxidisation. The foundations are submerged likely in a static more anoxic water-saturated state and are made from denser, less voided mass concrete, both these factors would have restricted access to gaseous oxygen. The dry inner leaves and the wetter outer leaves have been exposed to air and moisture through vents in the cavity wall and any failures in the external render. The inner leaves, being dry, would appear to be the most susceptible to air ingress and therefore carbonation and associated lowering of pH (neutral). In this case and in broad agreement with RSK's prior experience, the predominant iron sulfide oxidisation within the investigated concrete blockwork was related to oxygen and moisture supply primarily located where blockwork was directly exposed to wetting/drying cycles either in the outer leaves behind failures/cracks in the outer render or exposures around the DPM. However, it appears that enough moisture had reached the inner leaf to allow significant sulfide oxidisation to occur.

Similarly to the macro environment, the microscopic environment of the iron sulfides present within the concrete was observed to affect sulfide oxidisation. Sulfides were more commonly oxidised when exposed to the high pH (if uncarbonated) of the cement matrix. This primarily occurred as discrete matrix set grains typically (<1 mm in size) and on the margin or along internal fractures within sulfide-bearing aggregate particles. At these locations, the sulfides were exposed to either the interfacial transition zone (ITZ), high microporosity cement matrix (see **Figure 7-21**) or pore solutions all providing a pathway for oxygen and moisture to access the sulfides. However, even when matrix-set pyrrhotite was exposed to high pH, moisture and oxygen (e.g. failed outer leaf) sulfide oxidisation was still highly varied at the microscopic scale. This occurrence may be explained by highly localised differences in moisture or oxygen availability but also by the specific species of pyrrhotite present from within the non-stoichiometric range (the analysis of which is beyond the scope of this investigation).[80]

8.2.4 Mica content

The presence of micaceous aggregates within PHY and to a lesser extent SST resulted in discrete muscovite mica and chlorite grains, typically <10 µm but up to approximately

[78] I. Casanova, Aggregate expansivity due to sulfide oxidation, See [75]

[79] I. Casanova, Aggregate expansivity due to sulfide oxidation, See [75]

[80] Titon, B.; Duchesne, J.; Fournier, B. Characterization and distribution of pyrrhotite species in concrete aggregates: Insights into internal sulfate attack in Québec, CA. in Benoît Fournier, Josée Duchesne, Rodolfo Castillo Araiza, Andreia Rodrigues and Pierre-Luc Fecteau (eds), Proceedings of the First internal Conference on Iron Sulfide Reaction in Concrete, May 2024

100 µm in size with a flaky or platy morphology (**Figure 7-23**). These 'free' mica grains are limited by I.S. 465[81] to muscovite mica of <63 µm only. However, SEM phase mapping (**Figure 7-22**) shows that chlorite grains typically had similar morphologies present and other forms of sheet silicate were also suggested by XRD analysis (**Table 7-7**). In data not presented herein, the muscovite mica and chlorite content combined would present a proportional increase of approximately 7-50 % for test properties and 75-140 % for the control property, for reported 'free' mica totals dependent on the specific element. For this discussion, we chiefly considered the 'free', < 63 µm sized, muscovite mica content of the paste.

The test properties reported high to excessive 'free' mica content of the binder (cement matrix) between 24-40 % for concrete block elements and 13-18 % for foundations (**Table 7-5**). The higher cement:aggregate ratios observed in the foundations likely contribute to the lower 'free' mica contents in the binder. The control property had a further reduction in 'free' mica content, with a range of 6-10%, compared to the test properties (**Table 7-5**). The SST muscovite mica content was notably lower than that in the PHY lithologies mainly due to the presence of flaky, friable, easily split phyllite, comprising abundant sheet silicates, within PHY. However, the chlorite content of the SST aggregate in the control property appeared to be significantly higher proportionally than within PHY, sometimes exceeding muscovite mica content in places.

Figure 8-1 Comparison of 'free mica' content to OM determined soundness

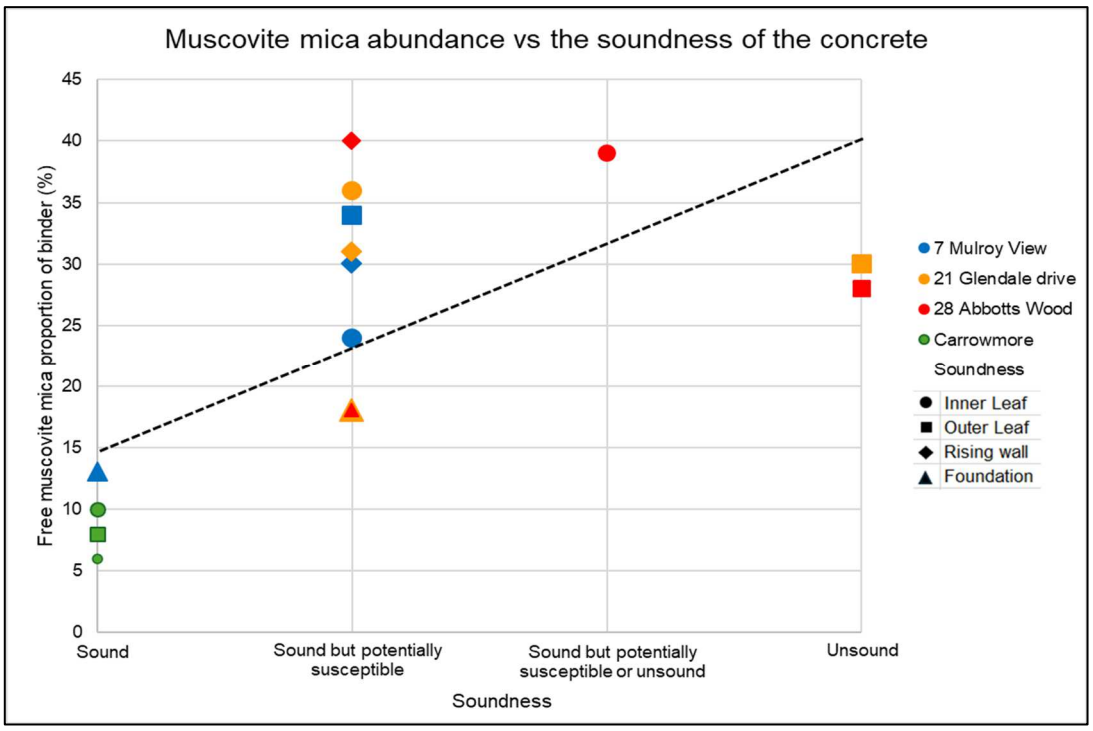

The values of the determined 'free' mica content of the binder appear relatively high when compared to XRD and petrographic analysis. The AOIs selected for SEM/EDX phase mapping were chosen to be most representative of areas of binder and the relatively high

[81] I.S. 465:2018+A1:2020, See [2]

microporosity of the binder (**Figure 7-21**). This combined with the resolution of analysis may account for some bias towards 'free' mica content at the scale of SEM analysis. Even given a nominal 5 % analytical overestimation, the calculated values for the test property concrete blocks almost certainly represent a significant exceeding of the 5 % limit for 'free' mica content of binder within concrete blocks for cases of poor concrete block durability.[82] When compared directly to the soundness of the concrete a loosely positive correlation can be seen (See **Figure 8-1**). However, this correlation may be thought of as a direct result of the phyllite content, which is both related to mica and sulfide occurrence, therefore this assertion is not conclusive proof that mica content relates to the soundness of concrete.

8.3 Cement matrix

8.3.1 Cement content

As no specific cement content is specified for concrete blocks (aggregate concrete masonry units) within EN 771-3,[83] as a performative specification standard no requirement exists for comparison. Typical concrete block cement contents of 100 kg/m^3 to 230 kg/m^3 are quoted within the literature[84,85], whilst RSK's experience of Irish concrete block assessments suggests typical cement content values for 7 N Blocks, commonly used for house superstructural walls of 150-200 kg/m^3. The cement content of the concrete blocks from all properties varied from 80-180 kg/m^3 (**Figure 7-30**), which would appear generally in line with the lower part of expected values. The relatively low cement contents of the inner and outer leaf concrete blocks may be the result of cement matrix conversion, deterioration or leaching within the test properties as seen within OM and SEM/EDX analyses (**7.1, 7.2**), however, this does not explain the low cement contents within the inner and outer leaves of the undamaged test property. The slightly elevated cement contents of the rising wall may be more representative of the original cement contents of the concrete blocks (140-180 kg/m^3) as less sulfide oxidisation, associated deterioration and cement matrix conversion were generally observed in these locations. As the rising wall is mostly assumed to be chiefly saturated there is likely to be a lower contribution of pumping wetting-drying cycles or any associated wicking effect removing any leached cement species out of the concrete.

A minimum value of >200kg/m^3 is prescribed within Irish building regulations for slit trench foundations at the time of the test properties construction (early 2000s).[86] No binding nationwide building regulations were known by the author to have existed in Ireland during the construction of the control property in the 1980s. The determined cement contents varied between 250-310 kg/m^3 within the test property foundations (**Table 7-8** and **Figure 7-30**) exceeding the minimum specified value at the time of construction. By

[82] Eden, M. Vickery, S., Investigating the causes of deterioration in concrete blocks in southern Ireland, 17th EMABM Toronto, Canada (2019) 228–234.

[83] EN 771-3:2011A1:2015 Specification for masonry units Part 3: Aggregate concrete masonry units (Dense and lightweight aggregates), CEN, Brussels

[84] Leemann, A. Lothenbach, B. Münch, B. Campbell, T. Dunlop, P., The "mica crisis" in Donegal, Ireland – a case of internal sulfate attack? Cem. Concr. Res. 168 (2023).

[85] Poole A. and Sims I., Concrete Petrography: A Handbook of Investigative Techniques, Second Edition, CRC Press, 2016, ISBN146658382

[86] Building regulations 1997, Technical Guidance Document A, Structure, Published by Irish Government, The Stationary Office, Department of Environment, Heritage and Local Government (1997).

Department of Housing, Local Government and Heritage and Geological Survey Ireland

Pyrrhotite-bearing concrete investigation, Co. Donegal - Laboratory Analysis Services in support of Geological Survey Ireland's "Irish Construction Materials" Project: Concrete Products, Phase 1 Report

comparison, the foundation of the control property contained a substantially lower cement content of 160kg/m^3 (**Table 7-8** and **Figure 7-30**). This may be down to the thinness (~10 cm) of the investigated control property foundation resulting in increased leaching over a greater amount of time or be due to the lack of regulation specifying a cement content. Perhaps a more pertinent observation is that all investigated foundations contained enough cement content to appear to be in relatively intact condition and with limited deterioration.

8.3.2 Internal sulfate attack (ISA)

Internal sulfate attack from the oxidisation of sulfides present within concrete aggregate results from the supply of oxygen and alkaline pore solution that can oxidise and produce ferric hydroxide ($Fe(OH_3)$), sulfuric acid (H_2SO_4) and sulfates[87]. It has been established in **8.2.3** that iron sulfides were present in the investigated concretes, and that *in situ* chiefly pyrrhotite oxidisation had occurred in various amounts and severity dependent on the concrete aggregate, concrete type, building element and associated exposure conditions. Therefore, we can suppose that some degree of sulfate had been released *in situ* within all investigated concretes with the potential to cause cement matrix deterioration (ISA).

8.3.2.1 Secondary sulfates

The acid soluble sulfate (ASS) represents the total easily soluble sulfates including secondary sulfates but typically not pyrite content,[88] with up to 0.5 % ASS (as SO_4) by mass deemed not abnormal due to the contribution of sulfates from the cement.[89] Although average concrete blocks with values above 0.4 % ASS (as SO_4) may indicate elevated levels of sulfates. The ASS results for the concrete investigated for all properties were typically between 0.3-0.5 % SO_4 by mass for EN 1744-1 and between 0.12-0.40 SO_4 by mass for EN 196-2 (see **7.4.5**) and considered normal but possibly indicative of some sulfate content in addition to that present in the cement. However, both EN 1744-1 and EN 196-2 ASS results indicated that 21GD inner and outer leaves returned between 0.49 % SO_4 and 0.6 % SO_4 by mass. These results were notably higher than the majority of other inner leaf, outer leaf and rising wall results for the other test and control properties and may indicate a relatively elevated presence of secondary sulfate deposits, such as ettringite and thaumasite, derived from ISA.

OM examinations found rare to numerous secondary sulfate deposits (see **Table 7-4**) with an uneven distribution dependent on property, secondary deposit and building element (see **Table 7-3**). Within OM and SEM/EDX analyses (see **Table 7-6**), the test properties typically exhibited a similar level of secondary deposits within the inner and outer leaves (see **Figure 7-22**). This always included ettringite within air voids or replacing cement matrix in isolated locations but variably included gypsum and other secondary deposits (**Figure 7-27**). 21GD inner and outer leaves were notable for also exhibiting moderate amounts of thaumasite at specific locations (see **Figure 7-27**), that converted C-S-H (the main strength-giving phases of the cement matrix). The presence of isolated point locations of cement matrix conversion to sulfates, albeit limited in

[87] Poole, A and Sims, I, Concrete Petrography 2, See [85]

[88] Longworth, I. (2011). Hardcore for supporting ground floors of buildings: Selecting and specifying materials. BRE Digest DG 522 Part 1. London: IHS BRE Press. ISBN 978 1 84806 216 0.

[89] RICS, The Mundic Problem, See [35]

occurrence, was conclusive evidence for the presence of ISA within the outer and inner leaves of the test properties. In comparison, the outer and inner leaves of the control property were devoid of secondary sulfates or signs of associated deterioration (see **Table 7-3** and **Table 7-4**), strongly indicative that no significant sulfide oxidation and associated ISA had occurred. It should be noted that due to the presence of excessive amounts of 'free' mica (see **Table 7-5**) coupled with the fine size of secondary deposits, an under-estimation and identification of observed finely disseminated deposits (possibly secondary sulfates) within the cement matrix during OM and SEM/EDX analyses is likely. This suggested that the degree of ISA discussed above may be an underestimate.

The test properties' rising walls contained varying amounts of secondary ettringite, gypsum, and other secondary deposits, which were typically only present within air voids. Only 7MV contained traces of thaumasite conversion of the matrix. This suggested that rising walls within the test properties exhibited a limited degree of ISA, however, as mentioned above this may be an underestimate. Alternatively, leaching of the cement matrix could explain the occurrence of the secondary deposits lining air voids within the concrete blocks, as possibly expected for relatively porous and permeable concrete masonry blocks within a variably saturated environment.

A largely similar distribution of secondary sulfates was present in the foundations of the test properties compared to their corresponding rising walls, although usually to a lesser extent (see **Table 7-3**, **Table 7-4** and **Table 7-6**). SEM/EDX evidence of limited ISA was observed with the rare, isolated conversion of the cement matrix by thaumasite and ettringite (7MV, **Figure 7-27**). The foundations of the control property exhibited significant delicate secondary ettringite deposits limited to air voids which can be just as easily supposed to be the result of leaching rather than ISA.

ISA within the test properties was observed to relatively increase as follows OL>IL>>RW≥F correlated to secondary sulfate formation, replacement of cement by secondary sulfates and overall associated damage and overall cracking/microcracking (

8.3.2.2 Sulfate mobilisation

Sulfate deposits and associated conversion of cement matrix are known to be commonly located in close proximity (e.g. reaction haloes) to the associated source of the sulfate (oxidised sulfides) as a localised expansive deterioration mechanism.[85,90,91,92] This occurrence was only rarely observed within the investigated samples (see **Figure 7-11** and **Figure 7-14**). Rather, secondary sulfate deposits and replacement of the investigated cement matrix of the test properties were variably distributed, chiefly within discrete areas of the cement matrix in isolated masses (see **Figure 7-22**). A notable exception was located within 21GD inner and outer leaves, where thaumasite was abundant at the interface with the adjacent mortar observed extensively within air voids and replacing the cement matrix (see **Figure 7-3** and **Figure 7-7**). Thaumasite formation requires a source of sulfate supply, calcium ions and low temperatures, plus a greater presence of water than conventional sulfate attack.[93] Given that OM and SEM/EDX analyses found no oxidised sulfides within the mortar, it would seem reasonable that the sulfates required

[90] RICS, The Mundic Problem, See [35]

[91] Rodrigues et al, 2012, See [5]

[92] Leeman et al, The "mica crisis" in Donegal Ireland, See [84]

[93] Poole, A and Sims, I, Concrete Petrography 2, See [85]

were transported from the adjacent concrete block to the mortar. Whilst the transportation mechanism was not investigated here, a reasonable assumption, seen by RSK in other similar investigations, can be made that a sulfate transportation gradient exists, based on the wicking (capillary absorption) properties of the finely porous and permeable sand cement mortar in contact with the more porous and permeable blockwork. The presence of a significant transport gradient through the concrete blocks of the IL and OL would help to explain the relative lack of sulfate deposits within the examined test property concrete samples. Additional evidence of sulfate mobilisation was observed within 28AW, where the abundance of secondary sulfate, particularly above ground level, did not necessarily correlate with the severity of damage observed. This occurrence can be explained by the saturated nature of the blocks upon extraction (**Figure 2-1**) and the extensive cracking present (**Figure 7-8** and **Table 7-4**). The presence of moisture ingress above ground and easily exploitable failures may have provided pathways for the leaching out or transportation of soluble sulfates released during oxidisation to areas distant from the oxidisation sites present within the samples.

8.3.3 Acid attack

The release of H^+ ions in solution is a well-established result of sulfide oxidisation. Within concrete this leads to the formation of gypsum in certain reducing low pH conditions.[94,95] Secondary gypsum was primarily found within the foundations and rising walls of the test properties but also rarely within the concrete blocks of the inner and outer leaves (see **Table 7-3** and **Table 7-6**). The stability of secondary gypsum in the presence of concrete suggests the pore solution below ground is slightly acidic to neutral, reflective of the expected groundwater redox conditions below ground and within the rising walls. The limited presence of secondary gypsum in the inner and outer leaves suggests that the cement matrix is still chiefly buffering the formation of gypsum by maintaining a high pH and promoting the formation of secondary ettringite.[96] In rare cases where gypsum is present within the IL of 21GD (see **Table 7-6**), we can assume some very localised form of acid concentration either from the release of acid by sulfide oxidisation or the ingress of rainwater through the system (see **Figure 2-1**). Evidence of acid or soft water attack is rarely confirmed by the presence of secondary carbonation within the foundations of 21GD (see **Figure 7-18**) suggesting a very localised minor effect. The inner and outer leaves typically exhibited areas of weak cement matrix, comprising high microporosity and low cement content. It was not possible to identify whether the areas of weak cement matrix were the result of concrete block production or acid attack and subsequent transportation of the resultant soluble phases away. This was particularly made more difficult to confirm due to the presence of fine mica within the cement matrix.

8.4 Physical properties

The compressive strengths of the concrete blocks ranged between 5.9-12.8 N/mm^2 for the test properties and between 12.8-14.1 N/mm^2 for the control property (see **Figure 7-28** and **Table 7-8**). The associated densities range between 2040-2220 kg/m^3 for the test properties and 2100-2270 kg/m^3 for the control property. When compared with the

[94] Leeman et al, The “mica crisis” in Donegal Ireland, See [84]

[95] Rodrigues et al, 2012, See [5]

[96] Leeman et al, The “mica crisis” in Donegal Ireland, See [84]

building regulations of the time[97,98] and more modern standards[99,100] (5 N/mm^2 to 7.5 N/mm^2) the concrete blocks from all properties appear to chiefly meet the typical or required values.

The notably lower strengths of the RWs from 21GD and 28AW, and the OL of 28AW can be correlated to concrete deterioration observed within these samples (see **Table 7-4**). What is not evident from the compressive strength results are the samples and sub-samples that were rejected for compressive strength testing because they were either too weak to sub-sample or were received partially fragmented or disintegrated (see **Table 3-1**). It should be appreciated that the physical results, therefore, often represent the worse condition of suitable samples supplied for the different elements rather than necessarily typical or indicative values. For instance, samples for the OL of 28AW initially comprised of two disintegrated cores, and two fragmented or crumbly, partial to near whole concrete blocks. Therefore, we can infer that the reported value of 7.2 N/mm^2 is easily the best case for the element when at least three of the other supplied samples would be considered as having already failed. This variation in condition can be explained by the observed localised deterioration associated with sulfide deterioration. As previously discussed above, this localised deterioration is moisture sensitive in an oxidising environment. In this case, being related to moisture ingress or cracking of the protective systems (render) in place, resulting in a block-level resolution of deterioration (see **Figure 2-1**).

The mass concrete foundation of the test properties varied between 14.2-29.9 N/mm^2 compressive strength and 2240-2260 kg/m^3 density. All but one of the calculated compressive strength values exceed the 15 N/mm^2 characteristic 28-day compressive strength for concrete strip foundations in non-aggressive ground, specified in Irish building regulations of the time and currently applicable.[101,102] It should be noted that 14.2 N/mm^2 does not necessarily indicate a failure of the concrete to attain the characteristic strength of 15 N/mm^2 as samples from *in situ* are less ideally compacted and cured compared with test cubes.[103] The relatively high sulfur as sulfide value and high associated risk (**Table 7-4**) for this sample may explain the relatively low strength of the sample, however, no conclusive explanation was apparent.

The concrete blocks of the control property exhibited substantially higher compressive strengths but comparable density results when compared to the test properties. Whilst many explanations could be possible for this variation including initial specification and production quality, the difference could be reasonably explained by the use of a more competent aggregate and the observed lack of *in situ* oxidisation and subsequent internal sulfate attack within the reference property concrete.

It is noted that it would have been preferential to test a representative number of samples per element, and all in accordance with the same methodology of compressive strength test. The number, size and condition of the samples combined with the intent to get as

[97] Building Regulation 1997, Ireland, See [86]

[98] I.S. 465:2018+A1:2020, See [2]

[99] I.S. 465:2018+A1:2020, See [2]

[100] EN 771-3, See [83]

[101] Building Regulation 1997, Ireland, See [86]

[102] Building regulations 2012, Technical Guidance Document A, Structure, Published by Irish Government, The Stationary Office, Department of Environment, Heritage and Local Government (1997).

[103] BS EN 12504-1, See [17]

much information from the same sub-sample as possible to correlate the results predicated this preferred testing arrangement. It is acknowledged that the results are at best only relatively indicative of the compressive strength of the samples. Given the observation of localised deterioration at the block scale and below, any comparisons to requirements for characteristic compressive strength of the elements they represent are unwise.

8.5 Condition summary of test property structural elements

The risk ratings in accordance with I.S. 465[104] are considered critical for test property elements given the presence of the PHY aggregate (see **Table 7-4**). However, when eliminating the consistent presence of PHY within the samples and when accounting for the other test data, it is possible to deduce the severity of the mechanisms of deterioration and factor in the influence of environmental conditions. A summary of the condition follows for each investigated building element in the test properties (see **Figure 8-2**), in order of relative severity of deterioration.

8.5.1 Outer leaf

The received test property outer leaf concrete blocks exhibited conditions ranging from intact to complete failure, representing the worst condition within the investigated samples. As previously discussed, the observed deterioration in the outer leaves of the test properties was primarily due to the presence of PHY aggregate containing significant amounts of pyrrhotite. The presence of significant amounts of accessible (matrix-set or exposed aggregate-set) pyrrhotite resulted in expansive *in situ* sulfide oxidisation within the outer leaves where a ready supply of oxygen was present in the wall cavity and the supply of moisture through the failed render. Where pyrrhotite had oxidised, expansive reaction products (iron oxides, iron hydroxides etc.) both within the cement matrix and within phyllite aggregate particles had commonly caused significant expansive cracking. The presence of widespread but localised *in situ* pyrrhotite oxidation led to a similarly localised distribution of small areas of severe ISA within the cement matrix. This resulted in the significant but limited formation of expansive secondary ettringite observed near oxidation sites or rarely within the cement matrix. Additionally, extensive thaumasite form of ISA had occurred at the outer leaf block-mortar/render interface, indicating sulfate movement (wicking) into the relatively cement-rich uncarbonated (higher pH) mortar or render. The carbonation of the cement matrix within the outer leaf indicated a lowered pH, restricting sulfide oxidisation[105], but also the ingress of oxygen that aids sulfide oxidisation. These factors had potentially restricted the degree of ISA within the outer leaf, as evidenced by the rareness of extensive masses of sulfate deposits. The sulfate and acid released into the concrete by pyrrhotite oxidisation may chiefly have resulted in the common weakening of the cement matrix. It is possible to speculate that the weakened areas of high microporosity cement matrix represent the resultant Al and Si-rich remnants of the cement matrix after the leaching/acidic removal of calcium (from C-S-H), and sulfate deposits from these areas.

[104] I.S. 465:2018+A1:2020, See [2]

[105] Divet, L. Davy, J.P. Étude des risques d'oxydation de la pyrite dans le milieu basique du béton, Bull. Lab. Ponts et Chaussées 204 (1996) 97–107.

The presence of excessive 'free' mica within the outer leaf had not caused any directly observable deterioration but may have been responsible for or contributed to the excessively high microporosity of the observed cement matrix even within intact samples through increased water demand during production.[106] Excessive 'free' mica can be speculated to have provided pathways for moisture transportation (leaching). Given the presence of sulfide oxidisation and ISA within the outer leaf samples, excessive 'free' mica content is found to be a limited contributory factor to the observed deterioration, primarily causing the relatively poor quality of concrete block, suspectable to deterioration mechanisms rather than being a direct cause of deterioration itself. The extensive cracking and failure of the concrete blocks, as well as the subsequent deterioration of the external render, were caused by significant primarily pyrrhotite oxidisation, localized severe internal sulfate attack (ISA), and the resulting weakening of the cement matrix within the outer leaf of test property concrete blocks.

8.5.2 Inner leaf

The same mechanisms of deterioration, localised occurrence and reactant pathways are present within the inner leaf as described within the outer leaf samples, except that the degree of pyrrhotite oxidisation, ISA, deterioration and moisture ingress was marginally less advanced (see **Figure 8-2**). The lack of moisture ingress within the inner leaf is expected given typical domestic cavity wall construction due to the greater distance to external moisture sources and the presumed influence of the relatively lower humidity environment of the house interior. Nevertheless, where moisture ingress was observed within the inner leaf (e.g. 28AW), excessively high microporosity, weakening of the matrix and increased *in situ* oxidisation of pyrrhotite were observed. The presence of rare secondary gypsum within the inner leaf, but not seen in the outer leaf, suggested that some limited degree of lower pH ISA had occurred when the required portlandite (i.e. uncarbonated cement matrix) was available for gypsum formation.

8.5.3 Rising wall

The redox environment of the rising walls will inherently be dependent on the degree of groundwater saturation present. When saturated with groundwater the conditions will be reducing but when partially saturated or unsaturated the environment is more likely to be oxidising.

Given the *in situ* conditions upon sampling, the predominantly wet conditions within the Donegal region,[107] and the mild acidity of most groundwater and rainwater an assumption of chiefly reducing conditions in the rising wall can be made. The test property rising wall concrete blocks exhibit a lack of significant carbonation of the cement matrix that can be attributed to block saturation restricting the permeation of oxygen. Accordingly, when compared with the outer leaf and inner leaf the *in situ* oxidisation of pyrrhotite within the rising walls was significantly decreased with the presence of secondary sulfate deposits chiefly limited to air voids and only rare possible observations of ISA within the cement matrix.

[106] Eden, M. Vickery, S. (2019), See [71]

[107] Met Eireann, Historical data, Available at, https://www.met.ie/climate/available-data/historical-data. Accessed 06/10/2024.

Figure 8-2 Cross section of element condition

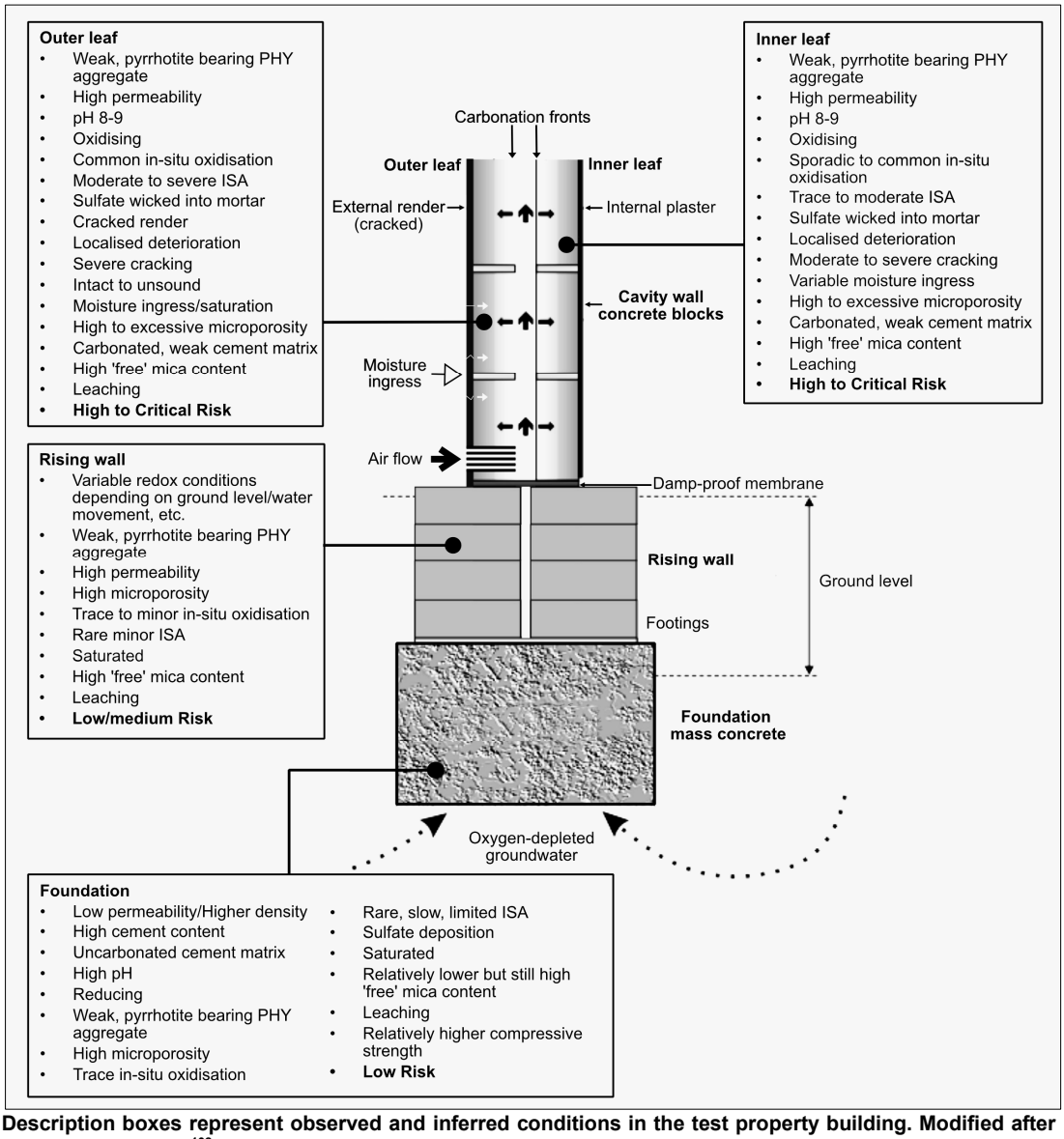

Description boxes represent observed and inferred conditions in the test property building. Modified after Poole & Sims 2016.[108] All risks are provisional, relative to each other and limited to the specific context.

8.5.4 Foundation

The mass concrete samples of the test property foundations were all received intact, in contrast to the concrete blocks of the other building elements described above. The use of stronger, more cementitious concrete in a likely reducing environment has largely inhibited *in situ* pyrrhotite oxidation and resisted physical deterioration. However, it has not eliminated internal sulfate attack (ISA) within the cement matrix, as inconsistently shown by rare, isolated masses of ettringite and thaumasite within the cement matrix, and the variable presence of secondary gypsum and ettringite within air voids (possibly leached from the rising walls). The presence of limited ISA within the concrete suggests that conditions for the ISA are possible within the foundations but that they are likely both rarer spatially (lower abundance) and occurring more slowly (~20 years). Given the

[108] Poole, A and Sims, I, Concrete Petrography 2, See [85]

investigations covered in this report, it is not possible to say that the mass concrete of the test properties foundations, whilst being able to resist significant pyrrhotite oxidisation and ISA-related deterioration to date, will continue to do so within the scope of future service. Further commentary on the foundations investigated in this project is covered within RSK report 1283831-03.

8.6 Control property

The condition of the control property was consistently superior relative to that of the test properties. The primary difference in condition was due to the species and morphology of the sulfides within the SST aggregate and the resultant, chiefly absent *in situ* oxidisation of sulfides within the inner leaf, outer leaf and foundations. Only secondary ettringite and calcite, consistent with leaching, and common traces of iron oxide/hydroxides were observed. Therefore, the control property was chiefly considered of low risk as supported by 40 years of service life without significant deterioration, likely due to the use of a stronger, lower oxidisation potential sulfide-bearing aggregate (SST) within the concrete.

8.7 Summary of main factors in the concrete deterioration

The 40-year service life of the control property has shown no significant deterioration to date. However, the test properties, with a service life of 15-25 years, have experienced failures within certain elements. This study suggests that the type, presence and exposure of sulfide minerals within the concrete aggregate, combined with the redox conditions and type of concrete present within different building elements, are the most important factors contributing to the observed deterioration in the test properties. Excessive muscovite mica is deemed to be a passive contributory secondary factor to the observed deterioration.

9 CONCLUSIONS

The presence of concrete block deterioration has been a significant problem within Donegal and other counties in the Republic of Ireland, leading to thousands of assessments in accordance with the I.S. 465[109] methodology. RSK has investigated the condition of different building elements and their potential for further deterioration primarily through sulfide oxidisation and ISA. This study reports Phase 1 of the investigation, considering the relative condition and deterioration mechanisms present within the inner leaf, outer leaf, rising wall and foundations within three test properties and one control property (no rising wall). The results presented here establish a baseline for the accelerated exposure testing in Phase 2 and a series of condition tests in Phase 3. The main conclusions are as follows:

- A total of 52 no. received samples consisted of IL, OL, and RW concrete block and F mass concrete elements.
- The as-received condition of the samples generally ranged in condition order F>RW>IL>OL.
- Test properties contained the problematic PHY aggregate in all elements.
- PHY aggregate contained weak phyllite and interbedded phyllite/quartzite lithologies that contained significant amounts of pyrrhotite, pyrite, other sulfides, muscovite mica and other mica group minerals.
- The test property concrete exhibited both evenly disseminated and lenses of aggregate-set sulfides chiefly within phyllite particles, and discrete matrix-set sulfides.
- The test property concrete exhibited high ‘free’ mica (<63 µm) contents of 24-40 % and 13-18 % proportion of the binder in concrete blocks and mass concrete respectively.
- High ‘free’ mica content was not necessarily the cause of observed deterioration other than potentially contributing to a high w/c ratio due to increased water demand, providing localised weaknesses and potential pathways for moisture movement.
- The control property contained the sulfide-bearing SST aggregate in all elements.
- SST contained pyrite, traces of pyrrhotite and relatively less muscovite mica and other mica group minerals.
- The control property concrete exhibited sandstone and siltstone aggregate-set and discrete matrix-set sulfides.
- Total sulfur content determined in accordance with EN 1744-1 by acid digestion and taking into account contributions from the cement, returned results (0.0-0.3 % S by mass) inconsistent with observed concrete containing sulfide-bearing lithologies. This would seem to be an analytical technique underestimation.

[109] I.S. 465:2018+A1:2020, See [2]

- Total sulfur content determined in accordance with EN 1744-1 by HTC and taking into account contributions from the cement, returned results of 0.5-0.9 % S by mass for test properties and 0.1-0.2 % S by mass for the control property. This was consistent with observed concrete containing sulfide-bearing lithologies.
- Total sulfur content determined in accordance with EN 1744-1 by HTC would appear to be the preferential method for determining the total sulfur in these concrete materials. Determination of sulfur or sulfates within the concrete elements, in particular the masonry blocks may have been underrepresented by wicking (transport gradient) of sulfates into the adjacent render/mortar during *in-situ* reactions.
- Sulfur content of the aggregate within the test properties was determined and calculated resulting in values (by mass) of 0.32-0.68 % S when using the test method given in EN 196-2 for cement (determination only).
- Acid digestion determination of sulfur content of concrete by EN 196-2 was deemed more consistent with the overall sulfur content than by the EN 1744-1 acid digestion test method.
- The vast majority of sulfur content of aggregate values both determined and calculated for PHY exceeded the 0.1 % S (by mass) limit for aggregate containing pyrrhotite specified in EN 12620.
- Pyrrhotite exhibited typically striped oxidisation morphology, whilst pyrite exhibited rare typically surface-type oxidisation morphology.
- The striped oxidisation of pyrrhotite appeared to give an approximation for the degree of oxidisation when comparing oxidised to unoxidised bands.
- Sulfide oxidisation was observed to have occurred either prior to use within the concrete or *in situ* within the concrete.
- The *in situ* oxidisation of the sulfides (primarily pyrrhotite) was observed within all test property elements and relatively ordered in terms of severity OL>IL>>RW≥F.
- The control property lacked significant *in situ* oxidisation of sulfides
- Oxidisation of sulfides was chiefly influenced by factors such as mineralogy, morphology and exposure of the sulfides, coupled with the redox conditions of the concrete element the sulfides were present in.
- The oxidisation of the sulfides had led to ISA in all elements variously across all test properties. The degree of ISA within the test properties was relatively ordered OL>IL>>RW≥F.
- Significant TSA was present at the interface between the concrete blocks and adjacent sand cement mortar, of a single test property for both the OL and IL, suspected to be caused by a transport gradient (wicking) of sulfates into the uncarbonated cement matrix of the mortar.
- Carbonation of the cement matrix within the test properties appeared to have restricted the amount of ISA in the OL and IL.
- Acid attack as the result of sulfide oxidisation within the test properties may have both caused or exploited weak areas of the cement matrix.

- Sulfide oxidisation and ISA had caused significant cracking within aggregate particles and the cement matrix, in good correlation with the degree/frequency of *in situ* sulfide oxidisation and ISA.
- Sulfide oxidation and ISA were generally highly localised but extensively distributed at the microscopic scale.
- Secondary reaction products/minerals identified consisted of iron oxide and hydroxides, ettringite, gypsum, thaumasite and portlandite.
- All but one of the elements tested satisfied both the compressive strength and cement requirements of the Irish building codes at the time of construction. However, it was important to note that these samples were of sufficient condition to permit testing for compressive strength and as such likely represent the best condition to the worst intact condition available. In particular test property ILs and OLs were variably intact, crumbly, deteriorated or disintegrated, to the extent that no meaningful strength tests could be undertaken on a number of these samples.
- The deterioration in test property ILs and OLs was highly localised at a block scale and likely correlated to moisture ingress through the outer render, particularly where it had failed.
- The mass concrete foundation of the test properties appeared in generally sound condition, significantly more so than the other elements investigated.
- Whilst secondary ettringite deposits within voids present in the test property foundations were more typical in morphology of leaching, the traces of *in situ* pyrrhotite oxidisation, secondary gypsum deposits and rare thaumasite and ettringite masses still suggested sulfide oxidation and associated ISA had occurred in some trace, likely isolated, degree even in the reducing environment of the foundations.
- Whilst no significant cracking or failures had occurred at the time of analysis within the PHY-bearing foundations of the test properties, these foundations are denser, stronger and undergoing a slightly different, much slower form of deterioration than other elements investigated. The findings presented within this report do not allow significant confidence as to whether the limited deterioration observed within PHY concrete foundations would pose a risk of further deterioration and thus may not have much confidence currently placed in the proposed low-risk ultimately due to the presence of reactive pyrrhotite. Phase 2 and Phase 3 investigations to comment further.
- All elements of the test properties exhibited some form of *in situ* oxidisation of sulfides and ISA.
- The relative condition and state of deterioration within the test properties was OL>IL>RW>F.
- The degree of relative risk associated with the samples can be considered as OL>IL>RW>F.
- The control property did not exhibit significant deterioration, sulfide oxidisation, or any ISA, even though it contains iron sulfides including rare traces of pyrrhotite.

- The control property was considered at low risk of deterioration in accordance with I.S. 465 due to the service history combined with the composition and abundance of sulfides within the SST aggregate.

10 REMARKS

These findings refer only to the samples sampled and tested and to any materials or areas properly represented by those samples.

Any assessment of risk mentioned herein is based upon the findings of these specific investigations and any information provided to the investigation. Extension of this assessment of risk to any properties not included in this investigation should be with caution and ideally should include site-specific assessment of the existing concrete.

Statements of uncertainty of test measurements are provided on test certificates only where these are specifically declared by the documented Test Method and are the result of a formal inter-laboratory precision trial.